https://ntrs.nasa.gov/search.jsp?R=19680027760 2020-03-12T05:46:35+00:00Z

General Disclaimer

One or more of the Following Statements may affect this Document

- This document has been reproduced from the best copy furnished by the organizational source. It is being released in the interest of making available as much information as possible.

- This document may contain data, which exceeds the sheet parameters. It was furnished in this condition by the organizational source and is the best copy available.

- This document may contain tone-on-tone or color graphs, charts and/or pictures, which have been reproduced in black and white.

- This document is paginated as submitted by the original source.

- Portions of this document are not fully legible due to the historical nature of some of the material. However, it is the best reproduction available from the original submission.

Produced by the NASA Center for Aerospace Information (CASI)

N68-37232
(ACCESSION NUMBER)

(THRU)

129
(PAGES)

1
(CODE)

CR-98035
(NASA CR OR TMX OR AD NUMBER)

10
(CATEGORY)

FACILITY FORM 602

WYLE LABORATORIES

TESTING DIVISION, HUNTSVILLE FACILITY

GPO PRICE $ ______

CFSTI PRICE(S) $ ______

Hard copy (HC) 3.00

Microfiche (MF) ______

ff 653 July 65

research

WYLE LABORATORIES - RESEARCH STAFF

REPORT NUMBER WR 67-17

INTERACTIONS OF A SHOCK WAVE WITH AN ENTROPY DISCONTINUITY

By

Elizabeth Cuadra

Work Performed Under Contract NAS 8-21100

Principal Investigator, M. V. Lowson

FEB 1968

12

FOREWORD

This report is submitted under Contract NAS 8-21100, Aerodynamic Noise Research. The program has been administered by the Unsteady Aerodynamics Branch, National Aeronautics and Space Administration, George C. Marshall Space Flight Center, Huntsville, Alabama

The author expresses her appreciation to the following Wyle Laboratories personnel: David M. Lister for computer programming, and Dr. Martin V. Lowson for guidance in the derivation for a random field of entropy waves and other helpful discussions.

SUMMARY

Numerical results (based on the theory of C. T. Chang) are presented for use in prediction of the perturbed downstream flow field resulting from the interaction of a planar entropy discontinuity with an infinite planar shock. Downstream pressure, vorticity, and entropy fluctuation values are presented in parametric form for normal shocks and for oblique shocks generated by wedge flow: for wedge half-angles from 4 to 30 degrees, for upstream Mach numbers from 1.4 to 10, and over the entire range of orientations of the oncoming entropy disturbance.

Discontinuous large values in the amplitudes of all flow perturbations occur at an "effective Mach number, M_e" value of unity in the flow. For $M_e > 1$ the generated pressure disturbance radiates as sound, while for $M_e < 1$ the pressure disturbance amplitude decays with distance from the shock. These numerical results, when combined with typical entropy fluctuation magnitudes, give sound pressure levels greater than those typical for boundary layer noise, and equal to those produced by shock-turbulence interactions, for typical aerospace applications.

For the case of a random field of entropy waves interacting with a shock, the required relations for the harmonic components of all three downstream modes are presented, and an expression is derived for the root-mean-square pressure amplitude caused by an isotropic entropy field, but this study has not progressed to the point of numerical results.

TABLE OF CONTENTS

LIST OF FIGURES

LIST OF FIGURES (Continued)

LIST OF FIGURES (Continued)

LIST OF SYMBOLS

Roman Symbols

A	speed of sound in downstream flow field
A_1	speed of sound in upstream flow field
$\tilde{A}$	ratio of transfer coefficients, π_{31}/π_{21}
a_p	downstream pressure fluctuation amplitude, harmonic case
a_s , b_s	downstream entropy perturbation amplitude, harmonic case
a_v , b_v	velocity perturbation amplitude, harmonic case
a_ψ , b_ψ	shock displacement amplitude components, harmonic case
B	ratio of transfer coefficients, $-\pi_{41}/\pi_{21}$
C	see Equation 52
c_p	specific heat at constant pressure
c_v	specific heat at constant volume
C_s	drift speed of the interaction point along the shock (trace velocity)
C_{s_1}	intersection of shock and sonic circle lying farthest from origin
C_{s_2}	intersection of shock and sonic circle lying nearest the origin
D	see Equation 52
$f(Y)$	vorticity generating function (Equation 41)
G	a nondimensional group in solution for Riemann invariants (Equation 40)
$g(Y^*)$	a function related to the strength of an equivalent source located on the shock plane (Equation 50)

LIST OF SYMBOLS (Continued)

k_1	upstream wavenumber, harmonic entropy wave
ℓ_1	$\cos\delta$
M	Mach number of the flow downstream of the shock
M_1	Mach number of the flow upstream of the shock
M_e	effective Mach number corresponding to U_e
m_1	$\sin\delta$
N	normal component of downstream Mach number
N_1	normal component of upstream Mach number
p_+	dimensionless magnitude of downstream pressure perturbation
q	one of the two Riemann invariants (Equation 36)
q_1	upstream dynamic pressure
R_s	upstream amplitude, harmonic entropy wave
s_-, s_1	upstream entropy perturbation magnitude
s_+	downstream entropy perturbation magnitude
T	temperature (absolute)
T_1 (δ)	an amplitude function for subsonic case (Equation 40)
T_2 (δ)	an amplitude function for supersonic case (Equation 39)
t	time

LIST OF SYMBOLS (Continued)

U	downstream mean flow velocity
U_1	upstream mean flow velocity
U_e	effective mean flow velocity (apparent velocity of downstream mean flow to an observer moving at trace velocity C_s)
u_1	dimensionless magnitude of velocity perturbation component along upstream mean flow direction
u^*	dimensionless magnitude of velocity perturbation component along shock plane direction
u_+	dimensionless magnitude of velocity perturbation component along downstream mean flow direction
VORT	vorticity magnitude parameter, $(u_1^2 + v_1^2)^{1/2}$
v_1	dimensionless magnitude of velocity perturbation component normal to upstream mean flow direction
v^*	dimensionless magnitude of velocity perturbation component normal to shock plane direction
v_+	dimensionless magnitude of velocity perturbation component normal to downstream mean flow direction
X, Y	coordinate axes along and normal to the effective velocity vector U_e
x, y	coordinate axes along and normal to the downstream mean flow
x_1, y_1	coordinate axes along and normal to upstream mean flow
x^*, y^*	coordinate axes along and normal to the shock plane

Greek Symbols

α	inclination of effective velocity U_e with respect to downstream mean flow velocity U
β	angle between the shock and the downstream mean flow velocity vector U_1

LIST OF SYMBOLS (Continued)

γ	ratio of specific heats
δ	inclination of upstream entropy wave with respect to main flow direction
ϵ	shock wave angle, referenced to x_1-axis
θ	enclosed angle between shock and that radius vector of the sonic circle ending at intersection of sonic circle and shock
θ'	enclosed angle between U_e and the x_1-axis
Λ_{ij}	transfer coefficients for the interaction (see text)
μ_e	effective Mach angle corresponding to M_e
π_{ij}	transfer coefficients for the interaction (see text)
ρ_m	mean density in downstream flow
ρ_{1m}	mean density in upstream flow
τ	a reduced space variable At
ϕ	velocity potential
χ	shock strength (ratio of mean static pressures across the shock)
Ψ_τ	local perturbation velocity of the shock
Ψ_y	local shock deflection
Ω_1	a grouping of transfer coefficients (Equation 40)
Ω_2	a grouping of transfer coefficients (Equation 40)
ω	vorticity

1.0 INTRODUCTION

Many of the important problems in gas dynamics are concerned with the effect of small disturbances in a supersonic flow with shock waves present. The impetus to study the resulting downstream perturbation field has come from such problems as oscillating shocks ahead of blunt bodies, Reference 1, or flared sections on launch vehicles, oscillating shocks in supersonic inlets and exit nozzles, and disturbances in supersonic wind tunnels, Reference 2. The major interest in several current investigations is in the pressure field generated by the interaction, since the fluctuating pressure field associated with a shock is thought to have been the cause of several catastrophic failures of launch vehicles; in any case,the pressure field must be predicted to enable minimum-weight design of such structures.

First-order perturbation theory indicates that the governing equations for a compressible, viscous, and heat-conducting gas can have three distinctively different types of disturbance fields: (a) entropy, (b) vorticity, (c) pressure and irrotational velocity (sound). When the intensity of the fluctuations is small, the three modes are independent. Non-linear coupling between the various modes can occur if the intensity of the disturbances is large or if interactions at boundaries occur (e.g., at a solid wall, a shock wave, or the boundary of a wake or a jet). Thus, when a shock wave is perturbed from its equilibrium configuration (as by interaction with any one of the three fundamental modes), the field downstream of the shock is composed of the original field plus perturbation fields of all three modes (vorticity, entropy and sound) generated by the interaction. When the perturbations are small, the three resulting fields are computable from separate systems of linear partial differental equations, connected only through the boundary conditions on the shock wave and any solid boundaries present. Since the equations are linear, Fourier synthesis can be applied, and so it is useful to consider the interaction of a single simple disturbance with a shock wave.

Although the problem of interactions between weak disturbances and shock waves in a uniform stream of perfect gas has received a good deal of attention, most of it has been concentrated on interaction of a plane shock with sound waves or with turbulence (vorticity). Sound-shock interactions were dealt with in References 3, 4, and 5, and Chu (Reference 5) included the effect of reflection between a wall and the shock wave. Regarding vorticity-shock interactions, Ribner (Reference 6) studied the interaction of a shear wave with a shock, and demonstrated the existence of sound waves and refracted shear-entropy waves in the flow behind the shock. In Reference 7 this work was generalized to give the noise radiated by the interaction of a shock with turbulence. Moore (Reference 8) analyzed the interaction of sound with an oblique shock wave. Lowson (Reference 9) extended the numerical information available based on theory in References 7 and 8, including the motion of the shock wave during the interaction, and showed that the fluctuating pressure field is of significant magnitude in typical supersonic flow problems.

The remaining mode, entropy waves, are represented by either temperature or density discontinuities (at constant pressure) in the gas and are carried along at the local mean flow velocity of the gas. Entropy waves may be due to such causes as temperature stratification in the medium, presence of an upstream shock wave undergoing perturbations, or an unsteady upstream heat source as can occur in combustors or in heated supersonic wind tunnels. Morkovin concluded in Reference 2, for example, that entropy wave interactions with shock waves can be the largest source of noise in supersonic wind tunnels. The entropy fluctuation mode has been analyzed by Chang, Reference 10, who gave the theory for interaction of a plane entropy wave with an oblique plane shock wave. In addition to giving solutions for a number of specific cases involving a shock produced by an infinite wedge (including reflections from the wedge) and several varieties of restriction on the nature and relative orientation of the entropy wave, Chang also gave the solution for the general case of the unsteady interaction of a single (step function) plane entropy disturbance and an infinitely extended oblique plane shock where the body causing the shock is tacitly assumed to be absent. It is Chang's solution of this general case that has been used to obtain the numerical results given here.

While the theoretical foundation exists in Reference 10, the method is unwieldy for routine engineering use, and only a few numerical results were previously available: Reference 1 for a sinusoidal entropy wave interacting with a normal shock at an upstream Mach number of 1.45 only, and Reference 1* for the same case over an extended range of Mach numbers up to Mach 10. It is the purpose of the present report to provide parametric numerical results for the downstream flow field, covering the range of flow conditions which might be encountered in practice, and to make order of magnitude estimates for the most extreme pressure fields which might be generated, based on existing data for entropy fluctuation magnitudes. The required equations for the root-mean-square pressure fluctuations resulting from a random field of entropy waves are also presented, but the random field case has not been carried to the point of numerical results.

* To be amended in a forthcoming corrigendum by Dr. Morkovin.

2.0 THE SHOCK-ENTROPY INTERACTION

2.1 Chang's Theory for the Shock-Entropy Interaction

Chang's analysis (Reference 10) begins with a unified treatment* concerning upstream disturbances of all three modes (vorticity, entropy, and sound) interacting with a shock wave, and then specializes on the entropy mode. The medium is taken to be a non-viscous ideal gas, and the analytical model is as follows: A wedge is placed in a uniform flow field and an oblique shock is formed at the wedge. The shock divides the flow field into two regions: An upstream region with uniform velocity U_1 and a downstream region with uniform velocity U, Figure 1. A plane entropy disturbance (simple step function in temperature) is introduced upstream and is convected with the main flow toward the shock. Since the main interest is the interaction of the shock with the upstream disturbance and its effect on the downstream flow field, the presence of the wedge is now ignored (ruling out reflection phenomena), and the shock is taken as infinitely extended.

Three sets of rectangular coordinate axes will be used, Figure 1: $x^* \, o \, y^*$, with $o y^*$ taken along the shock plane; $x_1 \, o \, y_1$, with $o x_1$ taken along the velocity vector U_1 of the upstream main flow; and $x \, o \, y$, with $o x$ taken along the velocity vector U of the downstream main flow.

The flow parameters will be replaced by their corresponding nondimensionalized ones. If Δp, $\Delta \rho$, Δs, and Δu denote the perturbations of pressure, density, entropy and velocity, their corresponding dimensionless parameters will be given by:

$$p = \frac{\Delta p}{\gamma \, p_m} \quad , \quad \rho = \frac{\Delta \rho}{\rho_m} \, , \quad s = \frac{\Delta s}{c_p} \, , \quad \vec{u} = \frac{\Delta \vec{u}}{A} \tag{1}$$

where subscript "m" refers to the unperturbed main flow. Whenever no number subscript is attached, reference is to the region downstream of the shock; for the region upstream of the shock a subscript 1 will be used.

The equations governing the flow field, both upstream and downstream of the shock, are the three conservation laws of mass, momentum and energy. The equation of state gives a relation among the three thermodynamic variables. After replacing the independent time variable t by two reduced space variables

$$\tau = A t, \quad \tau_1 = A_1 t = (A_1/A) \, \tau \tag{2}$$

---

* Chang's derivation is summarized here in some detail, since it is only available in his thesis on a loan basis.

the governing equations are:

Mass:

$$\frac{D\rho}{D\tau} + \operatorname{div} \vec{u} = 0 \tag{3}$$

Momentum:

$$\frac{Du}{D\tau} + \operatorname{grad} p = 0 \tag{4}$$

Energy:

$$\frac{Ds}{D\tau} = 0 \tag{5}$$

State:

$$s = p - \rho \tag{6}$$

where

$$\frac{D}{D\tau} = \frac{\partial}{\partial \tau} + M_1 \frac{\partial}{\partial x_1} \tag{7}$$

for flow in the upstream region, and

$$\frac{D}{D\tau} = \frac{\partial}{\partial \tau} + M \frac{\partial}{\partial x} \tag{8}$$

for flow in the downstream region.

The velocity field can be split into two parts, an irrotational part $\vec{u}_\ell$ and a rotational part $\vec{u}_s$, such that

$$\operatorname{curl} \vec{u}_\ell = 0, \quad \operatorname{div} \vec{u}_s = 0 \tag{9}$$

Then two potential fields can be introduced, a scalar potential ϕ and a vector potential $\vec{E}$, defined by

$$\vec{u}_\ell = -\operatorname{grad} \phi, \quad \vec{u}_s = \operatorname{curl} \vec{E} \tag{10}$$

The governing flow equations, in terms of the potentials, are:

$$\nabla^2 \phi - \frac{D^2 \phi}{D \tau^2} = 0 \qquad (11)$$

$$\text{div } \vec{E} = 0, \quad \frac{D \vec{E}}{D \tau} = 0 \qquad (12)$$

$$\frac{D s}{D \tau} = 0 \qquad (13)$$

The three modes (sound, vorticity, and entropy) are clearly indicated by Equations (5), (6), and (7) respectively. In terms of our non-dimensional parameters, the vorticity $\vec{\omega}$ is given by

$$\vec{\omega} = A \text{ curl } \vec{u_s} = A \text{ curl curl } \vec{E} \qquad (14)$$

The scalar potential ϕ represents the sound field, with pressure and velocity perturbations

$$p = - \left(\frac{\partial}{\partial \tau} + M \frac{\partial}{\partial x} \right) \phi \qquad (15)$$

and

$$\vec{u_\ell} = - \text{ grad } \phi$$

The governing equation for ϕ differs from the conventional wave equation only by a convective term

$$M \frac{\partial}{\partial x}$$

and could be reduced to the conventional wave equation by a Galilean transformation equivalent to using a frame of reference moving with the unperturbed mean flow:

$$x' = x - M \tau$$

$$y' = y$$

$$\tau' = \tau \qquad (16)$$

With the coordinate system $x^* \text{ o } y^*$ (with the oy^* axis along the mean position of the shock) the shock configuration can be given as

$$x^* = \Psi (y^* , \tau) \qquad (17)$$

To first order, the local perturbed velocity of the shock is $A\Psi_\tau$ $(= \Psi_t)$, and the deflection is Ψ_{y^*}, where this subscripting means partial differentiation. If one isolates a small element of the shock and superposes a velocity vector of the same magnitude but opposite direction as $A\Psi_\tau$ to the whole flow field fore and aft of the shock, and then applies the Rankine-Hugoniot equations to the flow parameters across the shock, the downstream perturbed flow parameters can be solved explicitly in terms of the given upstream flow parameters and the local shock deflection and velocity. This solution involves rewriting the conservation equations for mass, energy, momentum normal to the shock and momentum along the shock in terms of the sum of mean flow and perturbation quantities, retaining only the first order terms, and then using the fact that the mean flow must obey the same conservation laws. The result, shown in matrix notation for clarity, is:

$$\begin{bmatrix} s_+ \\ p_+ \\ u^*_+ \\ v^*_+ \end{bmatrix} = \begin{bmatrix} \Lambda_{11} & \Lambda_{12} & \Lambda_{13} & 0 \\ \Lambda_{21} & \Lambda_{22} & \Lambda_{23} & 0 \\ \Lambda_{31} & \Lambda_{32} & \Lambda_{33} & 0 \\ 0 & 0 & 0 & \Lambda_{44} \end{bmatrix} \begin{bmatrix} s_- \\ p_- \\ u^*_- \\ v^*_- \end{bmatrix} +$$

$$+ \begin{bmatrix} \pi_{11} \ M \cos \beta \\ \pi_{21} \ M \cos \beta \\ \pi_{31} \ M \cos \beta \\ \pi_{41} \end{bmatrix} \Psi_{y^*} + \begin{bmatrix} \pi_{11} \\ \pi_{21} \\ \pi_{31} \\ 0 \end{bmatrix} \Psi_\tau \qquad (18)$$

The subscripts + refer to flow properties immediately behind the shock; and subscripts −, to flow properties just ahead of the shock. The downstream perturbed velocity has been resolved into components Δu^* and Δv^* normal and tangential to the unperturbed shock plane respectively; u^* and v^* are their non-dimensionalized forms: $u^* = \Delta u^*/A$ and $v^* = \Delta v^*/A$.

The coefficients occurring in Equations (18) are given by

$$
\begin{aligned}
\Lambda_{1} &= \left(\frac{\rho_m}{\rho_{1m}}\right)^2 \left(\frac{N}{N_1}\right)^2 - (\gamma - 1)\left(1 - \frac{\rho_m}{\rho_{1m}}\right) N^2 \\
\Lambda_{21} &= \frac{N^2}{1 - N^2}\left\{\left(1 - \frac{\rho_m}{\rho_{1m}}\right)\left[1 + (\gamma - 1)\, N^2\right] + \left[1 - \left(\frac{\rho_m}{\rho_{1m}}\right)^2 \left(\frac{N}{N_1}\right)^2\right]\right\} \\
\Lambda_{31} &= \frac{-N}{1 - N^2}\left\{\left[1 - \left(\frac{\rho_m}{\rho_{1m}}\right)^2 \left(\frac{N}{N_1}\right)^2\right] + \left(1 - \frac{\rho_m}{\rho_{1m}}\right) \gamma N^2\right\} \\
\Lambda_{12} &= (\gamma - 1)\left(1 - \frac{\rho_m}{\rho_{1m}}\right)\left(1 - \frac{1}{N_1^2}\,\frac{\rho_m}{\rho_{1m}}\right) N^2 \\
\Lambda_{22} &= \frac{-N^2}{1 - N^2}\left\{\left(1 - \frac{\rho_m}{\rho_{1m}}\right) + \left(1 - \frac{1}{N_1^2}\,\frac{\rho_m}{\rho_{1m}}\right)\left[1 + (\gamma - 1)\left(1 - \frac{\rho_m}{\rho_{1m}}\right) N^2\right]\right\} \\
\Lambda_{32} &= \frac{N}{1 - N^2}\left\{\left[1 - \left(\frac{\rho_m}{\rho_{1m}}\right)^2 \left(\frac{N}{N_1}\right)^2\right] + \gamma\left(1 - \frac{\rho_m}{\rho_{1m}}\right)\left(1 - \frac{1}{N_1^2}\,\frac{\rho_m}{\rho_{1m}}\right) N^2\right\} \\
\Lambda_{13} &= (\gamma - 1)\left(1 - \frac{\rho_m}{\rho_{1m}}\right)^2 \frac{N^2}{N_1} \\
\Lambda_{23} &= -\frac{N}{1 - N^2}\left(1 - \frac{\rho_m}{\rho_{1m}}\right)\left\{2 + (\gamma - 1)\left(1 - \frac{\rho_m}{\rho_{1m}}\right) N^2\right\}\frac{N}{N_1} \\
\Lambda_{33} &= \frac{1}{1 - N^2}\,\frac{N}{N_1}\left\{1 - \left(\frac{\rho_m}{\rho_{1m}}\, N\right)^2 + \gamma\left(1 - \frac{\rho_m}{\rho_{1m}}\right)^2 N^2\right\} \\
\Lambda_{44} &= \frac{\rho_m}{\rho_{1m}}\,\frac{N}{N_1}
\end{aligned}
\qquad (19)
$$

$$\pi_{11} = -(\gamma - 1)\left(1 - \frac{\rho_{1m}}{\rho_m}\right)^2\left(\frac{\rho_m}{\rho_{1m}}\right) N$$

$$\pi_{21} = \frac{-N}{1 - N^2}\left(1 - \frac{\rho_{1m}}{\rho_m}\right)\left[2 + (\gamma - 1)\left(1 - \frac{\rho_m}{\rho_{1m}}\right) N^2\right]$$

$$\pi_{31} = \frac{1}{1 - N^2}\left(1 - \frac{\rho_{1m}}{\rho_m}\right)\left[1 + N^2 + (\gamma - 1)\left(1 - \frac{\rho_m}{\rho_{1m}}\right) N^2\right]$$

$$\pi_{41} = \left(\frac{\rho_m}{\rho_{1m}} - 1\right) N \qquad (19) \text{ Cont.}$$

With N_1 and N the Mach numbers upstream and downstream of an equivalent normal shock:

$$N_1 = M_1 \sin \epsilon, \qquad N = M \sin \beta \qquad (20)$$

Since all the coefficients Λ and π are functions only of N_1, N and the density ratio ρ/ρ_{1m}, then for any given value of γ they are only functions of the shock strength χ:

$$\chi \equiv \rho_m / \rho_{1m} \qquad (21)$$

Thus the obliqueness of the shock, or dependence on the shock angle β, enters only in terms involving Ψ_y*, the local shock inclination. It may also be noted that the system of Equations (19), containing one more unknown than the number of equations, is insoluble without the addition of another relation involving the shock configuration.

From the governing equation of the entropy mode, it can be seen that an arbitrary function in the form of a plane wave is a possible solution:

$$s_1 = s_1\left[\ell_1 M_1 \frac{A_1}{A} \tau - (\ell_1 x_1 + m_1 y_1)\right] \qquad (22)$$

where δ is the inclination of the normal to the entropy wave front with respect to the main flow velocity U_1 upstream of the shock, and

$$\ell_1 \equiv \cos\delta\,, \quad m_1 \equiv \sin\delta \tag{23}$$

This will be useful later on when the object is to synthesize a random field of entropy disturbances from such monochromatic spectral components.

The incoming disturbance drifts along the shock at a speed*

$$C_s = \frac{\cos\delta}{\cos(\delta - \epsilon)}\, U_1 \tag{24}$$

so that the flow pattern of the incoming disturbance appears stationary to an observer moving along the shock at this speed, and in such a reference frame the downstream flow field appears time independent. That is, with respect to the reference frame x', y', τ' obtained from the following Galilean transformation, the downstream flow solution is a function of x' and y' only:

$$\begin{aligned} x^* &= x' \\ y^* &= y' + \frac{C_s}{A}\,\tau \\ \tau &= \tau' \end{aligned} \tag{25}$$

This transformation is equivalent to superposing on the whole flow field a velocity $-C_s$; to an observer affixed to this moving coordinate system the downstream main flow has an apparent velocity U_e, which is the vectorial sum (Figure 2)

$$U_e = U + (-C_s) \tag{26}$$

and which has the magnitude and inclination α with respect to the main flow given by

$$\frac{C_s}{\sin\alpha} = \frac{U}{\sin(\alpha - \beta)} = \frac{U_e}{\sin\beta} \tag{27}$$

---

* One will note that this fails at $(\delta - \epsilon) = \pi/2$, i.e., where the oncoming entropy wave is parallel to the shock, and this special case is treated below in Section 2.1.4.

The vorticity and entropy trajectories are along the velocity vector U_e, and the system of governing equations can be simplified by rotating the coordinate axes along and normal to this direction. The problem has an effective Mach number $M_e = U_e/A$ and its corresponding effective Mach angle $\mu_e = \arcsin(1/M_e)$. This new reference frame XOY is specified by

$$\begin{bmatrix} X \\ Y \end{bmatrix} = \begin{bmatrix} \sin(\alpha - \beta) & -\cos(\alpha - \beta) \\ \cos(\alpha - \beta) & \sin(\alpha - \beta) \end{bmatrix} \begin{bmatrix} x' \\ y' \end{bmatrix} \tag{28}$$

In the reference frame the system of governing equations becomes

Mass:

$$M_e \frac{\partial p}{\partial X} + \frac{\partial U}{\partial X} + \frac{\partial V}{\partial Y} = 0$$

Momentum:

$$M_e \frac{\partial U}{\partial X} + \frac{\partial p}{\partial X} = 0$$

$$M_e \frac{\partial V}{\partial X} + \frac{\partial p}{\partial Y} = 0 \tag{29}$$

Energy:

$$\frac{\partial s}{\partial X} = 0$$

$$\text{for } X \sin(\alpha - \beta) + Y \cos(\alpha - \beta) > 0$$

The components of perturbed velocity U and V in the XOY reference frame are related to the components u^* and v^* in the original shock - affixed coordinate system by:

$$\begin{bmatrix} u^* \\ v^* \end{bmatrix} = \begin{bmatrix} \sin(\alpha - \beta) & \cos(\alpha - \beta) \\ -\cos(\alpha - \beta) & \sin(\alpha - \beta) \end{bmatrix} \begin{bmatrix} U \\ V \end{bmatrix} \tag{30}$$

In the coordinate frame XOY and restricting our interest to the entropy mode as the only upstream disturbance, the boundary conditions at the shock can be written as

$$
\begin{bmatrix} s_+ \\ p_+ \\ U_+ \\ V_+ \end{bmatrix} = \begin{bmatrix} \Lambda_{11} \\ \Lambda_{21} \\ \Lambda_{31} \sin(\alpha - \beta) \\ \Lambda_{31} \cos(\alpha - \beta) \end{bmatrix} s_-
$$

$$
+ \begin{bmatrix} \pi_{11} (M \cos\beta - C_s/A) \\ \pi_{21} (M \cos\beta - C_s/A) \\ \pi_{31} (M \cos\beta - C_s/A) \sin(\alpha - \beta) - \pi_{41} \cos(\alpha - \beta) \\ \pi_{31} (M \cos\beta - C_s/A) \cos(\alpha - \beta) + \pi_{41} \sin(\alpha - \beta) \end{bmatrix} \sin(\alpha - \beta) \Psi_y \tag{31}
$$

at $\quad X \sin(\alpha - \beta) + Y \cos(\alpha - \beta) = 0$

From the Y–component of the momentum equation,

$$
V = \phi_Y
$$

$$
p = -M_e \phi_X \tag{32}
$$

After the elimination of U, V, and p, a governing equation for the potential ϕ results:

$$
(M_e^2 - 1) \phi_{XX} - \phi_{YY} = 0 \tag{33}
$$

which is hyperbolic or elliptic depending on whether $M_e > 1$ or $M_e < 1$. Physically, this means that when $M_e > 1$ the sound field generated at a fixed point is affected only by a localized distortion of the shock; but in the case $M_e < 1$ it is affected by the whole shock configuration, and we must expect the subsonic case to involve an integral equation. Analogous to the classical wavy wall problem, the resulting pressure waves propagate downstream along a characteristic with constant amplitude for the supersonic regime ($M_e > 1$); but in the subsonic case ($M_e < 1$) the pressure disturbance amplitude diminishes with distance from the shock, part of the disturbance energy being fed back into the shock.

2.1.1 The Supersonic Case, $M_e > 1$

For $M_e > 1$, the governing equation for ϕ in the XOY reference frame reduces to a simple wave equation, which is also obeyed by the flow parameters p and V. By eliminating U between the equations of continuity and momentum, one obtains a pair of wave equations in terms of V and $q = -(\cos \mu_e)\, p$:

$$\begin{bmatrix} \frac{\partial}{\partial X} & -\tan \mu_e \frac{\partial}{\partial Y} \\ \tan \mu_e \frac{\partial}{\partial Y} & -\frac{\partial}{\partial X} \end{bmatrix} \begin{bmatrix} q \\ V \end{bmatrix} = 0 \qquad (34)$$

for $\quad X \sin(\alpha - \beta) + Y \cos(\alpha - \beta) > 0$

and subject to the boundary condition at the shock:

$$\begin{bmatrix} q \\ V \end{bmatrix} = \begin{bmatrix} -\Lambda_{21} \cos \mu_e \\ \Lambda_{31} \cos(\alpha - \beta) \end{bmatrix} s_- + \begin{bmatrix} -\pi_{21} \left(M \cos \beta - C_s/A\right) \cos \mu_e \\ \pi_{31} \left(M \cos \beta - C_s/A\right) \cos(\alpha - \beta) + \pi_{41} \sin(\alpha - \beta) \end{bmatrix}$$

$$\times \quad \sin(\alpha - \beta)\, \Psi_y \qquad (35)$$

at $\quad X \sin(\alpha - \beta) + Y \cos(\alpha - \beta) = 0.$

The field of characteristics associated with these wave equations are given by $X - Y \cot \mu_e$ = constant and $X + Y \cot \mu_e$ = constant, since the Riemann invariants along these lines are $(q - V)$ and $(q + V)$. The solutions to the wave equations (34), therefore, are:

$$q = F_1 (X - Y \cot \mu_e) + F_2 (X + Y \cot \mu_e)$$

$$V = - F_1 (X - Y \cot \mu_e) + F_2 (X + Y \cot \mu_e) \qquad (36)$$

Only one of the two functions F_1 or F_2 represents sound waves propagating downstream. In the case of a normal shock ($\beta = \pi/2$) it is F_1, and in the case of an oblique shock the choice depends on the magnitude of C_s, the trace velocity of the entropy wave along the shock. Referring to Figure 2, when C_s is on the lower segment (below the first intersection of the shock and the sonic circle), F_2 is to be taken; when C_s is on the upper segment ($C_s \geq C_{s_1}$) then F_1 is to be taken. Whenever C_s falls between C_{s_1} and C_{s_2}, then $M_e < 1$, a case considered later.

The boundary condition at the shock, after eliminating the shock inclination Ψ_y gives another relationship between q and V together with the given disturbance s_-, allowing the function F_1 or F_2 to be determined:

(a) When $C_s \leq C_{s_2}$:

$$q = F_2 = -T_2(\delta) \cos \mu_e \; s_- \tag{37}$$

(b) When $C_s \geq C_{s_1}$:

$$q = F_1 = -T_1(\delta) \cos \mu_e \; s_- \tag{38}$$

where

$$T_2(\delta) = \frac{\Omega_2 \cos(\alpha - \beta) - \Lambda_{21} G \sin(\alpha - \beta)}{\tilde{A} \cos(\alpha - \beta) - G \sin(\alpha - \beta) + \cos \mu_e} \tag{39}$$

$$T_1(\delta) = \frac{\Omega_1 \cos(\alpha - \beta) - \Lambda_{21} G \sin(\alpha - \beta)}{\tilde{A} \cos(\alpha - \beta) - G \sin(\alpha - \beta) - \cos \mu_e} \tag{40}$$

and

$$\tilde{A} = \pi_{31}/\pi_{21} , \quad B = -\pi_{41}/\pi_{21} ,$$

$$\Omega_1 = \Lambda_{21} \tilde{A} - \Lambda_{31} , \quad \Omega_2 = \Lambda_{21} B ,$$

$$G = \frac{B}{M \cos \beta - (C_s/A)}$$

By determining q from the appropriate equations above, and substituting this value of q back into the original equation relating the boundary conditions at the shock (35), one can find the local shock inclination Ψ_y . At this point, all the required quantities are available for the calculation of the downstream flow perturbations through Equations (31). As vorticity is preserved along streamlines, the vorticity-generating function $f(Y)$, which is defined by:

$$\omega = -A \frac{df}{dY} \tag{41}$$

can also be calculated.

2.1.2 The Subsonic Case, $M_e < 1$

For $M_e < 1$, the potential equation for ϕ reduces to the Laplace equation if the Prandtl-Glauert transformation is applied. Introduce a complex variable defined by

$$\xi = X + i\,\overline{Y}$$

where

$$\overline{Y} = \sqrt{1 - M_e^2}\;Y \tag{42}$$

and any analytic function $\phi(\xi)$ or $W(\xi) = d\phi/d\xi$ will be a solution. $W(\xi)$ is related to the physical parameters through

$$W(\xi) = V(X, \overline{Y}) + i\,\frac{\sqrt{1 - M_e^2}}{M_e}\;p(X, \overline{Y}) \tag{43}$$

Again eliminating V between the continuity and momentum equations, one obtains a pair of Cauchy-Riemann equations:

$$\frac{\partial V}{\partial X} = \frac{\partial}{\partial \overline{Y}}\left(\frac{\sqrt{1 - M_e^2}}{M_e}\;p\right)$$

$$\frac{\partial V}{\partial \overline{Y}} = \frac{\partial}{\partial X}\left(\frac{\sqrt{1 - M_e^2}}{M_e}\;p\right) \tag{44}$$

for the region

$$X \sin(\alpha - \beta) + \frac{\overline{Y}}{\sqrt{1 - M_e^2}}\cos(\alpha - \beta) > 0$$

The boundary conditions to be satisfied by $W(\xi)$ are (a) to remain bounded at infinity and (b) to satisfy

$$\left[\tilde{A}\cos(\alpha - \beta) - G\sin(\alpha - \beta)\right]p - V$$
$$= \left[\Omega_1 \cos(\alpha - \beta) - \Lambda_{21}\,G\sin(\alpha - \beta)\right]s_- \tag{45}$$

at the shock, i.e., at $X \sin(\alpha - \beta) + \dfrac{\overline{Y}}{\sqrt{1 - M_e^2}}\cos(\alpha - \beta) = 0$

It is more convenient to work with a set of coordinate axes rotated into the shock position, through the transformation

$$\begin{bmatrix} X^* \\ Y^* \end{bmatrix} = \begin{bmatrix} \cos\lambda & \sin\lambda \\ -\sin\lambda & \cos\lambda \end{bmatrix} \begin{bmatrix} X \\ Y \end{bmatrix} \tag{46}$$

where λ is defined by

$$\cot\lambda = \sqrt{1 - M_e^2}\ \tan(\alpha - \beta) \tag{47}$$

and the boundary condition at the shock is now specified along $X^* = 0$.

A solution for $W(\xi^*)$ which satisfies the boundary condition at infinity is

$$W(\xi^*) = \frac{i}{2\pi}\int_{-\infty}^{\infty} \frac{g(\eta)}{\xi^* - \xi_1^*}\, d\eta \tag{48}$$

where

$$\xi^* = X^* + i\,Y^*$$

with $g(\eta)$ bounded and continuous in the half-plane $X^* \geq 0$.

Chang compares the conventional complex potential with $W(\xi) = d\phi/d\xi$ and notes that the function $g(\eta)/2\pi$ can be interpreted as the strength of a source located on the shock plane at a distance η from the origin, or can be interpreted as a dipole moment with respect to the sound field (p and V) generated downstream.

The real and imaginary parts of $W(\xi^*)$ are:

$$\frac{\sqrt{1 - M_e^2}}{M_e}\, p = \frac{1}{2\pi}\int_{-\infty}^{\infty} \frac{X^*}{X^{*2} + (Y^* - \eta)^2}\, g(\eta)\, d\eta \tag{49a}$$

$$V = \frac{1}{2\pi}\int_{-\infty}^{\infty} \frac{(Y^* - \eta)}{X^{*2} + (Y^* - \eta)^2}\, g(\eta)\, d\eta \tag{49b}$$

which one may substitute back into the shock boundary condition, Equation (45), and obtain the following integral equation to be used in determining $g(Y^*)$:

$$\frac{M_e}{\sqrt{1 - M_e^2}} \left\{ \tilde{A} \cos\ (\alpha - \beta) \ - \ G \sin\ (\alpha - \beta) \right\} \frac{g\ (Y^*)}{2}$$

$$+ \ P \left\{ \frac{1}{2\pi} \int_{-\infty}^{\infty} \frac{g\ (\eta)}{\eta - Y^*}\ d\eta \right\} = \left\{ \Omega_1 \cos\ (\alpha - \beta) - \Lambda_{21}\ \ G \sin\ (\alpha - \beta) \right\} s_- \qquad (50)$$

To obtain (50) Chang has used the fact that

$$\lim_{X^* \to 0} \ \frac{1}{2\pi} \int_{-\infty}^{\infty} \frac{X^*\ g\ (\eta)}{X^{*2} + (Y^* - \eta)^2}\ d\eta \ = \ \frac{g\ (Y^*)}{2} \qquad (51)$$

and the notation " P " for Cauchy's principal value for the improper integral.

At this point, for any given set of conditions, everthing in Equation (50) is known numerically except $g\ (Y^*)$, which is to be found, and the principal value of the integral. Compressing Equation (50) for convenience into the form

$$D\ \ g\ (Y^*) \ + \ P \left\{ \frac{1}{2\pi} \int_{-\infty}^{\infty} \frac{g\ (\eta)}{\eta - Y^*}\ d\eta \right\} \ = \ C \qquad (52)$$

where

$$D \ = \ \frac{1}{2} \ \frac{M_e}{\sqrt{1 - M_e^2}} \left\{ \tilde{A} \ \cos\ (\alpha - \beta) \ - \ G \sin\ (\alpha - \beta) \right\}$$

and

$$C \ = \left\{ \Omega_1 \cos\ (\alpha - \beta) - \Lambda_{21}\ \ G \sin\ (\alpha - \beta) \right\} s_-$$

let us find the principal value of the integral. Applying Picard's iteration method, setting $g\ (\eta) = 0$ in (52) requires the trivial result that $g\ (Y^*) = 0$. Setting $g\ (\eta)$ equal to a constant, K, gives an integral of the form

$$\frac{K}{2\pi} \int_{-\infty}^{\infty} \frac{d\eta}{\eta - Y^*}$$

From residue theory, and based on the boundary condition at infinity giving a closed contour, the value of the integral is $2\pi i$, giving:

$$\frac{K}{2\pi}\int_{-\infty}^{\infty}\frac{d\eta}{\eta - Y^*} = \frac{K}{2\pi}(2\pi i) = iK \tag{53}$$

Inserting this into Equation (52), since D and C are real numbers, K is complex. Equating real and imaginary parts gives two equations to solve for K_i and K_r. After retaining only the real part, the solution for $g(Y^*)$ is:

$$g(Y^*) = \frac{DC}{1+D^2} \tag{54}$$

Next, one may solve for the pressure perturbation immediately downstream of the shock (at $X^* = 0$) from Equation (49a). Utilizing the limit value of the integral as $X^* \rightarrow 0$ as given by (51), Equation (49a) becomes:

$$p)_{x^*=0} = \frac{M_e}{\sqrt{1-M_e^2}}\,\frac{g(Y^*)}{2} \tag{55}$$

Having the pressure perturbation at the shock, then the shock displacement Ψ_y can be found from

$$p = \Lambda_{21}\, s_- + \pi_{21}\left(M\cos\beta - \frac{C_s}{A}\right)\sin(\alpha-\beta)\,\Psi_y \tag{56}$$

Having Ψ_y, all the remaining downstream flow perturbations and the vorticity generating function can be calculated also.

2.1.3 The Case $M_e = 1$

At $M_e = 1$, the governing equation for the potential ϕ reduces to the parabolic form

$$\phi_{YY} = 0 \tag{57}$$

As $M_e \rightarrow 1$, the Mach angle $\mu_e \rightarrow \pi/2$, and the two characteristics coalesce into a single line, X = constant. The drift velocity in a sound wave being normal to the wave front, then

$$\phi_Y = 0$$

In this case one can determine the pressure field p directly, from

$$p = -F(X) = \frac{\Omega_1 \cos(\alpha - \beta) - \Lambda_{21} G \sin(\alpha - \beta)}{\tilde{A} \cos(\alpha - \beta) - G \sin(\alpha - \beta)} s_- \tag{58}$$

2.1.4 Special Case of Parallel Entropy and Shock Waves

One may note from Equation (24) that the foregoing derivation fails in the case of parallel shock and oncoming entropy wave (that is, for $(\delta - \epsilon) = \pi/2$), and so this case is handled separately. The oncoming entropy wave can be expressed in the form

$$s = s \left\{ M_1 \frac{A_1}{A} (\cos \delta) \tau - x^* \right\} \tag{59}$$

For an observer moving along the shock (along the y^* axis, there is no transverse disturbance. The entire shock is struck by the entropy wave instantaneously, and the shock remains plane and simply oscillates along the x^* axis. This is in contrast to the case $(\delta - \epsilon) \neq \pi/2$, where a ripple moves along the shock at the trace velocity C_s. Hence $\Psi_y{}^* = 0$ in Equation (18), and it follows that $v^* = 0$, so that the flow field downstream of the shock is one-dimensional. Chang here makes a substitution of variables:

$$x' = x^* - N\tau$$

$$\tau' = \tau$$

and rewrites the conservation equations for mass, momentum and energy accordingly, from which it can be seen that $(-p)$ and u^* form a pair of simple wave equations. Since no disturbance can propagate upstream of the shock, only the right-running wave is taken:

$$p_+ = u_+ = F(\tau' - x') \tag{60}$$

When transformed back into the original x^*, τ coordinates, the downstream flow field is completely determined by the two functions $s_+ (N\tau - x^*)$ and $F\left\{(1 + N)\tau - x^*\right\}$. From the boundary conditions at the shock (at $x^* = 0$) these functions are

$$\frac{F}{s_-} = -\frac{p_+}{s_-} = \frac{u_+}{s_-} = \frac{\Lambda_{31} \pi_{21} - \Lambda_{21} \pi_{31}}{\pi_{21} - \pi_{31}} \tag{61}$$

and

$$\frac{s_+}{s_-} = \Lambda_{11} + \frac{\pi_{11}\,(\Lambda_{21} - \Lambda_{31})}{\pi_{21} - \pi_{31}} \tag{62}$$

If the shock displacement is also desired, it can be obtained from

$$x^* = \Psi = \frac{\Lambda_{31} - \Lambda_{21}}{\pi_{21} - \pi_{31}} \int s_-(\tau)\, d\tau \tag{63}$$

One may note that restriction to parallel waves, with the resulting one-dimensional downstream flow field, gives an immensely simplified problem, involving only six of the fourteen transfer coefficients, Equations (14).

2.2 Numerical Results

The computer program described in the appendix, based on the above analysis, has been used to obtain values defining the perturbed downstream flow field resulting from the interaction of a single entropy discontinuity with a shock wave. While a number of intermediate quantities (such as the transfer coefficients, vorticity generating function, and local shock deflection) are available in the printout, only those quantities useful for engineering estimates or for understanding of the results are presented here. They include the effective Mach number; the downstream fluctuations of entropy, pressure, and vorticity; and an alternate presentation of the pressure fluctuations referenced to free-stream dynamic pressure.

The results presented are for two cases of practical interest: (1) Normal shocks, and (2) Oblique shocks arising from wedge flow. While it is possible to calculate a downstream perturbed flow field for free combinations of ϵ (the shock wave angle) and β (the angle between the shock wave and the downstream mean flow velocity vector; see Figure 1), at each upstream Mach number there is only one value of flow deflection angle or wedge half-angle ($\epsilon - \beta$) which will produce the shock angle β. For each wedge half-angle ($\epsilon - \beta$), the lower limit of free stream Mach number has been taken as the value at which the mean flow behind the shock remains supersonic, Reference 12, and results are given from this lower limit to Mach 10. The wedge half-angles ($\epsilon - \beta$) covered in the numerical cases reported here range from 4 degrees (corresponding to a flat plate with boundary layer) to 30 degrees. This range should cover most cases of interest for external flows over high-speed aircraft and separation shocks produced by conical flares on launch vehicles.

The value of the entropy discontinuity orientation, δ, has been varied from one degree (nearly normal to the free-stream flow direction, see Figure 2) to 89 degrees (nearly parallel to the free-stream flow. For parallel shock and entropy waves, $(\delta - \epsilon) = \pi/2$, the general method for oblique shocks fails and these results are shown separately. For normal shocks, this is an important case, as it corresponds to temperature discontinuities normal to the flow. Because of the bulk of the data involved, results are shown only for the extremes of the δ range and for that region of δ's giving maximum flow perturbations.

Some of the results have been plotted as functions of δ rather than M_1; these graphs, in conjunction with the graphs of effective Mach number M_e, show how the flow perturbation values reach anomalous maxima at values of δ corresponding to $M_e = 1$. This trend agrees with the single published result of Chang in Reference 10. Referring to Figure 2, the occurrence of $M_e = 1$ corresponds to values of the trace velocity, C_s, of the entropy disturbance front along the shock such that the vector C_s just intersects the sonic circle. For C_s between the two possible intersection points, $M_e < 1$, and for any other values of C_s, $M_e > 1$. As discussed above, when $M_e < 1$ the generated pressure disturbance propagates with constant amplitude, but when $M_e < 1$ the amplitude decays with distance from the shock. For any given combination of ϵ and β, there is a bounded region of the Mach number and entropy wave inclination plane where the effective Mach number is subsonic, and energy can be fed back into the shock. As an example, Figure 9 shows this boundary in terms of critical angle δ^* for $\epsilon = 50$ degrees, $\beta = 30$ degrees, corresponding to a wedge angle of 20 degrees. The two branches of the boundary, δ_1^* and δ_2^*, arise from values of C_s corresponding to the two intersections of the shock and the sonic circle, Figure 2. For more accuracy in the perturbation values at $M_e = 1$, it would be desirable either to use more closely spaced input values for near the region of the peak, or to set $M_e = 1$ and compute the value of the peak directly. In the results shown here, the peak was sometimes obtained by extrapolating the adjacent curves to intersect at the value of M_1 or δ known to correspond to $M_e = 1$; however, the numbers are sufficiently accurate for engineering predictions.

With δ below used to indicate perturbation values (e.g., $\delta p = p - p_m$, where p is the mean value), and with subscripts 1 and (-) used to indicate the region upstream of the shock, the perturbed flow quantities shown in the figures are defined as follows:

For the entropy fluctuations,

$$\left(\frac{s_+}{s_-}\right) = \frac{\left(\delta s/C_p\right)_-}{\left(\delta s/C_p\right)_+} = \frac{\left(\delta\ T/T_m\right)_-}{\left(\delta\ T/T_m\right)_+} \tag{64}$$

For the pressure fluctuations,

$$\left(\frac{p_+}{s_-}\right) = \frac{\left(\delta p/\gamma\, p_m\right)_+}{\left(\delta\ T/T_m\right)_-} \tag{65}$$

In this form, the fluctuating pressure magnitudes are referenced to the local mean pressure, but the upstream mean flow conditions are sometimes more conveniently known. The dynamic pressure is given by

$$q = \frac{1}{2}\ \rho V^2 = \frac{\gamma}{2}\ p\, M^2$$

Hence, the downstream pressure fluctuation magnitude, referenced to twice the upstream dynamic pressure is:

$$\left(\frac{p_+}{s_-}\right) \cdot \frac{\chi}{M_1^2} = \left(\frac{\delta p}{\gamma\, p_1 M_1^2}\right) \Big/ \left(\frac{\delta T}{T}\right)_1 = \left(\frac{\delta p}{2\, q_1}\right) \Big/ \left(\frac{\delta T}{T}\right)_1 \tag{66}$$

where χ is the shock strength (or static pressure ratio) and q_1 is the upstream dynamic pressure.

The vorticity generation is shown here in terms of the magnitude of the vector sum of the two velocity perturbation components:

$$\frac{VORT}{s_-} = \frac{\sqrt{u_1^2 + v_1^2}}{s_-} \tag{67}$$

where

$$u_1 = \frac{\delta u_1}{A} \quad \text{and} \quad v_1 = \frac{\delta v_1}{A} ,$$

measured along and normal to the x_1 axis (free-stream direction) respectively, and A is the local sonic velocity behind the shock.

It should be noted that a single value of specific heat ratios,

$$\gamma = \frac{C_p}{C_v} ,$$

has been used in the calculations, $\gamma = 1.40$. For strong shocks (i.e., large upstream normal Mach number components), molecular dissociation begins to absorb part of the total energy of the flow, and the value of γ decreases slightly, affecting all the ratios of flow properties across the shock. However, this effect is not significant in the present results, since (1) in the most extreme case for the oblique shock results (Mach 10 and a flow deflection angle of 30 degrees) the error in the present coefficient across the shock, for example, due to use of $\gamma = 1.40$ would only be 3 percent; and (2) the flow purturbation results, shown up to Mach 20 for the normal shock case, are insensitive to Mach number for values above Mach 8.

Reviewing the trends of the results, for the special case of parallel shock and entropy wave inclination, Figure 3 shows the relative magnitude of the downstream entropy wave decreasing steadily from unity for the lowest possible shock strength to values below 0.03 for upstream normal components of Mach number $N_1 > 10$. The downstream disturbances of pressure and velocity increase from zero at the lowest possible shock strength to an asymptotic value of about -0.4 at high Mach numbers. The generated pressure and velocity disturbances are of opposite sign to the oncoming temperature discontinuity; that is, a positive step increase in temperature will generate a rarefaction; and a negative change in temperature, a compression. The entire entropy wave strikes the shock wave simultaneously, giving an infinite effective Mach number M_e.

The reader should not attempt to compare the present numerical results for pressure and velocity perturbation with those of Morkovin, Reference 1, as his results are being corrected in a forthcoming corrigendum, in accordance with Reference 13.

Continuing to the normal shock cases (taken from the computer results) Figure 4 shows the variation of effective Mach number M_e with entropy wave inclination angle δ, for upstream Mach numbers M_1 from 1.1 to 20. As δ approaches zero, M_e approaches infinity as described above. The effective Mach number decreases through the critical $M_e = 1$ within the range $60^\circ < \delta < 70^\circ$ for all these upstream Mach numbers. Judging from Chang's single numerical example, we should expect discontinuous maxima of the flow perturbation quantities to occur near $\delta = 70^\circ$, and this is borne out in Figures 5 through 8. The values shown for $\delta = 0$ are taken from the parallel wave solution, above. For the pressure perturbation, the results lie too close to the curve for $5^\circ \leq \delta \leq 30^\circ$ to be shown separately. All the results become insensitive to Mach number for $M_1 > 8$.

In the oblique shock cases, for any given shock strength and shock angle β it is possible to have two values of entropy wave inclination δ which will result in a critical effective Mach number $M_e = 1$, corresponding to the two branches bounding the subsonic region, Figure 9. Depending on the wedge half-angle and upstream Mach number, there may be either one or two values of δ at which $M_e = 1$. This is apparent in Figures 10 through 12, which show the variation of M_e with δ, with upstream Mach number M_1 as a parameter, for three wedge half-angles $(\epsilon - \beta) = 4^\circ$, 12°, 30°. As the upstream Mach number increases, the critical values of δ (corresponding to $M_e = 1$) shift to lower values.

The effect of the shock interaction on the strength of the temperature discontinuity is given in Figures 13 through 21 in terms of the ratio (s_+/s_-). Since $s_+ = (\delta T)/T$ and $s_- = (\delta T)_1/T_1$, where subscript 1 refers to the upstream conditions, then the meaning of the ratio (s_+/s_-) in terms of temperature discontinuity magnitudes and local mean static temperatures can also be expressed as:

$$\frac{s_+}{s_-} = \frac{(\delta T)}{(\delta T)_1} \cdot \frac{T_1}{T} \tag{68}$$

where T_1/T is the inverse static temperature ratio across the shock and always has a value less than unity.

Figures 13 through 18 show s_+/s_- plotted versus upstream Mach number up to $M_1 = 4$, with a single value of δ for each figure. The peaks in the curves correspond to values of M_1 at which the effective Mach number $M_e = 1$; and the minima (as in Figure 16), to minima in the corresponding curves of effective Mach number. For those regions of δ where the effective Mach number is supersonic for all values of wedge half-angle, the effect of the interaction on the entropy discontinuity magnitude increases steadily with increasing wedge half-angle (that is, with increasing shock strength) for any given upstream Mach number. When both subsonic and supersonic effective Mach numbers occur, as in Figure 14, this simple trend no longer occurs.

In Figures 19 through 21, the results for s_+/s_- are plotted as a function of δ, one figure for each upstream Mach number, for $M_1 = 3, 6, 10$. Here the occurrence of peak values at critical values of δ is more readily apparent. As the value of the wedge half-angle increases, the magnitude of the peak corresponding to $M_e = 1$ increases and occurs at higher values of δ. For those values of $(\epsilon - \beta)$ where the curve of M_e crosses unity twice, there are two amplitude peaks; again, the amplitude minima correspond to minima in the effective Mach number curves.

The amplitude of the pressure pulse generated by the interaction is given in Figures 22 through 31, in a sequence paralleling that for the presentation of s_+/s_-. The results are shown in terms of p_+/s_-, which is defined above in Equation (79). The general trends are the same as discussed above for the entropy disturbance magnitudes, with sharp maxima occurring where $M_e = 1$. However, in the case of the pressure disturbances the minima (corresponding to minima in the curves of M_e) also have discontinuous slopes. The range of p_+/s_- encountered extends from -0.8 to +3, with the largest value of the maximum occurring near $M_1 = 3$, $\delta = 80$ degrees, $(\epsilon - \beta) = 30$ degrees.

These pressure magnitude values are also shown, in Figures 36 through 39, in a form more convenient for calculations, since the pressure perturbation values are referenced entirely to upstream conditions, in accordance with Equation (66). These results are shown only for the extremes of the range of δ and for those values of δ corresponding to maximum pressure disturbance. It should be emphasized that for $M_e < 1$ these pressure pulse magnitudes exist only immediately behind the shock and decay thereafter.

The vorticity generation parameter, as defined above in Equation (67), is shown in Figures 32 through 35. It shows maxima with discontinuous slopes, similar to the other interaction results, with the magnitude of the peak increasing with upstream Mach number M_1 and with wedge half-angle $(\epsilon - \beta)$. The largest values of the vorticity parameter (over the range $1.1 \leq M_1 \leq 10$, $1^\circ \leq \delta \leq 89^\circ$, and $4^\circ \leq (\epsilon - \beta) \leq 30^\circ$) occurs in the vicinity of $M_1 = 3$, $\delta = 80^\circ$, $(\epsilon - \beta) = 30^\circ$, as did the largest peaks in the pressure perturbation magnitude.

It would be useful next to estimate the magnitudes of pressure perturbations which might be experienced in practice. Two cases will be considered: (a) the separation shock ahead of a conical flare on a cylindrical body, as on a launch vehicle, at a low supersonic Mach number, and (b) oblique shocks on a supersonic aircraft at cruise Mach number and altitude. On the basis of the scant experimental results available for temperature fluctuation magnitudes (discussed further in Section 2.3), a value of 2 percent of the <u>total</u> temperature is taken here.

For a separation shock standing ahead of a conical flare on a cylindrical body, the shock angle β varies with free-stream Mach number only, and is nearly independent of flare angle, Reference 9. Therefore, as a first estimate, the wedge flow results given here can be used to predict the pressure perturbation, simply by taking the correct wedge half-angle to produce the equivalent shock angle at any given Mach number, Figure 40. For Mach numbers from 1 to 4, the required wedge half-angle varies from 0 to 14.6 degrees. Taking a flight condition of $M_1 = 1.2$, $h = 25{,}000$ ft. (corresponding to a dynamic pressure of $q_1 = 800$ lb /ft^2), and with the appropriate wedge half-angle of $(\epsilon - \beta) = 4^\circ$, values of

$$\left(\frac{\delta p}{2q_1}\right) \Big/ \left(\frac{\delta T}{T}\right)_1$$

as large as (- 2) can occur.

When the temperature fluctuation magnitude is translated into a static temperature reference at this Mach number, $(\delta T/T)_1 = 0.0258$. Hence the pressure pulse would be $\delta p = 82.5$ lb /ft^2, or in terms of sound pressure level, referenced to 0.0002 dynes/cm^2, SPL = 166 dB.

For a supersonic aircraft cruising at Mach 3, $h = 70{,}000$ ft., and again taking extreme values of $(\epsilon - \beta) = 30^\circ$, an upstream temperature discontinuity of 0.01 referenced to the total temperature, and the value of δ which gives the largest pressure perturbation, a value of

$$\left(\frac{\delta p}{2q_1}\right) \Big/ \left(\frac{\delta T}{T}\right)_1$$

as high as (+2) can occur. The resulting pressure pulse has a magnitude of 144 dB, substantially lower than that for the launch vehicle case, primarily, because the free stream dynamic pressure is lower by an order of magnitude.

It should be emphasized that these numbers represent extreme values reached by the selection of what are probably extreme values for $(\delta T/T)_1$ and δ, and that most levels encountered in practice will be lower. Further, these are instantaneous pressure pulses and not a continuous level.

3.0 TYPICAL ENTROPY FLUCTUATION MAGNITUDES

In Section 2.2, an entropy fluctuation magnitude (step amplitude) of 2 percent of the free stream (absolute) total temperature was used to make a first estimate of the downstream pressure fluctuation to be expected from entropy-shock interactions. A number of researchers have measured values of temperature or density fluctuation intensity in jets, wakes, and boundary layers (References 14 through 20); maximum values from some of these results are shown in Table I. Caution must be applied in interpreting these values, as not the same reference conditions were given for all the data. In general, the jet and boundary layer data are root mean square temperature fluctuations referenced to jet or free-stream total temperature, while the wake data are mostly root mean square density fluctuations referenced to local mean density in the wake, all taken by hot-wire anemometry. The data of Clay, et al., are amplitude values estimated from Schlieren photographs.

The data fall into two magnitude categories: (a) Maximum fluctuation intensities between 15 and 40 percent for jets and wakes, and (b) maximum fluctuation intensities between 2 and 5 percent for boundary layers. There is no discernible trend with Mach number, but aside from Kistler's boundary layer data there are too few Mach number points to provide any conclusion about trends. It is difficult to imagine a trend with Mach number, however, in which the temperature fluctuation would not asymptotically approach some fraction of a typical driving temperature difference in the flow, such as the difference between recovery temperature and wall temperature in a boundary layer or the temperature defect in a wake.

Entropy fluctuations in wakes persist for long distances downstream of the body, still showing significant magnitudes at 1,000 diameters. For launch vehicles, the wakes of upstream protuberances may be the most important source of strong entropy fluctuations to interact with downstream standing shocks.

Attempts to obtain large but pure entropy fluctuations (without vorticity fluctuations present) for experimental purposes were reported by Morkovin (Reference 2) and by Hamernik (Reference 21). Morkovin used electrically heated rods in the Johns Hopkins Supersonic Tunnel and produced entropy fluctuations dominant over the vorticity and sound signals, but only of about 0.2 percent intensity when referenced to the total temperature. Hamernik used an exploding wire to produce a temperature spot to interact with a reflected normal shock in a shock tunnel and obtained a peak density amplitude $\Delta\rho/\rho_{ref} \cong$ 4 percent, where the reference density was the local condition after passage of the shock front, for a shock strength of 1.8, corresponding to a shock Mach number of 1.3.

Typical temperature fluctuation values for the background in wind tunnels are less than half a percent of the total temperature. For example, Reference 16 cites a measured value of 0.04 percent in the Johns Hopkins 7" x 11" supersonic (Mach 1.75) tunnel. In the first few feet of the atmosphere, temperature fluctuations as large as 3 to 4 percent sometimes occur near highly heated surfaces such as airport runways.

TABLE I

ENTROPY FLUCTUATION DATA (EXTREME VALUES)

Flow	Mach Number Range	Reference	Entropy Data (Extreme Values)
Free Jet, Round Heated	Subsonic	14	18 percent (r.m.s. fluct. temp., ref. to centerline static temp.)
Boundary Layer, Flat Plate	$M_\infty = 1.75$	15	2.5 percent (fluct. amplitude, ref. to tunnel total temperature)
Boundary Layer, Flat Plate	$M_\infty = 1.72$ 3.56 4.67	17 •	4.8 percent 3.6 percent 2.1 percent (r.m.s. fluct. temp. ref. to tunnel total temperature)
Wake of Axisymmetric Rod	$M_\infty = 1.75$	16	2-3 percent (r.m.s. temp. fluct. ref. to tunnel total temperature)
Wake of Axisymmetric Rod	$M_\infty = 3.0$	18	7 percent (r.m.s. fluct. temp. ref. to local center-line total temperature)
Wake of Sphere	$M_\infty \cong 8$	19	15 percent (density fluct. amplitude ref. to local mean density)
Wake of Sphere	$M_\infty = 8.5$	20	30 percent (r.m.s. density fluct. ref. to local mean density)
Wake of 12-degree Cone	$M_\infty = 22.8$	20	40 percent (r.m.s. density fluct. ref. to local mean density)

4.0 RANDOM FIELD OF ENTROPY DISTURBANCES INTERACTING WITH A SHOCK WAVE

According to the Fourier integral theorem, a random field can be represented as a superposition or spectrum of elementary waves. A single spectrum wave can be interpreted physically as a plane sinusoidal wave of temperature or density variation, being convected downstream at the local mean flow velocity. Before synthesizing the random field, one must consider a single harmonic component. Again following Chang, Reference 10, the description of the interaction of a single harmonic entropy wave with a shock wave is given below.

4.1 The Harmonic Components

The plane upstream entropy wave can be characterized by its amplitude R_s, its wave number k_1, and its inclination δ with respect to the flow velocity U_1:

$$s_1 = R_s \cos k_1 \left\{ \ell_1 M_1 \frac{A_1}{A} \tau - (\ell_1 x_1 + m_1 y_1) \right\} \tag{69}$$

where (see Figure 41)

$$\ell_1 = \cos\delta, \quad m_1 = \sin\delta$$

Initially, let us restrict attention to the special case of a normal shock. Here, some simplification occurs, since the three sets of coordinate axes $x_1 o y_1$, $x o y$, and $x^* o y^*$ coincide, and the unperturbed shock plane can be taken along the y axis. For the "supersonic" case $M_e > 1$ the function F_1 becomes

$$F_1 = -\cos\mu_e \, a_p \cos \left\{ k_1 m_1 \frac{\sin\mu_e}{\cos(a + \mu_e)} (X - Y \cot\mu_e) \right\} \tag{70}$$

where

$$a_p = \frac{\left(\frac{C_s}{A}\right) \Omega \sin a - \Omega_2 \cos a}{\left(\frac{C_s}{A}\right) (\tilde{A} \sin a - \cos\mu_e) - B \cos a} \cdot R_s$$

$$a = \arctan \left\{ -\cot \left(\delta \frac{U_1}{U} \right) \right\}$$

$$\mu_e = \arcsin \left\{ -\frac{\cos a}{M} \right\}$$

The local displacement of the shock is given by

$$\Psi = b_\psi \sin (k_1 m_1 y') \tag{71}$$

where

$$k_1 m_1 b_\psi = \frac{\left(\frac{\Lambda_{31}}{\pi_{21}}\right) \sin \alpha - \left(\frac{\Lambda_{21}}{\pi_{21}}\right) \cos \mu_e}{\left(\frac{C_s}{A}\right) (\tilde{A} \sin \alpha - \cos \mu_e) - B \cos \alpha} \cdot R_s$$

The vorticity - generating function f (Y) and the entropy are given by:

$$f(Y) = \left(a_U + \frac{a_p}{M_e}\right) \cos (k_1 m_1 Y/\cos \alpha) \tag{72}$$

and

$$s(Y) = a_s \cos (k_1 m_1 Y/\cos \alpha) \tag{73}$$

where

$$a_U = \left\{ \tilde{A} \left(\frac{C_s}{A}\right) \cos \alpha + B \sin \alpha \right\} \pi_{21} (k_1 m_1 b_\psi) - \Lambda_{31} R_s \cos \alpha$$

and

$$a_s = \Lambda_{11} R_s - \pi_{11} \left(\frac{C_s}{A}\right) (k_1 m_1 b_\psi)$$

For the "subsonic" case $M_e < 1$, the function $g(\eta)$ is given by

$$\frac{g(\eta)}{2\pi} = \frac{1}{\pi} \frac{\sqrt{1 - M_e^2}}{M_e} \left\{ a_p \cos \left(k_1 m_1 \frac{\eta}{\sqrt{1 - M^2}}\right) + b_p \sin \left(k_1 m_1 \frac{\eta}{\sqrt{1 - M^2}}\right) \right\} \tag{74}$$

where

$$a_p = \left\{ \tilde{A} \frac{C_s}{A} \sin a - B \cos a \right\} \times$$

$$\times \frac{\Omega_1 \frac{C_s}{A} \sin a - \Omega_2 \cos a}{\left\{ \tilde{A} \frac{C_s}{A} \sin a - B \cos a \right\}^2 + \frac{1 - M_e^2}{M_e^2} \left(\frac{C_s}{A} \right)^2} \cdot R_s$$

and

$$b_p = \frac{\Omega_2 \cos a - \Omega_1 \frac{C_s}{A} \sin a}{\left\{ \tilde{A} \frac{C_s}{A} \sin a - B \cos a \right\}^2 + \frac{1 - M_e^2}{M_e^2} \left(\frac{C_s}{A} \right)^2} \cdot \times$$

$$\times \frac{\sqrt{1 - M_e^2}}{M_e} \cdot \frac{C_s}{A} \cdot R_s$$

The local shock displacement is

$$\Psi = a_\psi \cos (k_1 m_1 y') + b_\psi \sin (k_1 m_1 y') \qquad (75)$$

where

$$k_1 m_1 a_\psi = \frac{1}{\pi_{21}} \frac{\Omega_2 \cos a - \Omega_1 \frac{C_s}{A} \sin a}{\left\{ \tilde{A} \frac{C_s}{A} \sin a - B \cos a \right\}^2 \div \frac{1 - M_e^2}{M_e^2} \left(\frac{C_s}{A} \right)} \cdot \frac{\sqrt{1 - M_e^2}}{M_e} \cdot R_s$$

and

$$k_1 m_1 b_\psi = \frac{1}{\pi_{21}} \frac{\Lambda_{21} \dfrac{C_s}{A} \dfrac{1-M_e^2}{M_e^2} + \Lambda_{31} \sin a \left\{ \tilde{A} \dfrac{C_s}{A} \sin a - B \cos a \right\}}{\left\{ \tilde{A} \dfrac{C_s}{A} \sin a - B \cos a \right\}^2 + \dfrac{1-M_e^2}{M_e^2} \left(\dfrac{C_s}{A} \right)^2} \cdot R_s$$

Finally, the vorticity and entropy generating functions are given, respectively, by

$$f(Y) = \left(a_U + \frac{a_p}{M_e} \right) \cos \left(k_1 m_1 \frac{Y}{\cos a} \right) - \left(b_U + \frac{b_p}{M_e} \right) \sin \left(k_1 m_1 \frac{Y}{\cos a} \right) \tag{76}$$

and

$$s(Y) = a_s \cos \left(k_1 m_1 \frac{Y}{\cos a} \right) - b_s \sin \left(k_1 m_1 \frac{Y}{\cos a} \right)$$

where

$$a_s = \Lambda_{11} R_s - \pi_{11} \left(\frac{C_s}{A} \right) (k_1 m_1 b_\psi)$$

$$b_s = \pi_{11} \left(\frac{C_s}{A} \right) (k_1 m_1 a_\psi)$$

By rewriting the solution in the original physical coordinates, i.e., the x, y, τ reference frame, the three modes can be expressed explicitly. For $M_e > 1$,

$$p = a_p \cos k_p \left\{ (1 + M \cos \theta_p) \tau - (\ell_p x + m_p y) \right\} \tag{77}$$

$$s = a_s \cos k \left\{ \ell M \tau - (\ell x + m y) \right\} \tag{78}$$

$$\frac{\omega}{A} = \left\{ -k \left(a_U + \frac{a_p}{M_e} \right) \right\} \sin k \left\{ \ell M \tau - (\ell x + m y) \right\} \tag{79}$$

where

$$k_p = k_1 \left(\frac{m_1}{m_p} \right)$$

$$\ell_p = \cos\theta_p = \sin(\alpha + \mu_e)$$

$$k = k_1 (m_1/m)$$

$$\ell = \sin\alpha$$

For $M_e < 1$, the three modes are given by

$$p = e^{-x/d} \left\{ a_p \cos k_p \left[(1 + M\cos\theta_p)\tau - (\ell_p x + m_p y) \right] + b_p \sin k_p \left[(1 + M\cos\theta_p)\tau - (\ell_p x + m_p y) \right] \right\} \tag{80}$$

$$s = a_s \cos k \left[\ell M\tau - (\ell x + m y) \right] - b_s \sin k \left[\ell M\tau - (\ell x + m y) \right] \tag{81}$$

$$\frac{\omega}{A} = -k \left\{ \left(a_U + \frac{a_p}{M_e} \right) \sin k \left[\ell M\tau - (\ell x + m y) \right] + \left(b_U + \frac{b_p}{M_e} \right) \cos k \left[\ell M\tau - (\ell x + m y) \right] \right\} \tag{82}$$

where

$$k_p = k_1 (m_1/m_p)$$

$$\ell_p = \frac{\left(\dfrac{M^2}{1 - M^2} \right) \tan\alpha}{\left[1 + \left(\dfrac{M^2}{1 - M^2} \tan\alpha \right)^2 \right]^{1/2}}$$

$$k = k_1 (m_1/m)$$

$$\ell = \sin\alpha$$

and

$$d = \frac{1 - M^2}{k_1 M_1 (1 - M_e^2)^{1/2}}$$

The amplitudes of the wave generated at a given value of the shock strength are functions of δ, the inclination of the incoming disturbance. For $M_e < 1$, the amplitudes of the flow parameters refer to values immediately after the shock.

Now that the expressions are available for the downstream flow perturbations due to the interaction of a single Fourier component of entropy with a normal shock, the corresponding random field can be constructed. The method follows that used by Ribner to treat the case of a convected field of vorticity interacting with a shock. Just as Ribner used an aggregate of vorticity waves with a suitable distribution of amplitudes among the various wave lengths and inclinations to represent a turbulent field, so can an aggregate of entropy waves represent a random field of entropy spots.

4.2 The Random Field

Following Ribner, (Reference 7), expressions are next derived for the root-mean-square amplitude of the downstream pressure field generated by a random field of entropy waves (of given r.m.s. amplitude) interacting with a normal shock.

In general vector notation, and referring to any general physical quantity η, an elementary spectrum wave (harmonic component) is also expressible as:

$$d\eta = d\,Z_\eta \; e^{i\underline{k}\cdot\underline{x}} \tag{83}$$

where k is the wavenumber vector directed normal to the wavefronts and of magnitude $2\pi/\lambda$ (Figure 41), and $d\,Z_\eta$ is the complex amplitude of the wave. When η stands for a scalar quantity (such as temperature, density, entropy, or pressure), these are simple scalar waves.

The mean square level of a random disturbance η is

$$\overline{\eta^2} = \int [\eta\,\eta]\; d\,\underline{k} \tag{84}$$

where $[\eta\,\eta]$ is the spectral density, and $[\eta\,\eta]$ is in turn related to the complex amplitude $d\,Z_\eta\,(\underline{k})$ and its complex conjugate by:

$$[\eta\,\eta]\; d\,\underline{k} = \overline{d\,Z^*_\eta\,(\underline{k})\; d\,Z_\eta\,(\underline{k})} \tag{85}$$

For the specific case of random upstream entropy disturbances generating downstream pressure disturbances, the oncoming entropy wave is expressible as

$$d\,s = d\,Z_s\; e^{i\underline{k}_1\cdot\underline{x}} \tag{86}$$

and the downstream pressure disturbance as

$$d\,p = d\,Z_p\, e^{\,i\,\underline{k}\cdot\underline{x}} \tag{87}$$

and the direction of the wavevector for pressure is normal to the wavefronts of sound. The pressure wave amplitudes and entropy wave amplitudes are connected by the transfer function

$$d\,Z_p = P_s\, d\,Z_s \tag{88}$$

where P_s is the single-wave transfer function between entropy and pressure, which is wavenumber dependent.

The desired r.m.s. pressure fluctuation will be given by

$$\overline{p^2} = \int [p\,p]\; d\,\underline{k} \tag{89}$$

Through Equations (85) and (88),

$$[p\,p]\; d\,\underline{k} = \left| P_s \right|^2 \;\overline{d\,Z_s^*\, d\,Z_s} \tag{90}$$

and

$$\overline{p^2} = \int \left| P_s \right|^2 [s\,s]\; d\,\underline{k} \tag{91}$$

This relates the r.m.s. pressure fluctuation to the spectral density of the oncoming entropy field and the wavenumber-dependent transfer function. For an isotropic field of oncoming entropy waves (i.e., a scalar field with spherical symmetry), the spectral density has the general form

$$[s\,s] = k^2\, F(k) \tag{92}$$

where $F(k)$ is an arbitrary function of k that will finally cancel out in forming ratios.

Going over the spherical polar coordinates, the wavenumber components are

$$k_1 = -k \sin\delta$$
$$k_2 = k \cos\delta \cos\phi$$
$$k_3 = k \cos\delta \sin\phi$$

and

$$d\,\underline{k} = k^2 \cos\delta \; d\,k \; d\phi \; d\,\delta \tag{93}$$

Then the r.m.s. pressure fluctuation becomes

$$\overline{p^2} = \int_0^{\infty} k^2 F(k)\, dk \int_0^{2\pi} d\phi \int_{-\pi/2}^{+\pi/2} \left| P_s \right|^2 \cos\delta \; d\delta \tag{94}$$

Also, the r.m.s. entropy fluctuation is

$$\overline{s^2} = \int [s\,s] \; d\underline{k} = \int_0^{\infty} k^2 F(k)\, dk \int_0^{2\pi} d\phi \int_{-\pi/2}^{+\pi/2} \cos\delta \; d\delta \tag{95}$$

Therefore, the ratio of r.m.s. pressure fluctuation to r.m.s. entropy fluctuation produced by an isotropic field of entropy waves is

$$\overline{p^2}/\overline{s^2} = \int_0^{\pi/2} \left| P_s \right|^2 \cos\delta \; d\delta \tag{96}$$

including entropy waves of all wavelengths and orientations.

The required single wavenumber transfer function was defined, in Equation (88), as the ratio $d\,Z_p/d\,Z_s$, the ratio of the complex amplitude of a single harmonic pressure wave to the complex amplitude of the single harmonic entropy wave that produced it. Its absolute value $\left| P_s \right|$ will be obtained from section 4.1. The absolute value of the upstream entropy wave amplitude is obtained from Equation (69); and those of the downstream pressure fluctuation, from Equation (80) for the subsonic case, and from Equation (77) for the supersonic case. It must be remembered that the point of transition from subsonic to supersonic case is also a function of vector wavenumber $\underline{k}$ through the wave inclination δ.

For the supersonic case, $M_e > 1$, the transfer function is:

$$\left| P_s \right|^2 = \frac{\left| p \right|^2}{\left| s \right|^2} = \left(\frac{a_p}{R_s} \right)^2 \tag{97}$$

and for the subsonic case, $M_e < 1$, the transfer function is:

$$\left|P_s\right|^2 = \frac{\left|p\right|^2}{\left|s\right|^2} = \left(\frac{a_p}{R_s}\right)^2 + \left(\frac{b_p}{R_s}\right)^2 \tag{98}$$

where the amplitude components a_p/R_s and b_p/R_s are given for the supersonic case by:

$$\frac{a_p}{R_s} = \frac{\left(\frac{C_s}{A}\right)\Omega_1 \sin a - \Omega_2 \cos a}{\left(\frac{C_s}{A}\right)(\tilde{A}\sin a - \cos \mu_e) - B\cos a} \tag{99}$$

and for the subsonic case by:

$$\frac{a_p}{R_s} = \left\{\tilde{A}\,\frac{C_s}{A}\sin a - B\cos a\right\} \frac{\Omega_1\,\frac{C_s}{A}\sin a - \Omega_2 \cos a}{\left\{\tilde{A}\,\frac{C_s}{A}\sin a - B\cos a\right\}^2 + \frac{1-M_e^2}{M_e^2}\left(\frac{C_s}{A}\right)^2} \tag{100}$$

$$\frac{b_p}{R_s} = \frac{\Omega_2 \cos a - \left(\frac{C_s}{A}\right)\Omega_1 \sin a}{\left[\tilde{A}\left(\frac{C_s}{A}\right)\sin a - B\cos a\right]^2 + \frac{1-M_e^2}{M_e^2}\left(\frac{C_s}{A}\right)^2} \cdot \times \frac{\sqrt{1-M_e^2}}{M_e}\left(\frac{C_s}{A}\right) \tag{101}$$

From the complexity of the expressions for the transfer functions in both Mach number regions (mainly the form of their dependence on wave inclination δ), as well as the fact that the boundary of validity of the two expressions also depends on δ, then a numerical integration of Equation (96) will be involved in applying these expressions to obtain numerical results. Qualitative conclusions which may be drawn from the equations themselves include:

1) When $M_e > 1$, the waves generated downstream are in phase with the incoming disturbance, but when $M_e < 1$ there is a phase shift across the shock.

2) When $M_e > 1$, the pressure waves generated have a permanent waveform, but when $M_e < 1$ they decay with distance. At a fixed value of shock strength the absorption distance d is a function of the inclination of the oncoming disturbance δ, larger values of δ (or oncoming wave fronts more nearly normal to the shock) corresponding to shorter absorption distances. Increasing shock strengths also result in increasing decay rate with distance from the shock.

5.0 CONCLUSION AND RECOMMENDATIONS

The strength of the pressure disturbance generated by an entropy disturbance interacting with a shock wave depends strongly upon the inclination angles of the entropy wavefront and of the shock. For every flow condition there is a region of entropy disturbance angles for which an "effective Mach number" in the flow is subsonic, and the pressure wave amplitudes decay with distance from the shock, part of the disturbance energy being fed back into the shock. For all other entropy disturbance angles, the "effective Mach number" is supersonic and the pressure disturbance propagates at constant amplitude. Entropy disturbance angles encountered in practice will depend upon the source of the disturbances, but will most often be a mixture of all angles, so that part of the generated pressure field will propagate as acoustic waves while the remainder decays with distance.

Example estimates, based on flight conditions typical for launch vehicles and supersonic cruise vehicles, and using entropy disturbance inputs typical for boundary layers, show pressure fluctuation magnitudes larger than for boundary layer noise and equal to those produced by shock-turbulence interactions. Therefore, the entropy-shock interaction can cause serious levels of fluctuating pressure and should be explored further.

The large density fluctuations measured in supersonic wakes, and the persistence of the density fluctuations over large downstream distances, make wakes of upstream protuberances on launch vehicles particularly suspect if there are standing shocks downstream. Since several of the trends and conclusions in Reference 2 are subject to revision, the possibility of resonant oscillations of standing shocks (driven by entropy-shock interactions and by acoustic reflections between the body and the shock) should be re-examined.

Regarding entropy fluctuations in jets, the cited data (for a subsonic, heated jet) showed maximum values almost an order of magnitude larger than those used in the sample predictions. In a hot, supersonic rocket exhaust with oblique shocks, the shock-entropy interaction could be a major source of noise. Typical entropy fluctuation magnitudes and shock conditions for rocket exhausts should be applied to estimate the importance of this interaction as a noise source, compared to the strengths of other sources present.

As foundation for further assessment of the pressure fields from shock-entropy interactions, the analysis methods should be based on improved models of the actual flows. The first step would be to complete the random entropy field case, since a random field of entropy spots could then be represented by a field synthesized from all wavelengths and orientations of harmonic components.

Previous work has concentrated upon one of the three modes at a time (entropy, vorticity, sound) interacting with a shock, the present being no exception. Yet natural flows contain all three modes, with one sometimes dominant; and in an experiment it is difficult to generate significant entropy or vorticity fluctuations without also generating the other. The foundation exists (in Reference 2) for obtaining the downstream perturbed flow field from an upstream flow containing all three modes, without superposing individual solutions. Experimental data suggest that temperature disturbances are negatively correlated with velocity disturbances. Then the combined effect of temperature and velocity fluctuations interacting with a shock would not be a simple addition of the results for each, but must consider the cross-terms arising in the interaction. The combined result for a spatially homogeneous field of temperature and vorticity discontinuities, plus sound waves, interacting with a shock should be determined.

REFERENCES

1. Morkovin, M. V., "Note on the Assessment of Flow Disturbances at a Blunt Body Traveling at Supersonic Speeds Owing to Flow Disturbances in Free Stream," J. Applied Mech., ASME Trans. No 60-APM-10 (1960).

2. Morkovin, M. V., "On Supersonic Wind Tunnels with Low Free-Stream Disturbances," J. Applied Mech., ASME Trans. No. 59-APM-10 (1959).

3. Adams, M. C., "On Shock Waves in Inhomogeneous Flow," J. Aero. Sci. 16, 11, 685-690 (1949).

4. Lighthill, M. J., "The Flow Behind a Stationary Shock," Phil. Mag. 40, Ser. 7, No. 301, 214-220 (1949).

5. Chu, B. T., "On Weak Interaction of Strong Shock and Mach Waves Generated Downstream of a Shock," J. Aero. Sci. 19, 7 (1952).

6. Ribner, H. S., "Convection of a Pattern of Vorticity Through a Shock Wave," NACA Report 1164 (1954).

7. Ribner, H. S., "Shock-Turbulence Interaction and the Generation of Noise," NACA Report 1233 (1955).

8. Moore, F. K., "Unsteady Oblique Interaction of a Shock Wave with a Plane Disturbance," NACA Report 1165 (1954).

9. Lowson, M. V., "The Fluctuating Pressures Due to Shock Interactions with Turbulence and Sound," NASA CR-77313 (June 1966).

10. Chang, C.-T., "On the Interaction of Weak Disturbances and a Plane Shock of Arbitrary Strength in a Perfect Gas," Ph.D. Thesis, Johns Hopkins University (1955).

11. Chang, C.-T., "Interaction of a Plane Shock and Oblique Plane Disturbances with Special Reference to Entropy Waves," J. Aero. Sci. 24, 675-682 (1957).

12. "Equations, Tables, and Charts for Compressible Flow," NACA Report 1135 (1953).

13. Personal Communication, E. Cuadra to M. V. Morkovin (August 3, 1967).

14. Corrsin, S., and M. S. Uberoi, "Further Experiments on the Flow and Heat Transfer in a Heated Turbulent Air Jet," NACA Report 998, 1950. (Supersedes NACA TN 1865, 1949).

15. Kovasznay, L.S.G., "Turbulence in Supersonic Flow," Jour. Aero Sciences 20, 10 657-682, October 1953.

16. Kovasznay, L.S.G., "Interaction of a Shock Wave and Turbulence," Proc. Heat Transfer and Fluid Mechanics Inst., 1955.

17. Kistler, A. L., "Fluctuation Measurements in a Supersonic Turbulent Boundary Layer," Physics of Fluids 2, 3, 290-296, 1959.

18. Demetriades, A., "Turbulence Measurements in an Axisymmetric Compressible Wake," Philco-Ford Corporation Technical Report No. UG-4118, August 1, 1967.

19. Clay, W. G., Heerman, J., and R. E. Slattery, "Statistical Properties of the Turbulent Wake Behind Hypervelocity Spheres," Physics of Fluids 8, 10, 1792-1801, 1965.

20. Webb, W. H., "Self-Preserving Fluctuations and Scales for the Hypersonic Turbulent Wake," AIAA Journal 2, 11, 2031-2033, 1964.

21. Hamernik, R. P., "Interaction of an Advancing Shock Front with a Concentrated Heat (Entropy) Source," M.M.E. Thesis, Syracuse University, January 1967.

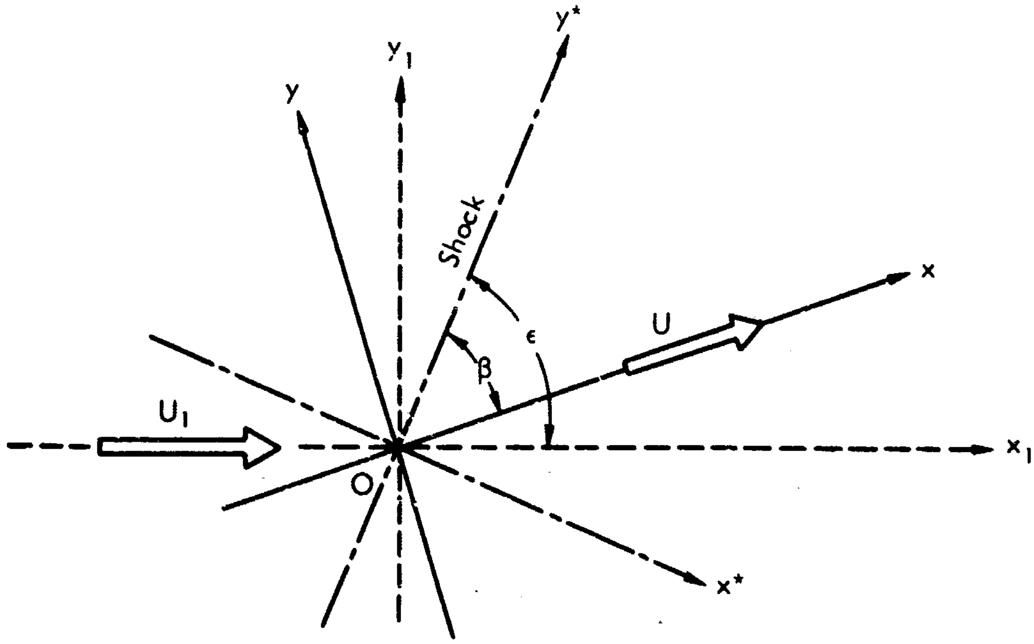

Figure 1. Basic Flow Coordinate Systems

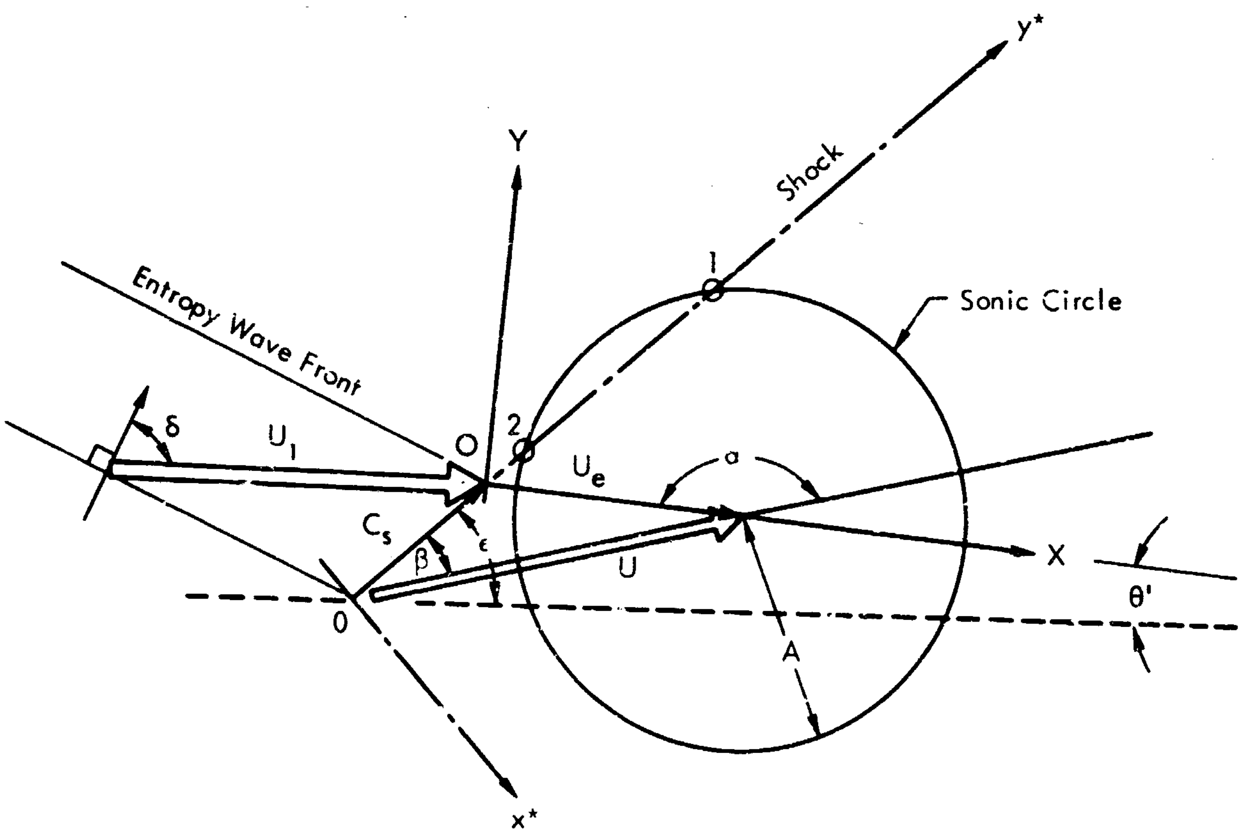

Figure 2. Intrinsic Frame of Reference with Respect to Downstream Flow Field

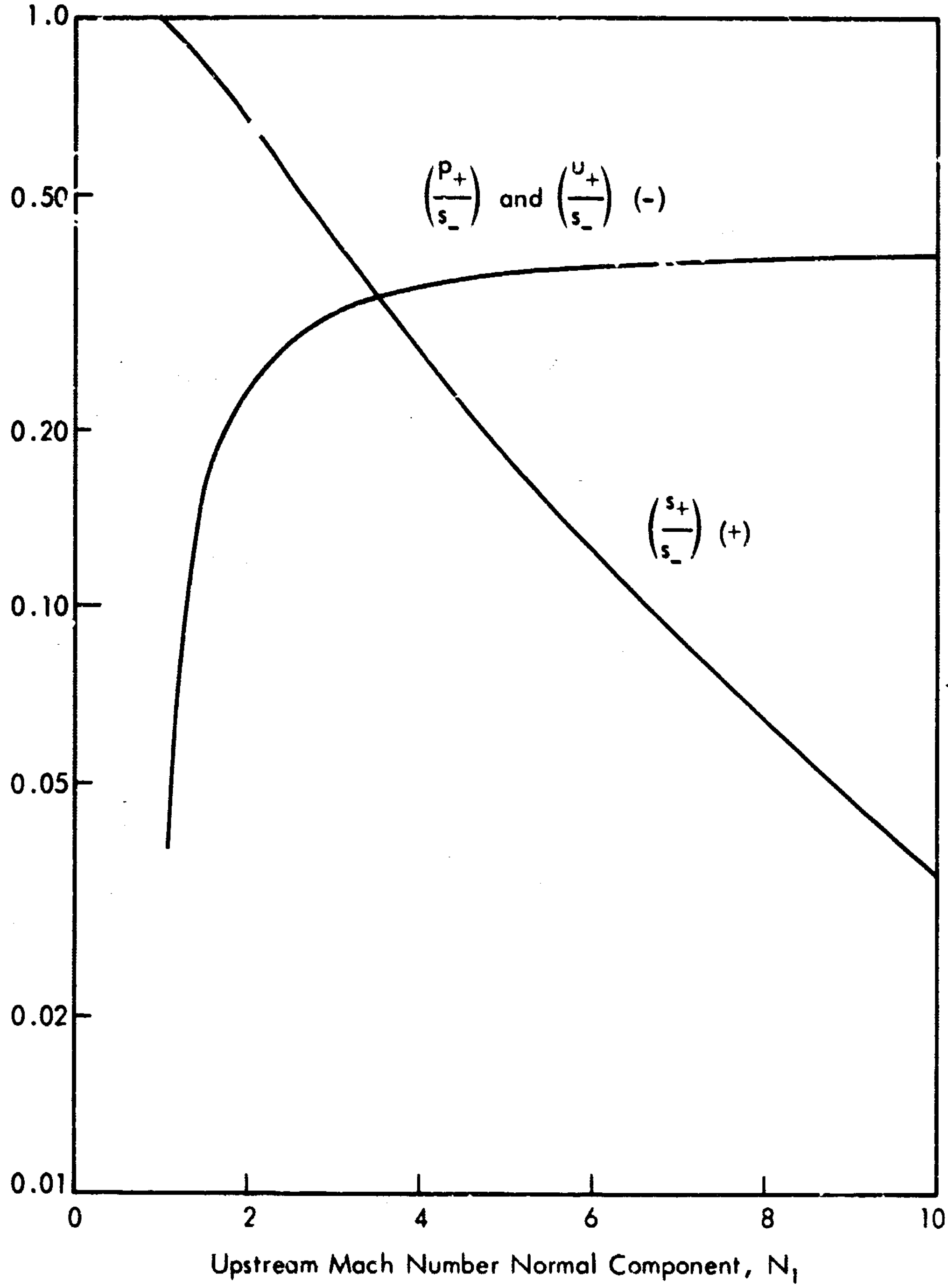

Figure 3. Special Case of Parallel Shock and Entropy Wave, $(\delta-\epsilon) = \pi/2$

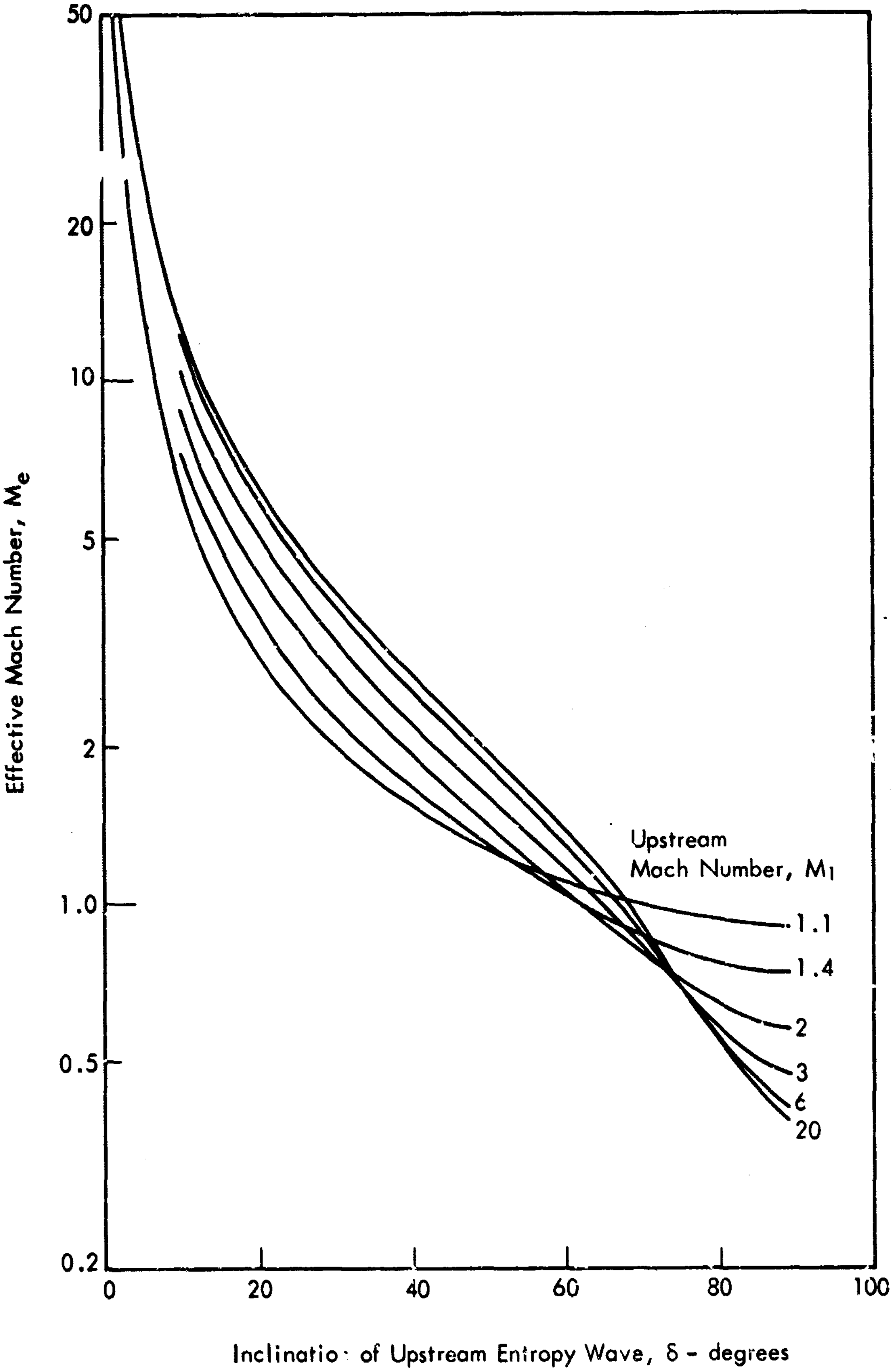

Figure 4. Variation of Effective Mach Number, Normal Shock Case

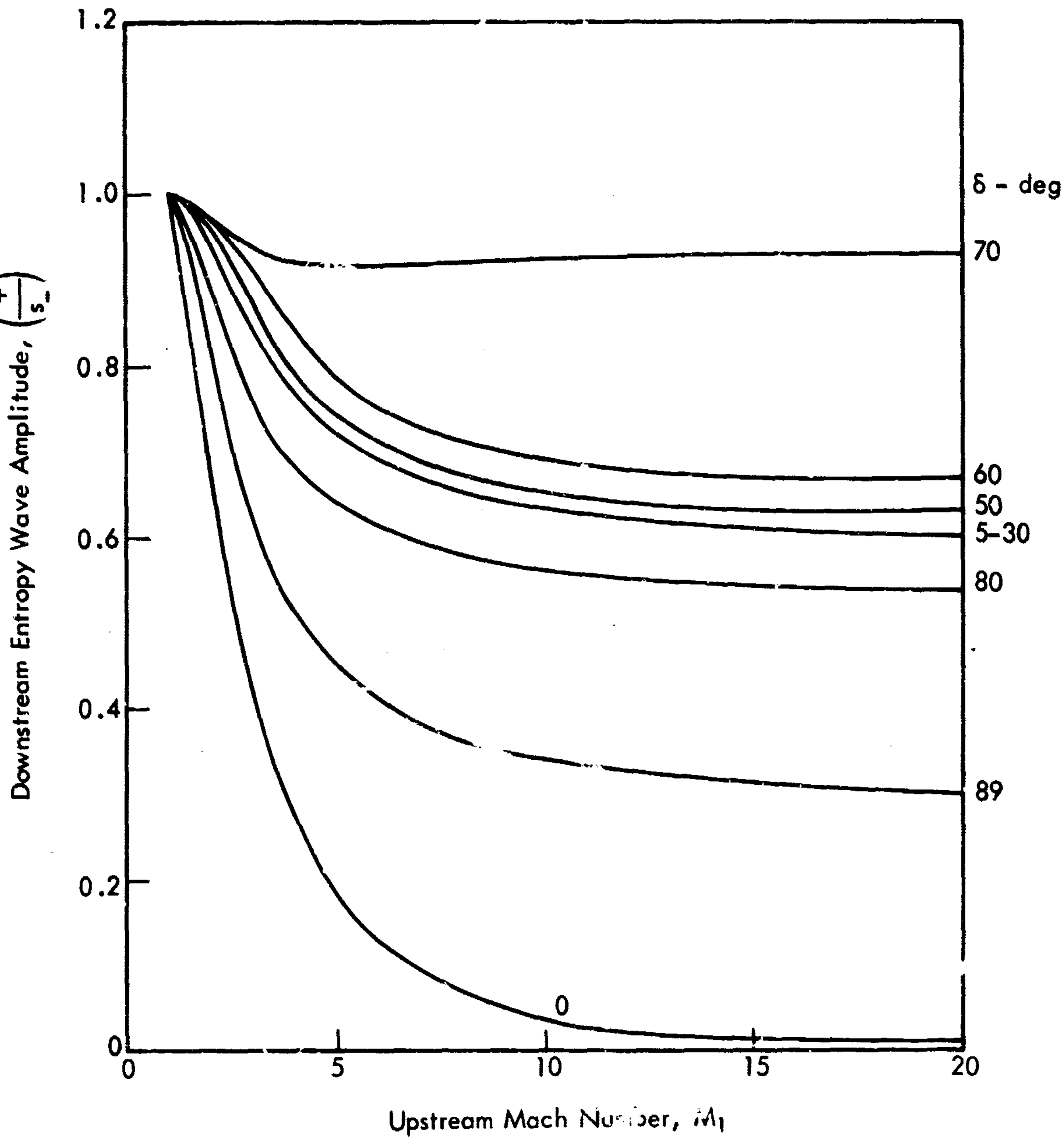

Figure 5. Downstream Entropy Wave Amplitude, Normal Shock Case

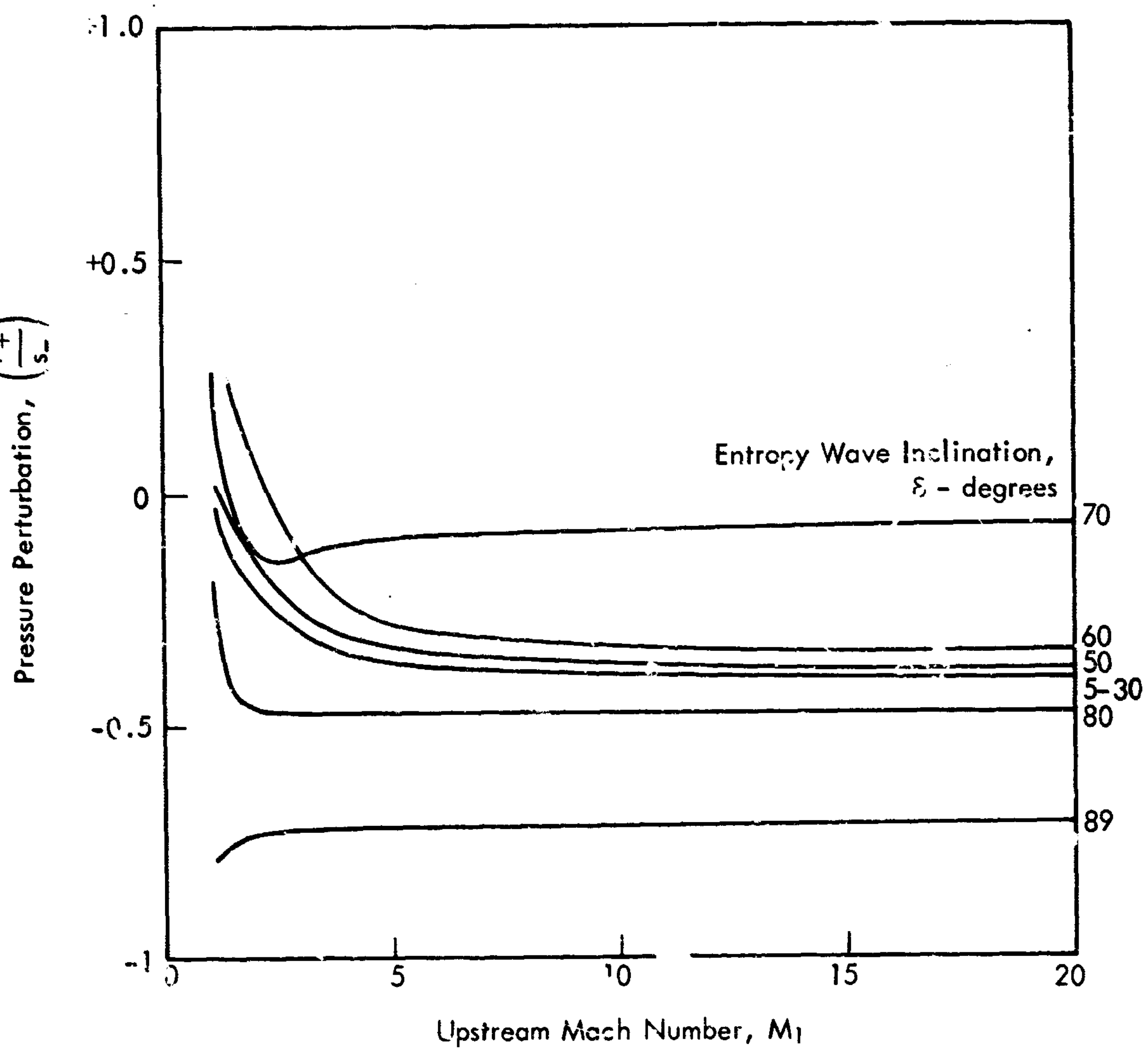

Figure 6. Generated Pressure Disturbance, Normal Shock Case

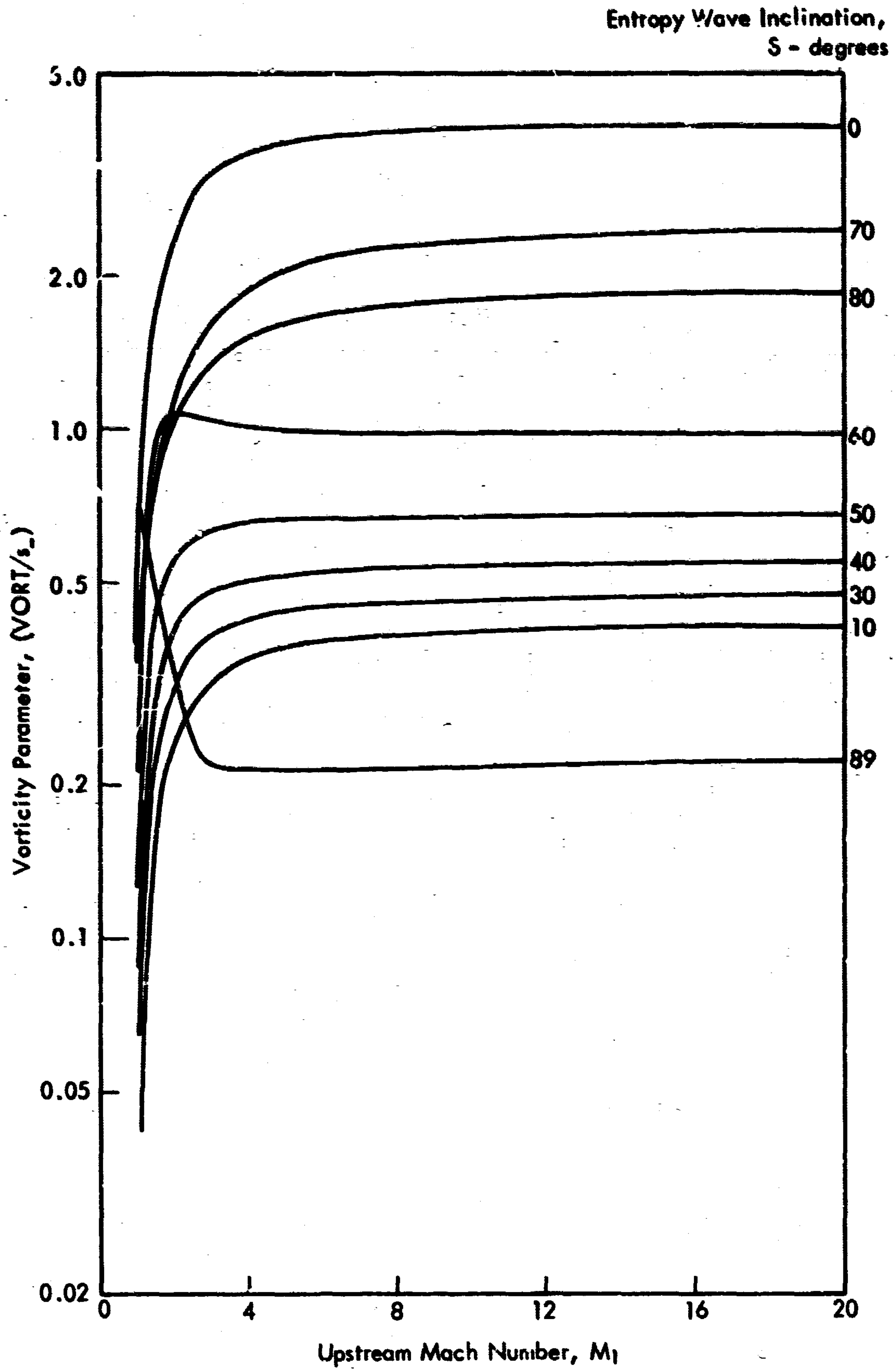

Figure 7. Generated Vorticity, Normal Shock Case

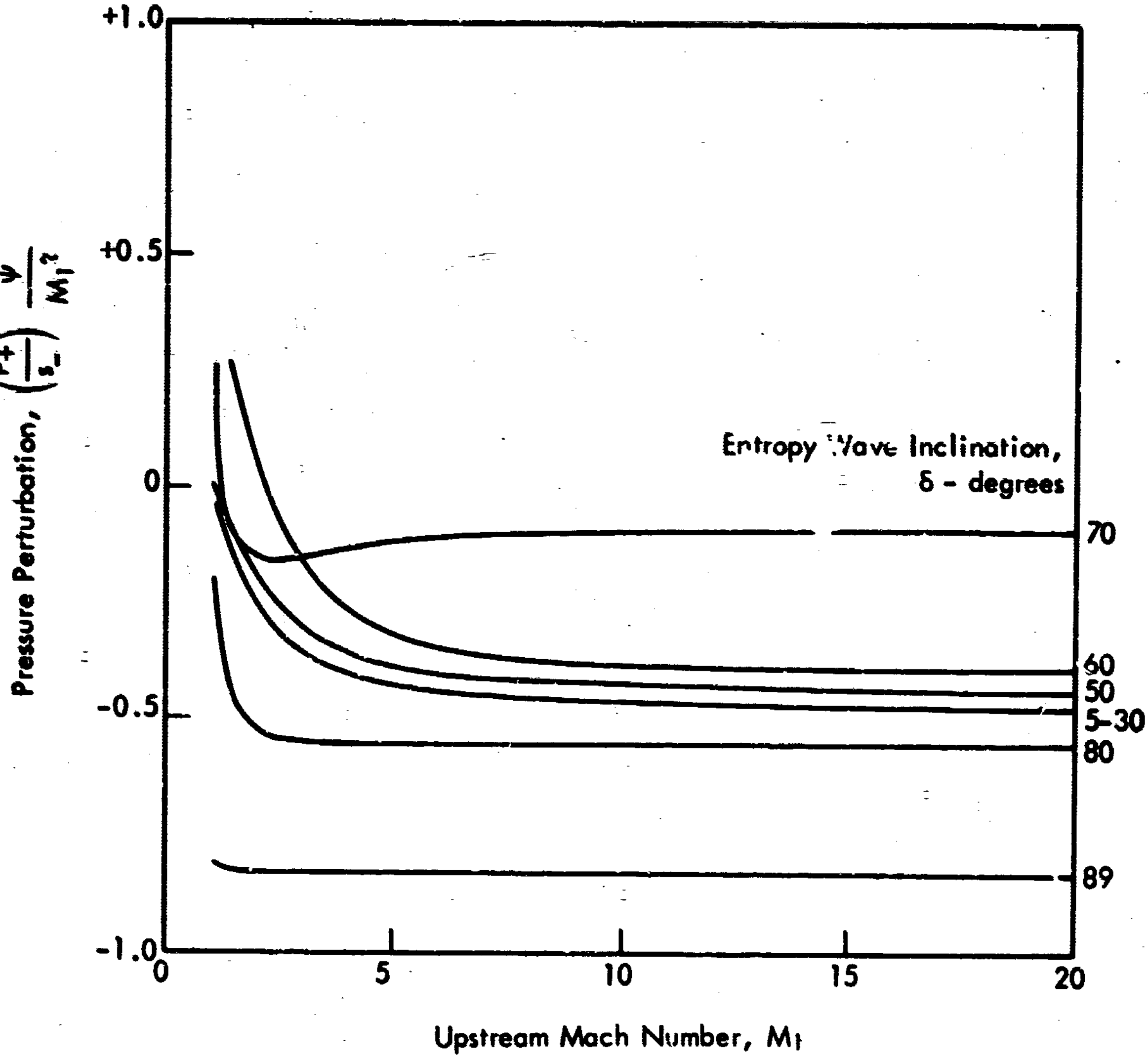

Figure 8. Pressure Disturbance Referenced to Free-Stream Conditions, Normal Shock Case

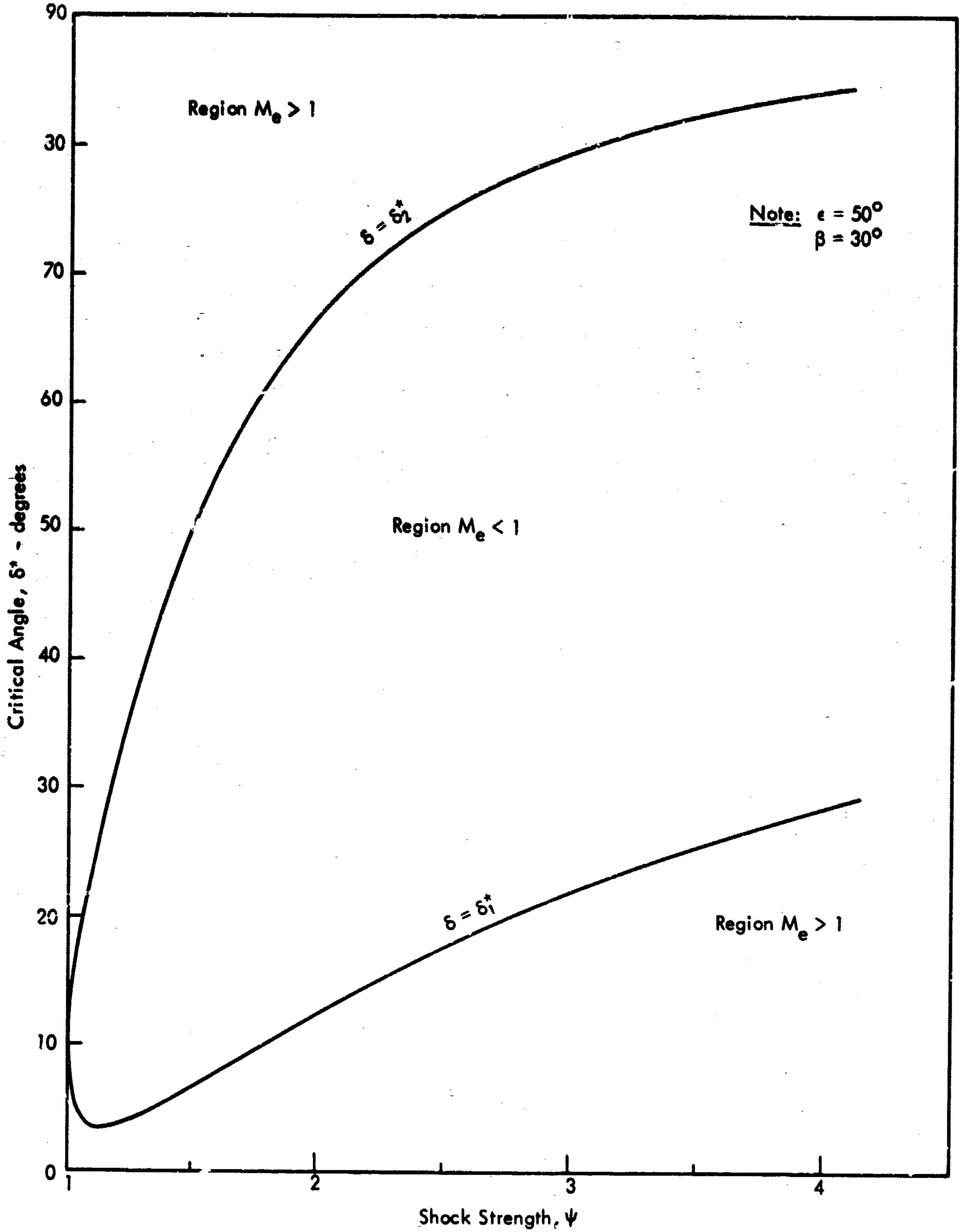

Figure 9. Typical Boundaries of Subsonic Region

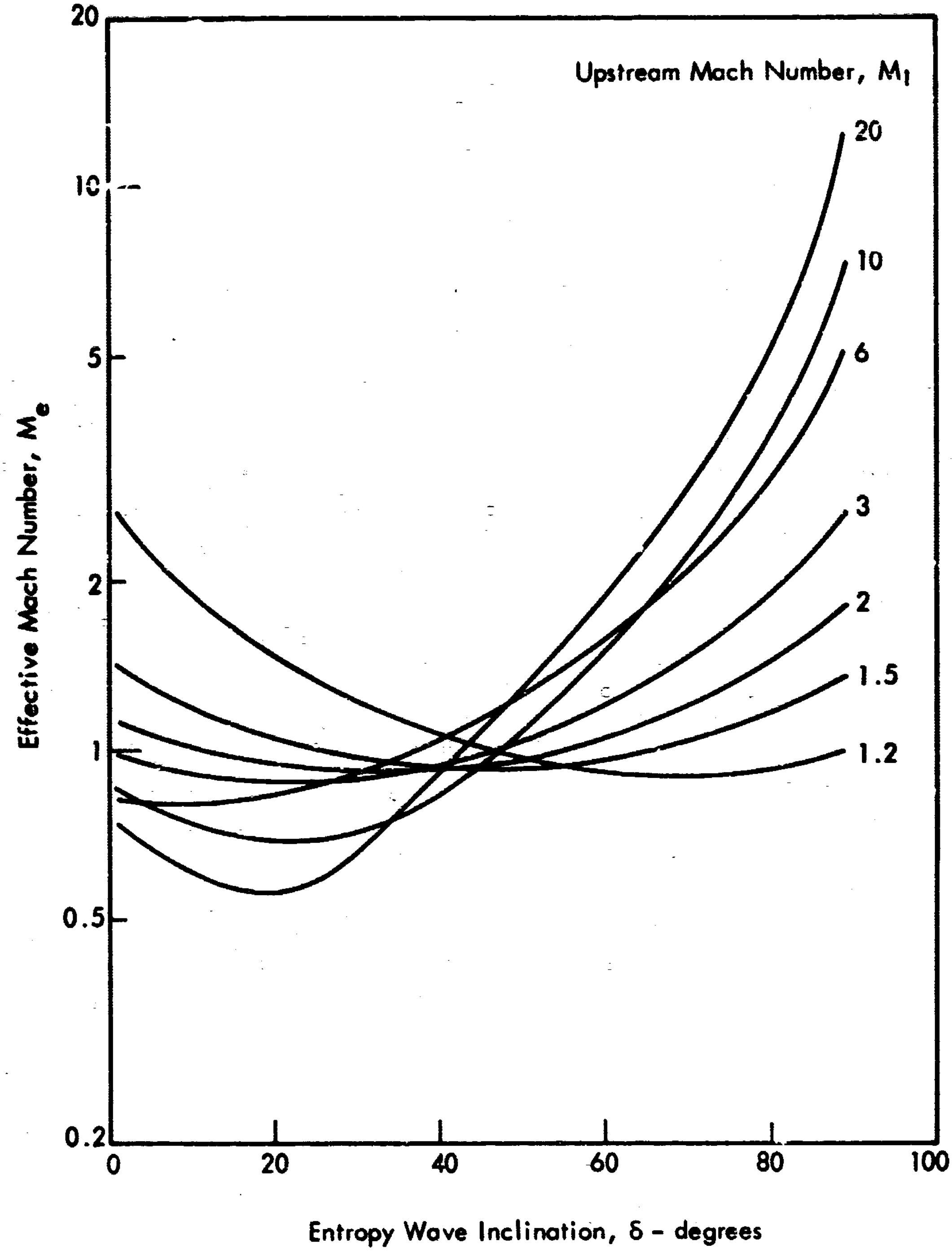

Figure 10. Effective Mach Number, Oblique Shock Case, Wedge Half-Angle $(\epsilon-\beta) = 4^{\circ}$

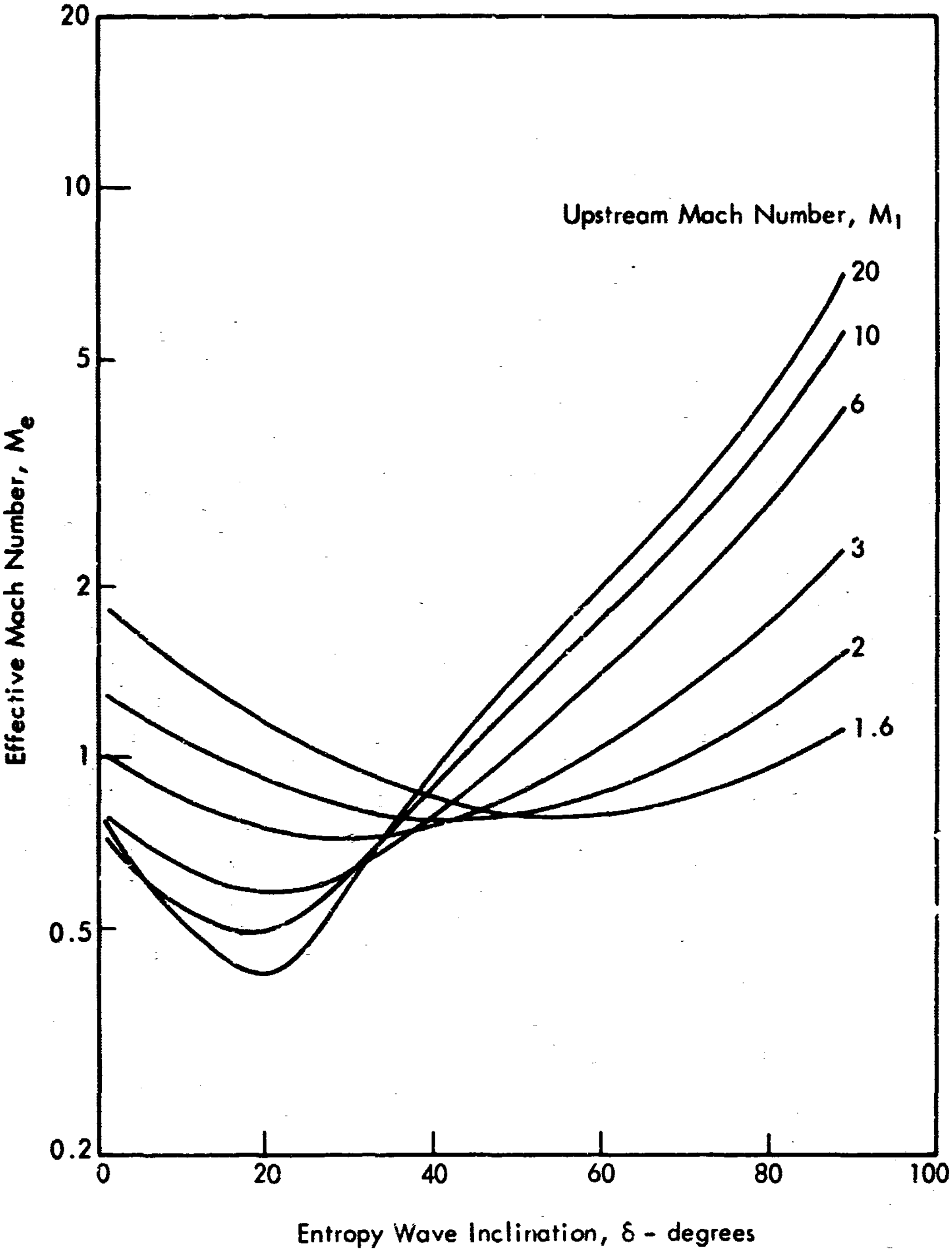

Figure 11. Effective Mach Number, Oblique Shock Case, Wedge Half-Angle $(\epsilon-\beta) = 12°$

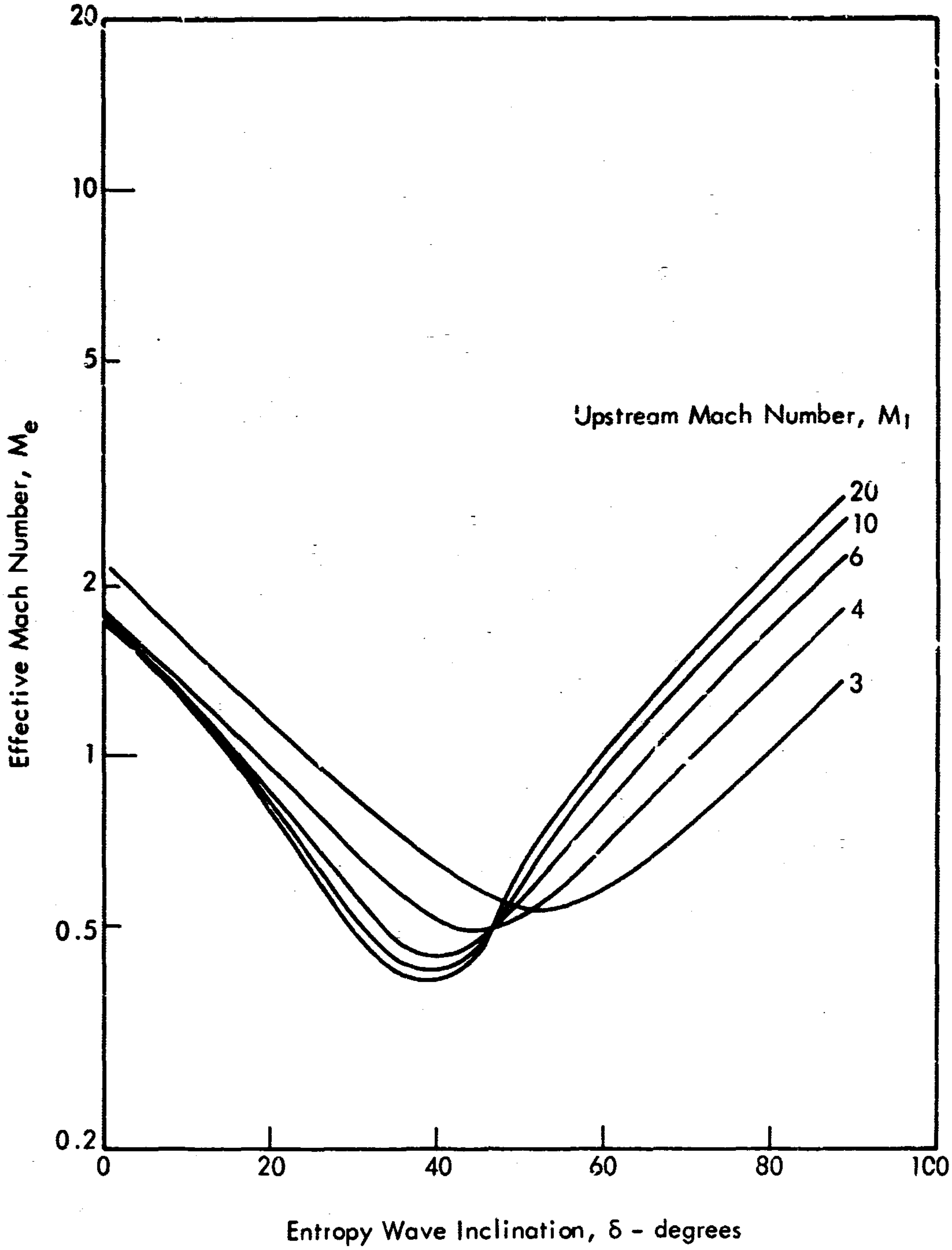

Figure 12. Effective Mach Number, Oblique Shock Case, Wedge Half-Angle $(\epsilon-\beta) = 30^{\circ}$

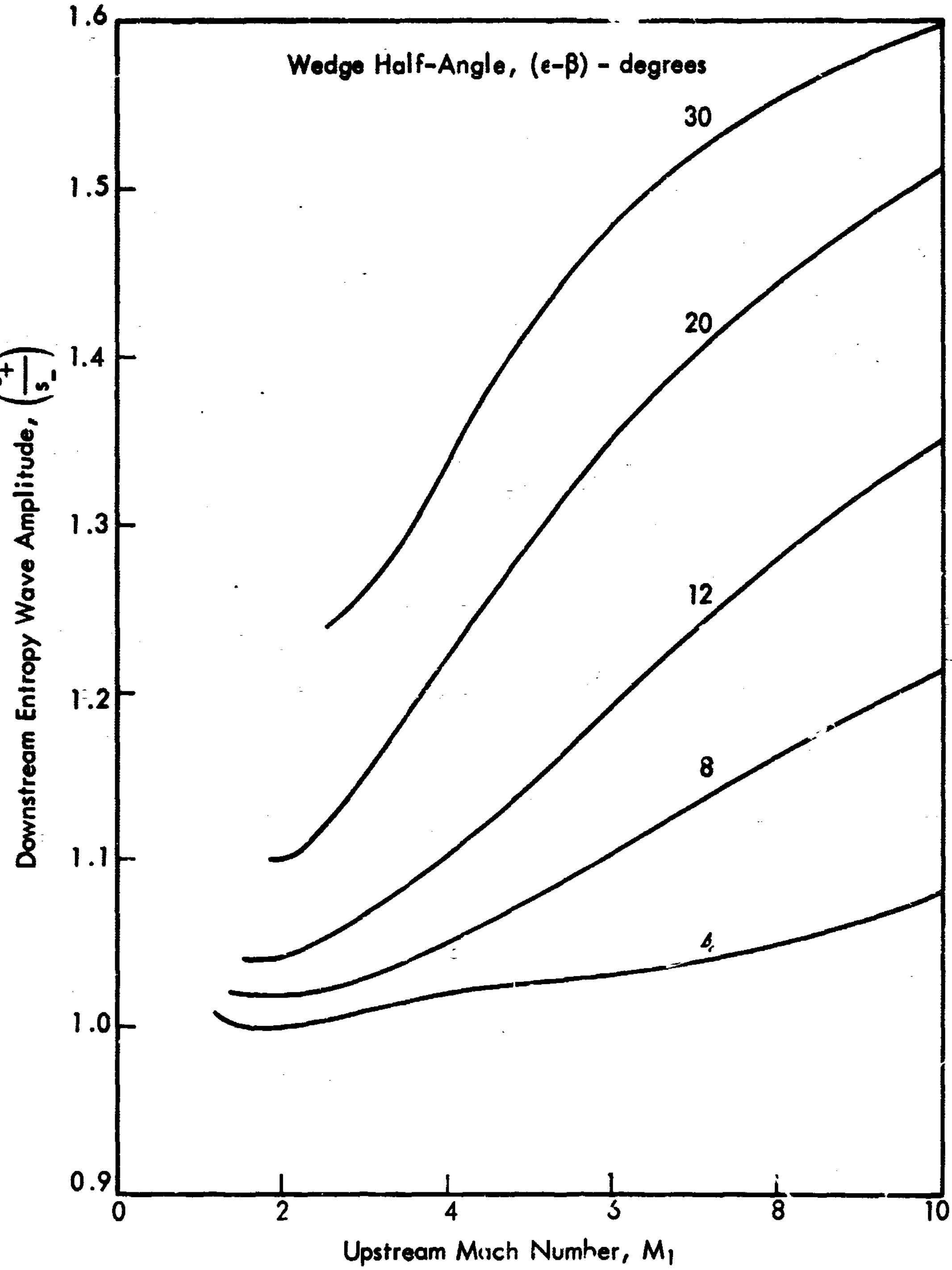

Figure 13. Downstream Entropy Wave Amplitude, Oblique Shock Case, $\delta = 1^\circ$

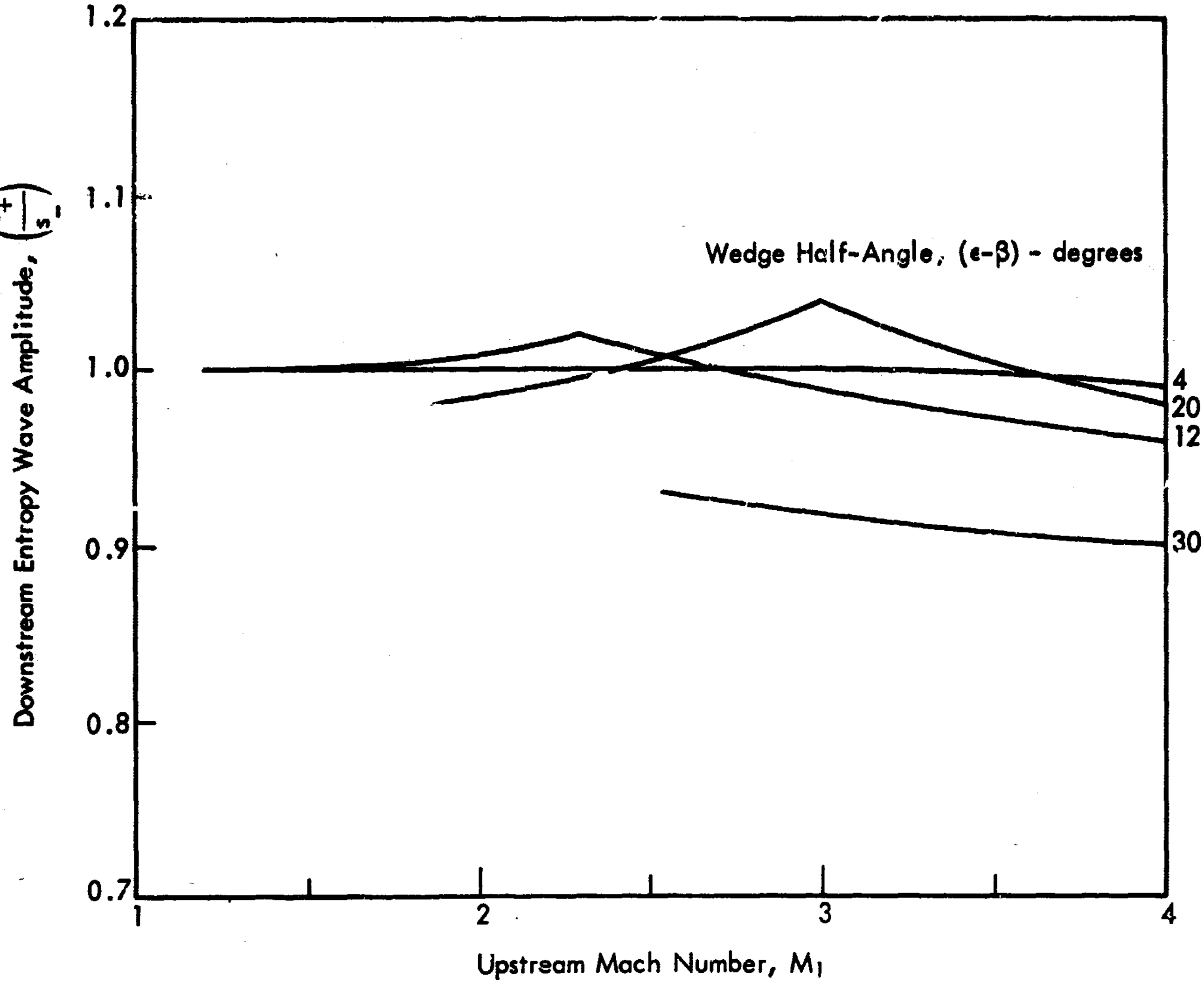

Figure 14. Downstream Entropy Wave Amplitude, Oblique Shock Case, $\delta = 10^{\circ}$

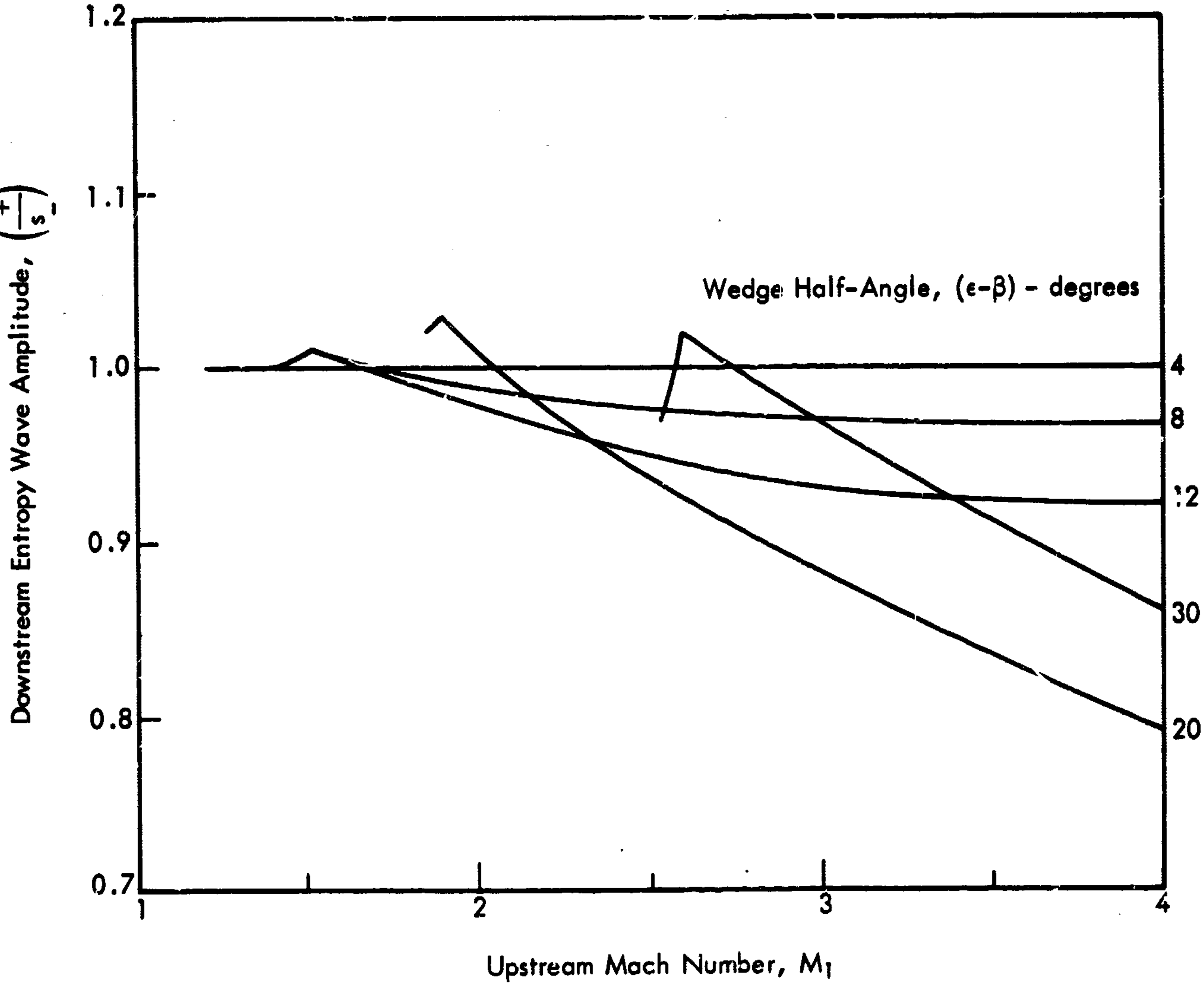

Figure 15. Downstream Entropy Wave Amplitude, Oblique Shock Case, $\delta = 30°$

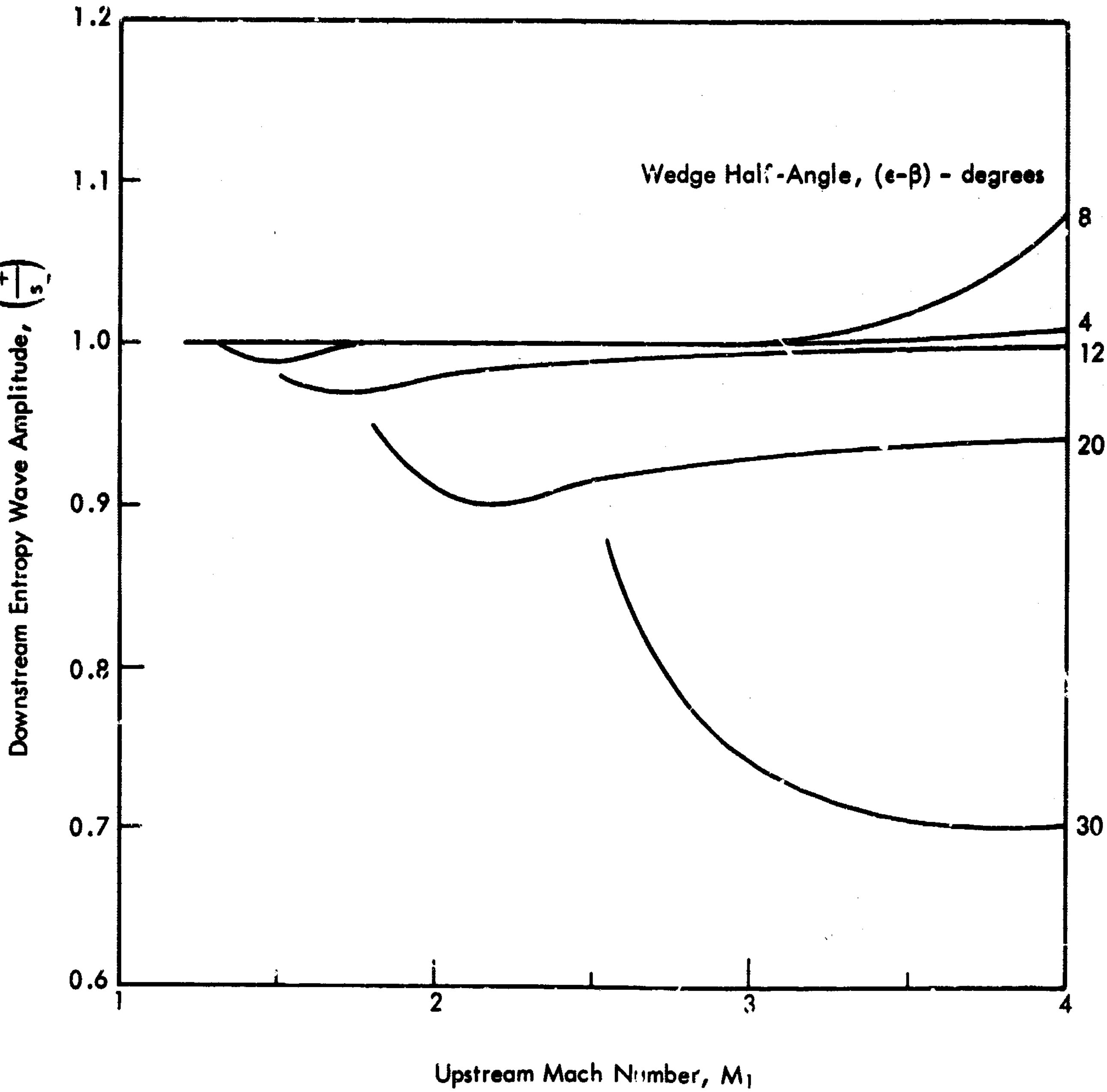

Figure 16. Downstream Entropy Wave Amplitude, Oblique Shock Case, δ = 50°

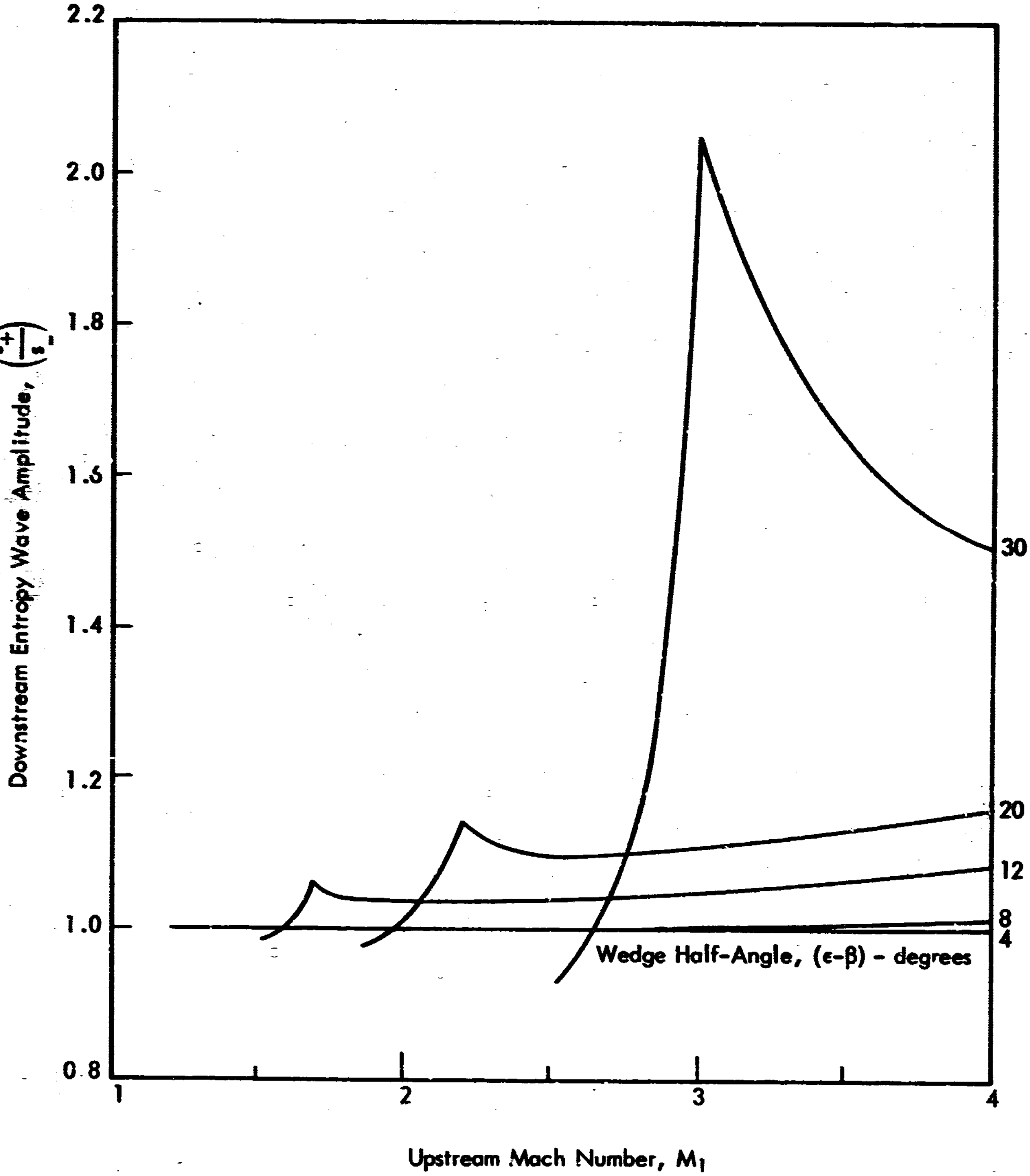

Figure 17. Downstream Entropy Wave Amplitude, Oblique Shock Case, $\delta = 80^{\circ}$

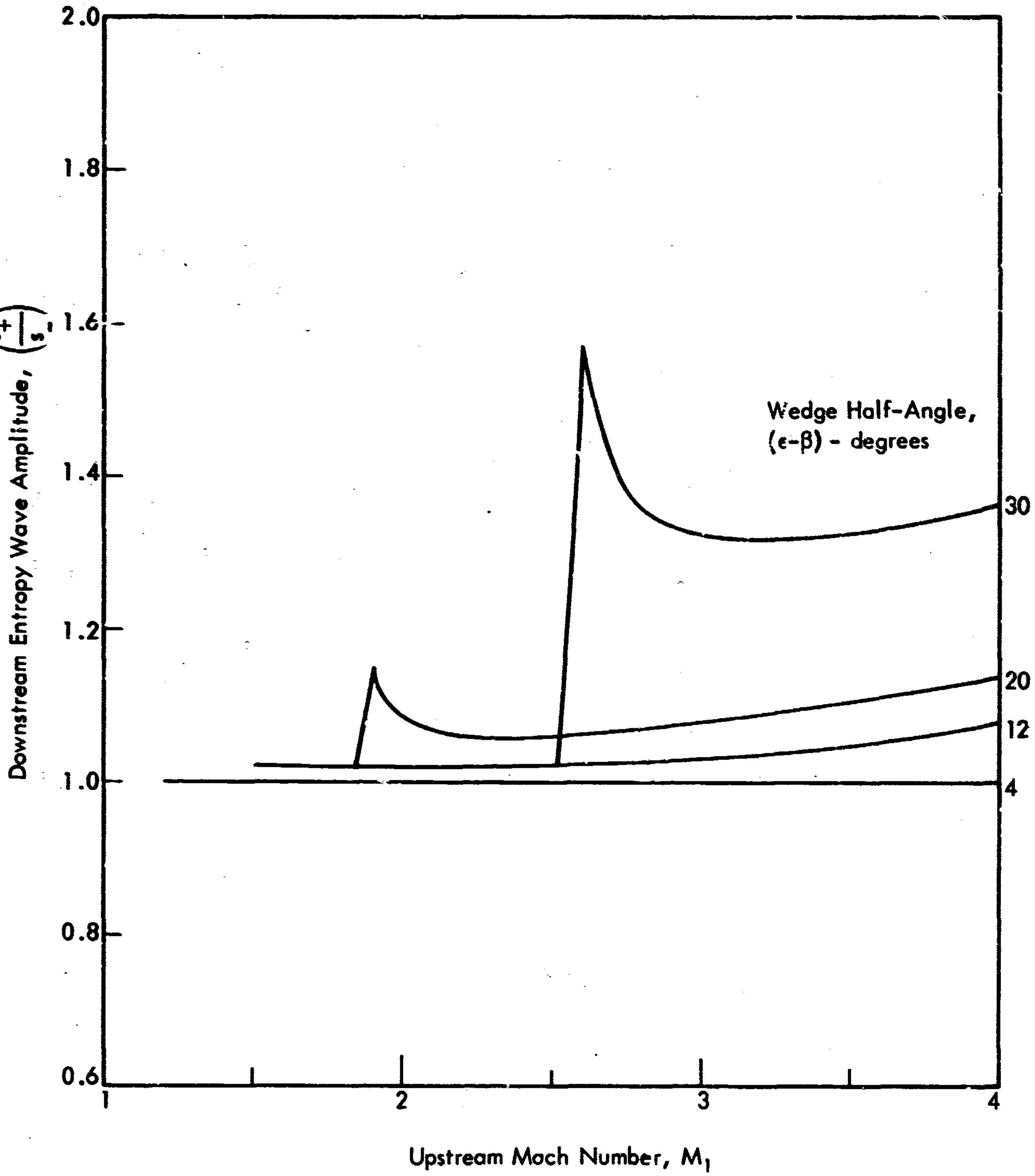

Figure 18. Downstream Entropy Wave Amplitude, Oblique Shock Case, $\delta = 89^{\circ}$

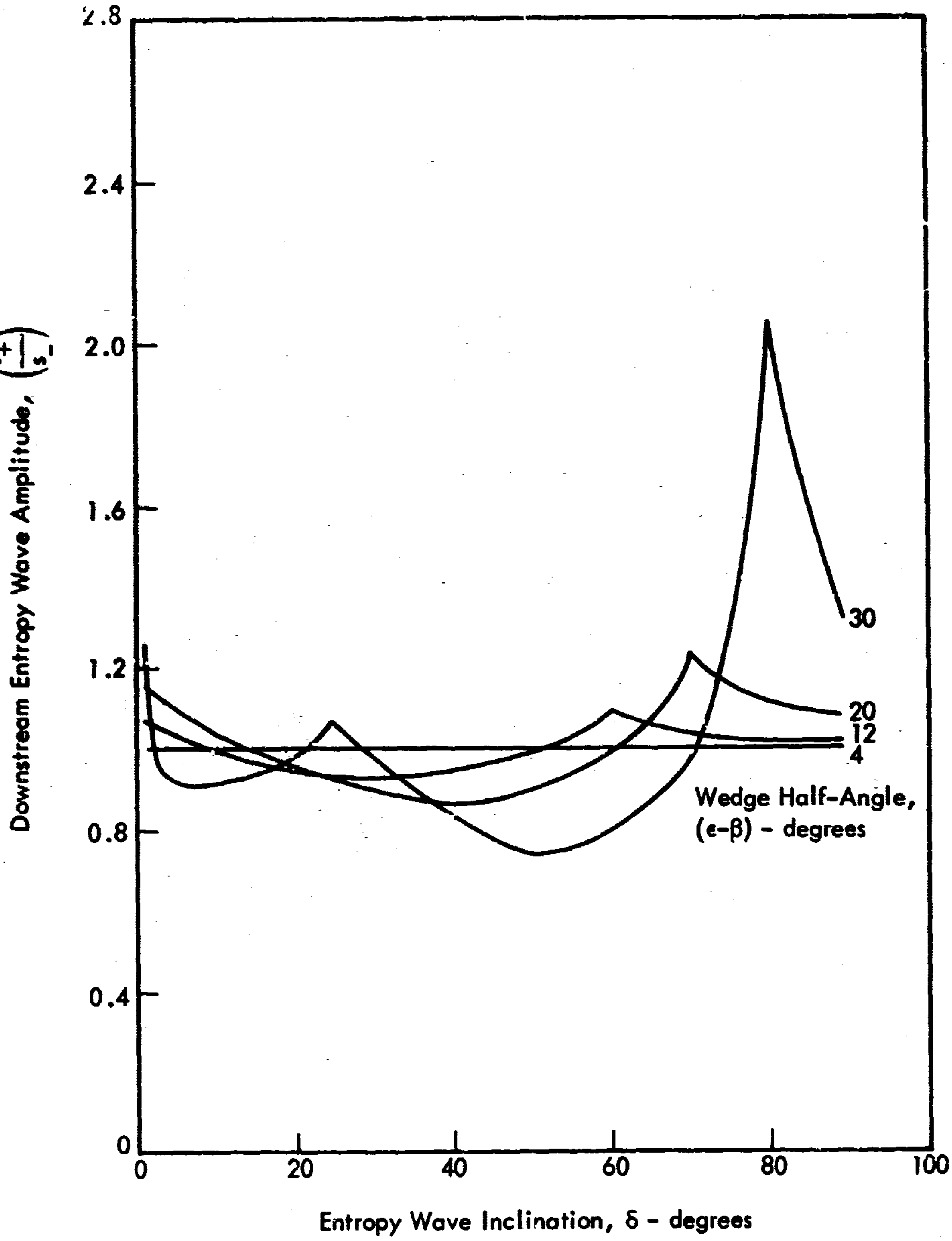

Figure 19. Downstream Entropy Wave Magnitude, Oblique Shock Case, $M_1 = 3$

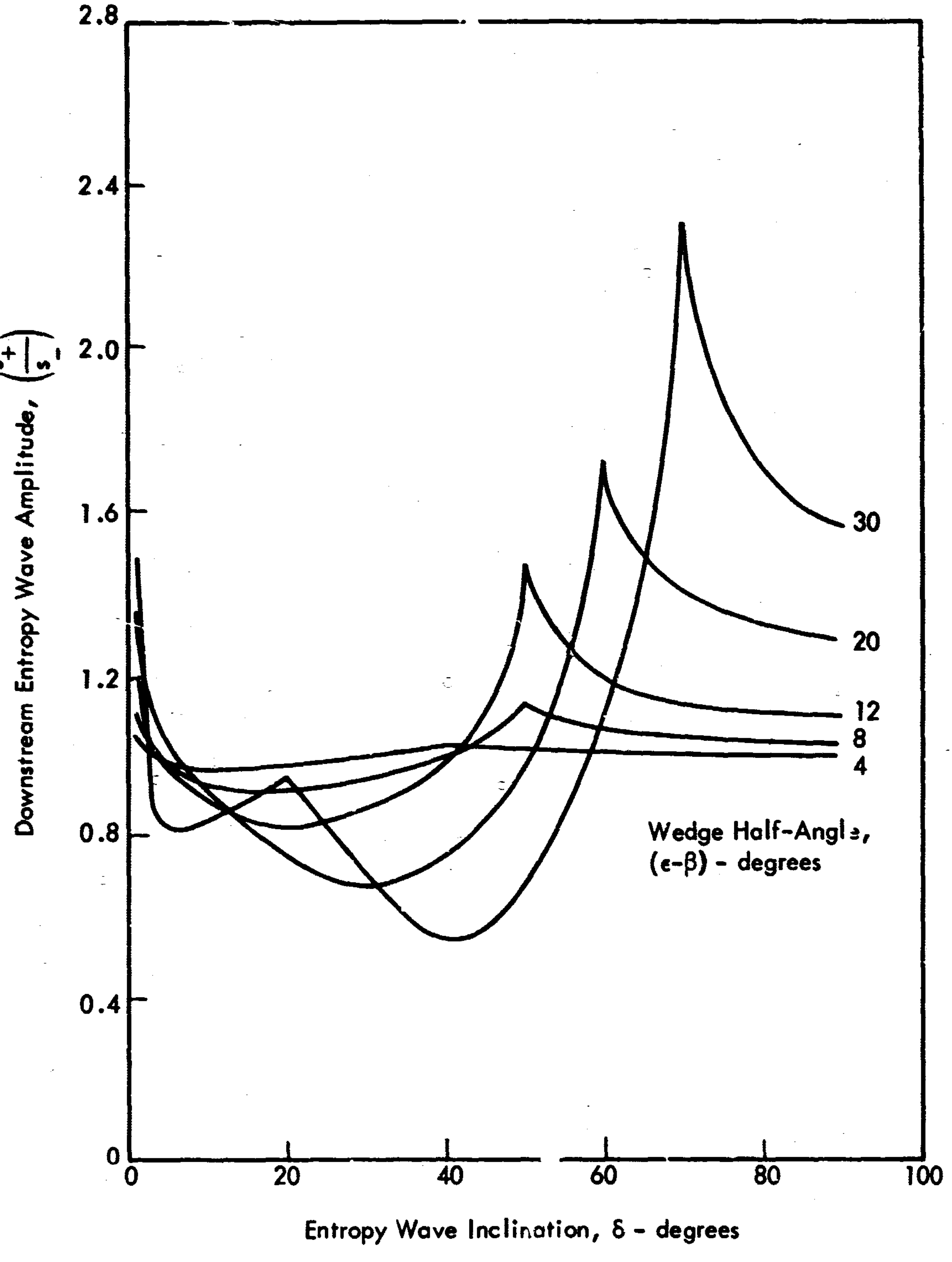

Figure 20. Downstream Entropy Wave Magnitude, Oblique Shock Case, $M_1 = 6$

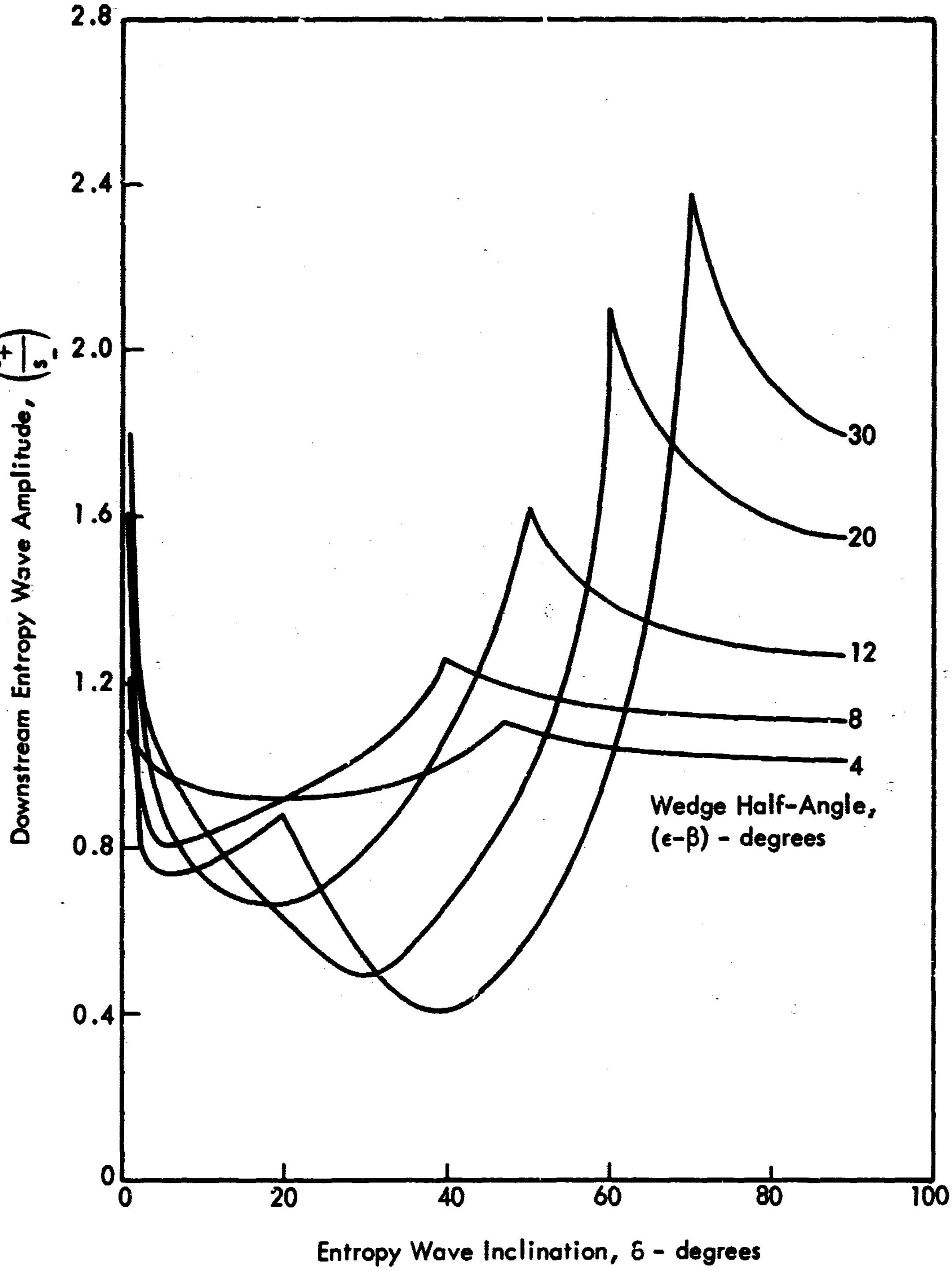

Figure 21. Downstream Entropy Wave Magnitude, Oblique Shock Case, $M_1 = 10$

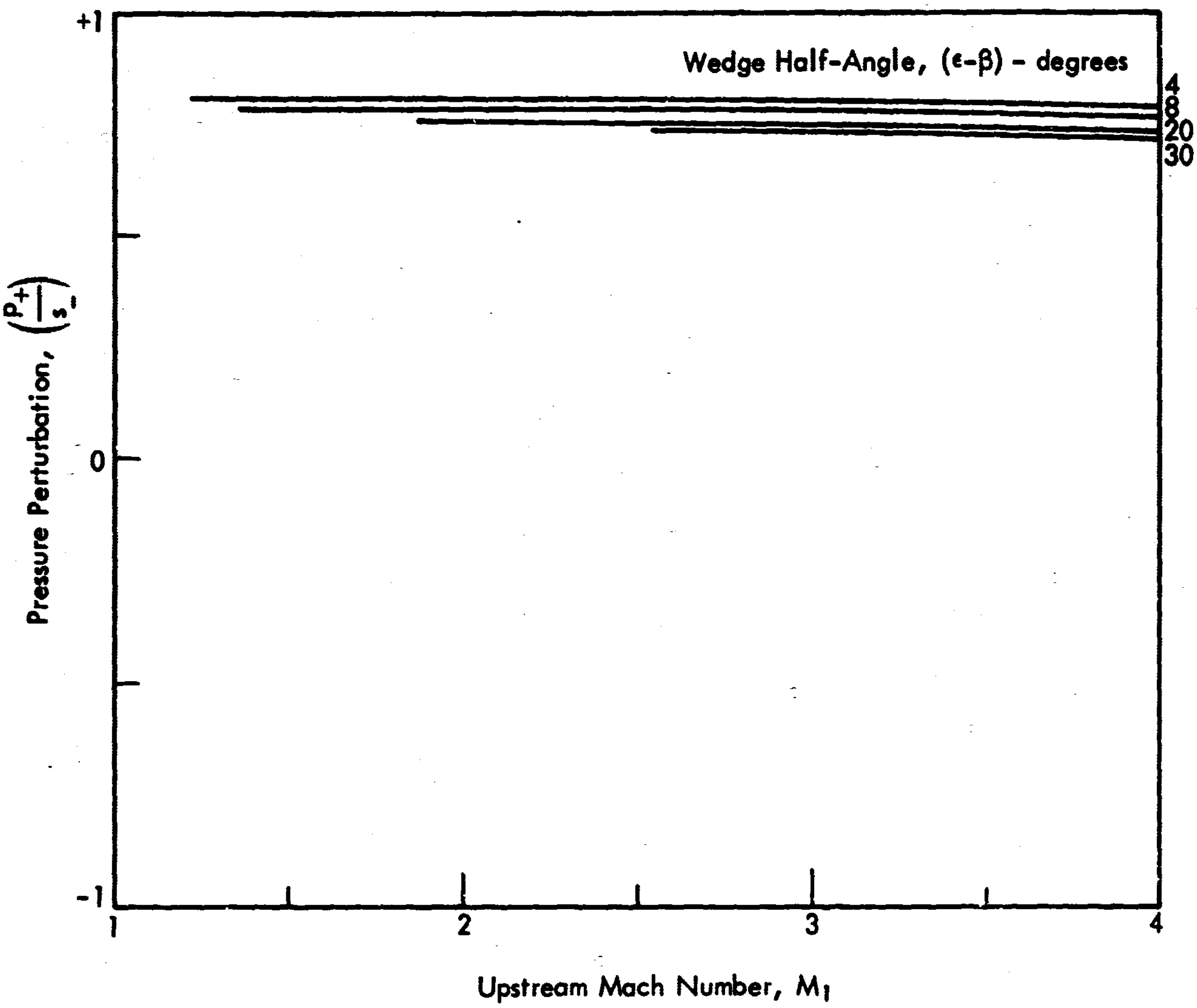

Figure 22. Generated Pressure Disturbance, Oblique Shock Case, $\delta = 1^o$

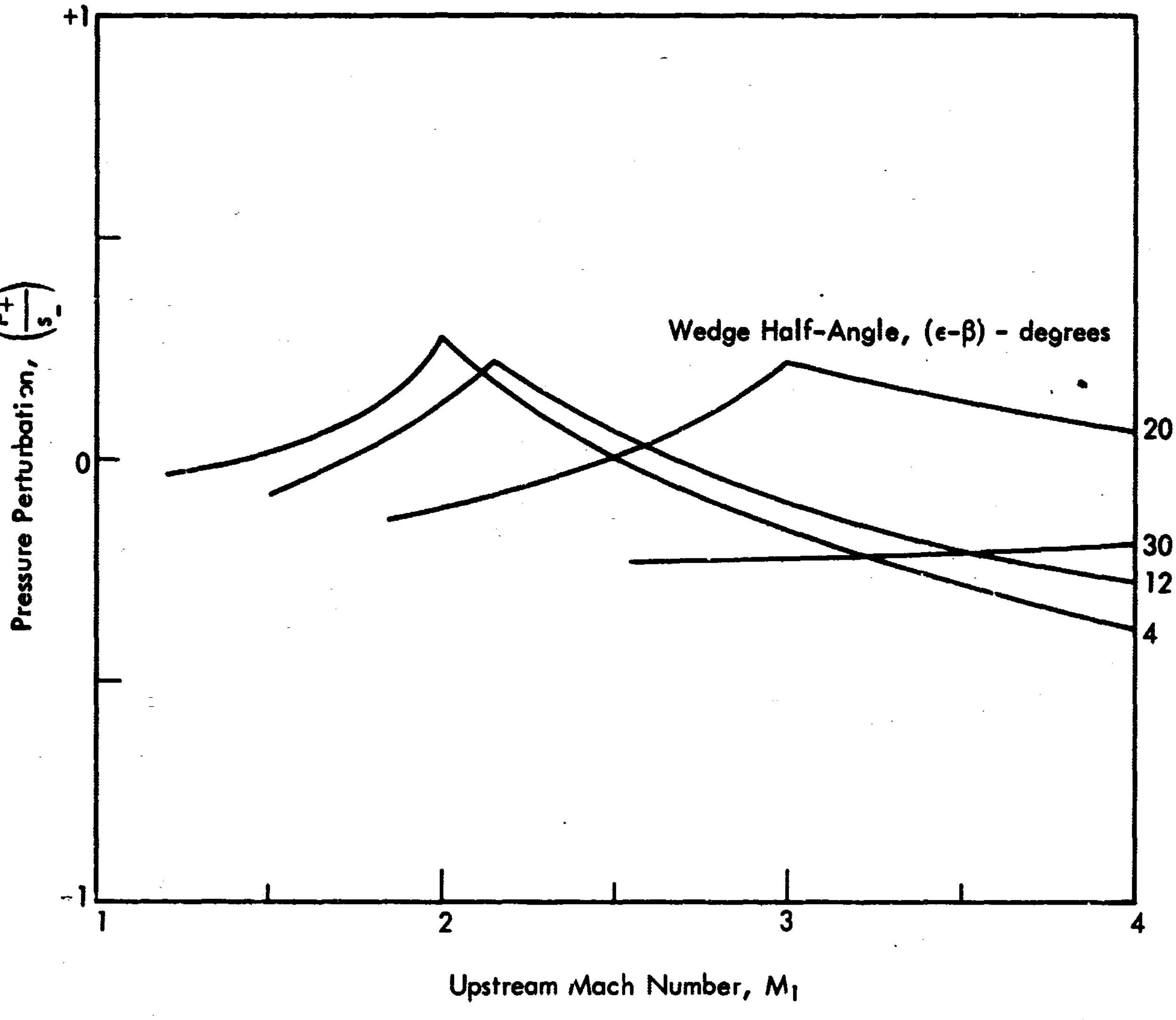

Figure 23. Generated Pressure Disturbance, Oblique Shock Case, $\delta = 10^{\circ}$

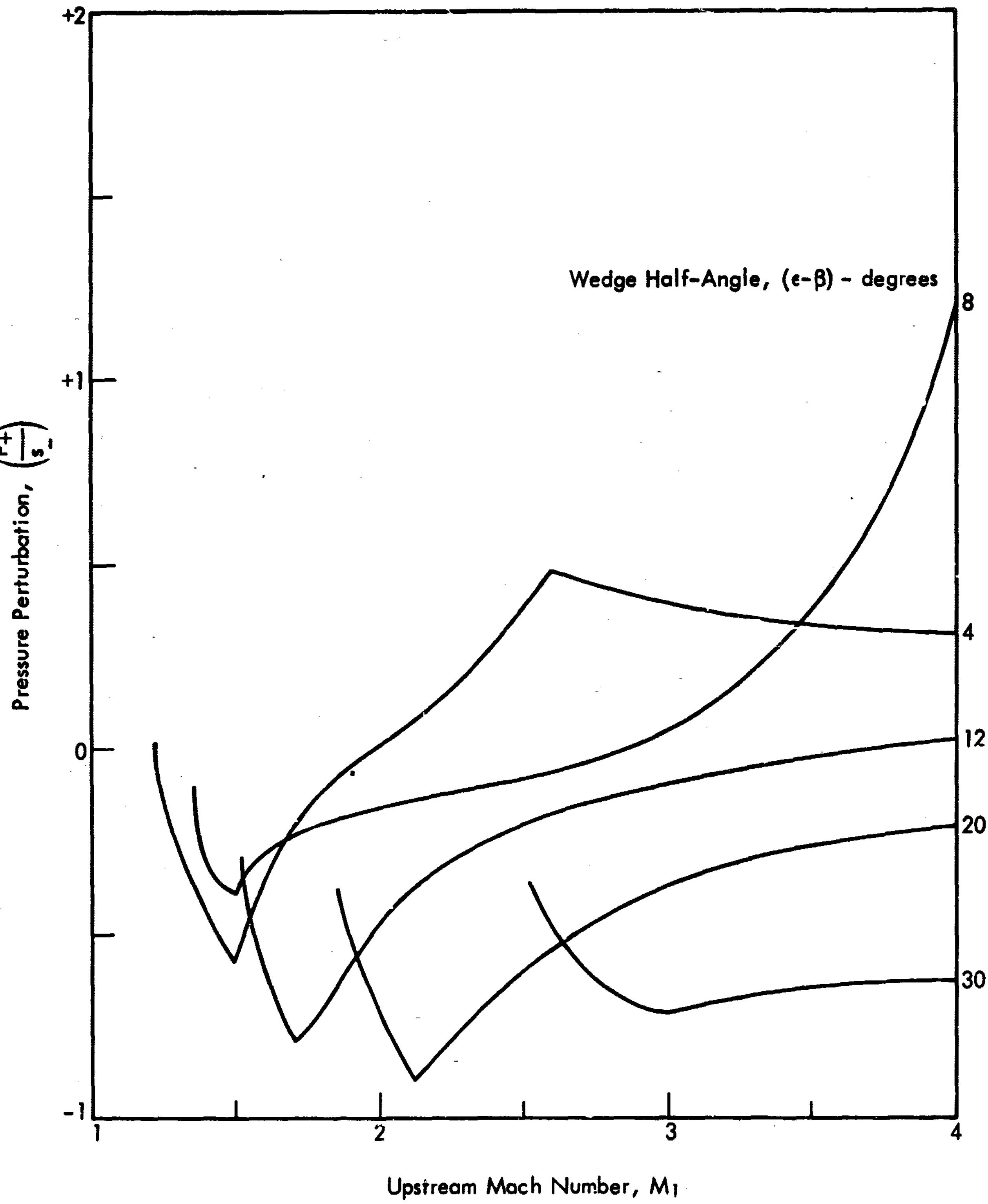

Figure 24. Generated Pressure Disturbance, Oblique Shock Case, δ = 50°

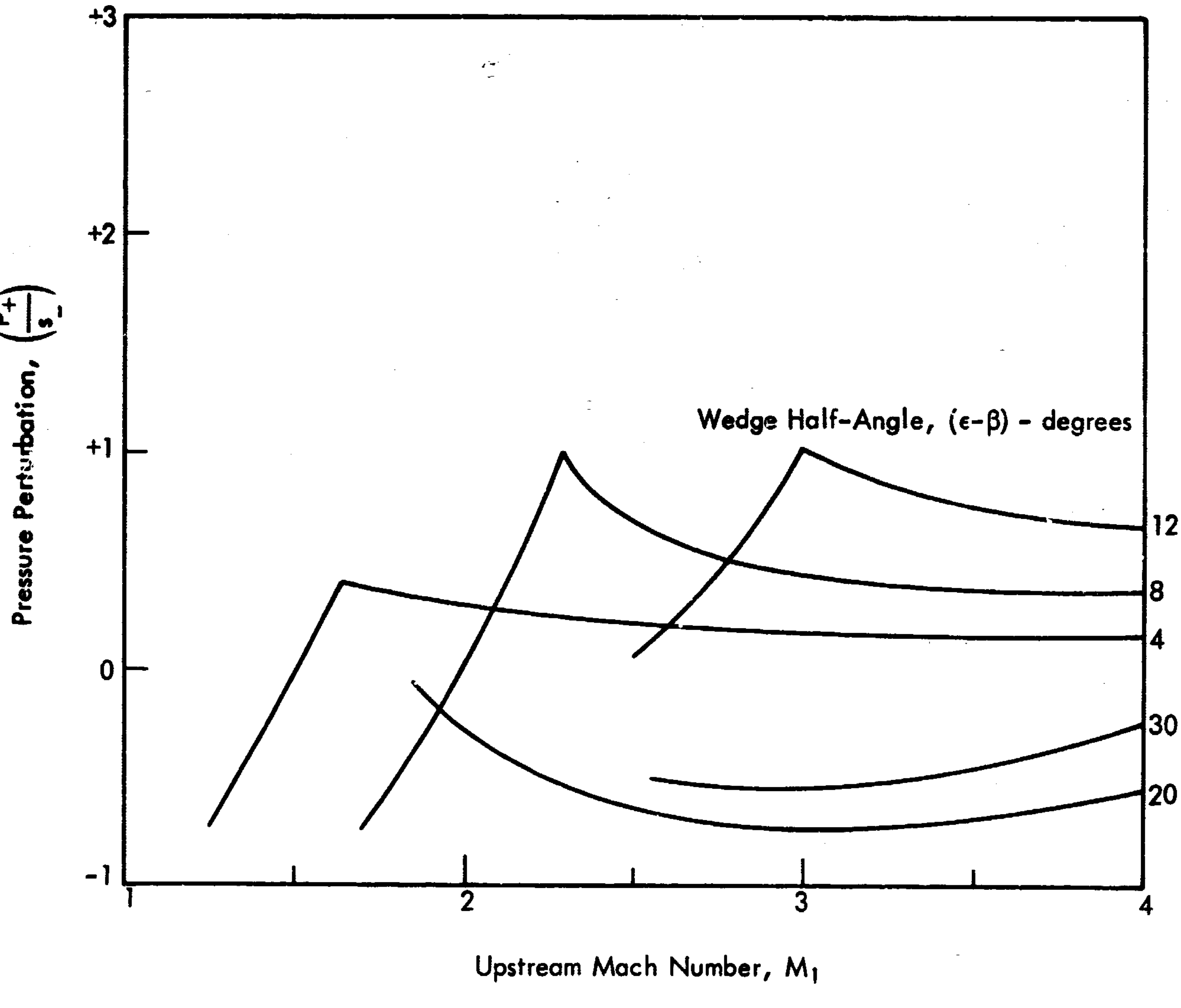

Figure 25. Generated Pressure Disturbance, Oblique Shock Case, $\delta = 60^\circ$

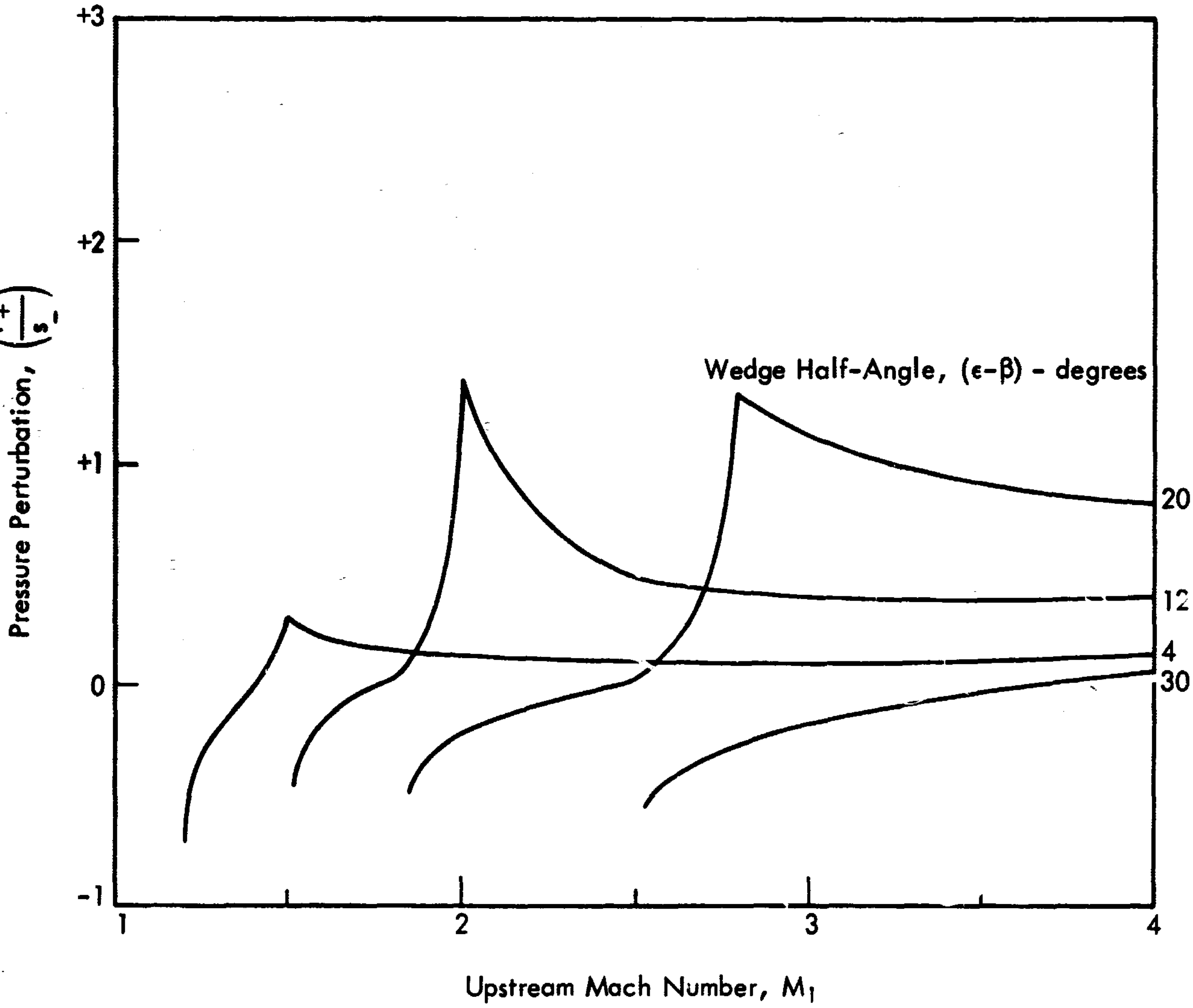

Figure 26. Generated Pressure Disturbance, Oblique Shock Case, $\delta = 70°$

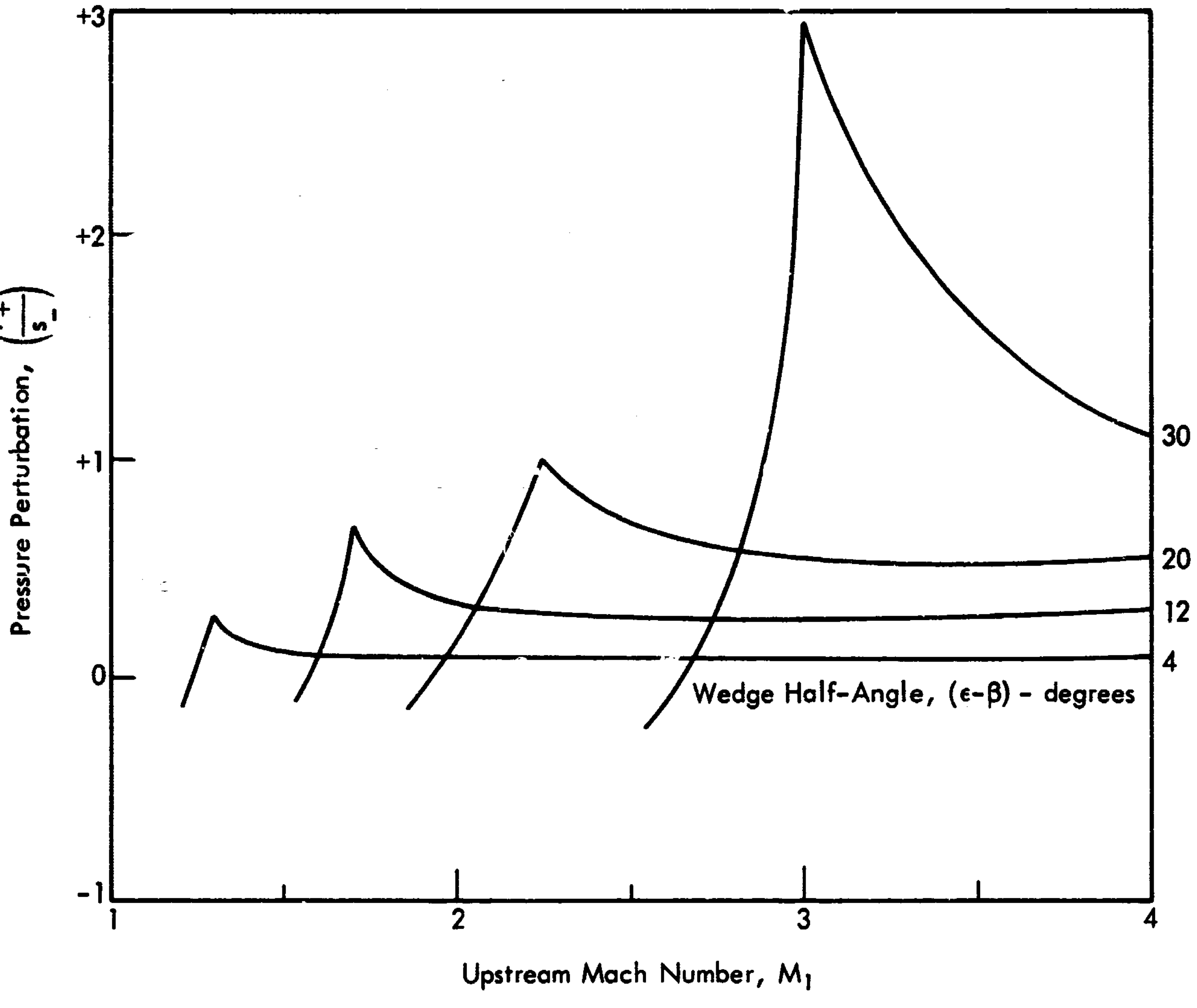

Figure 27. Generated Pressure Disturbance, Oblique Shock Case, $\delta = 80^{\circ}$

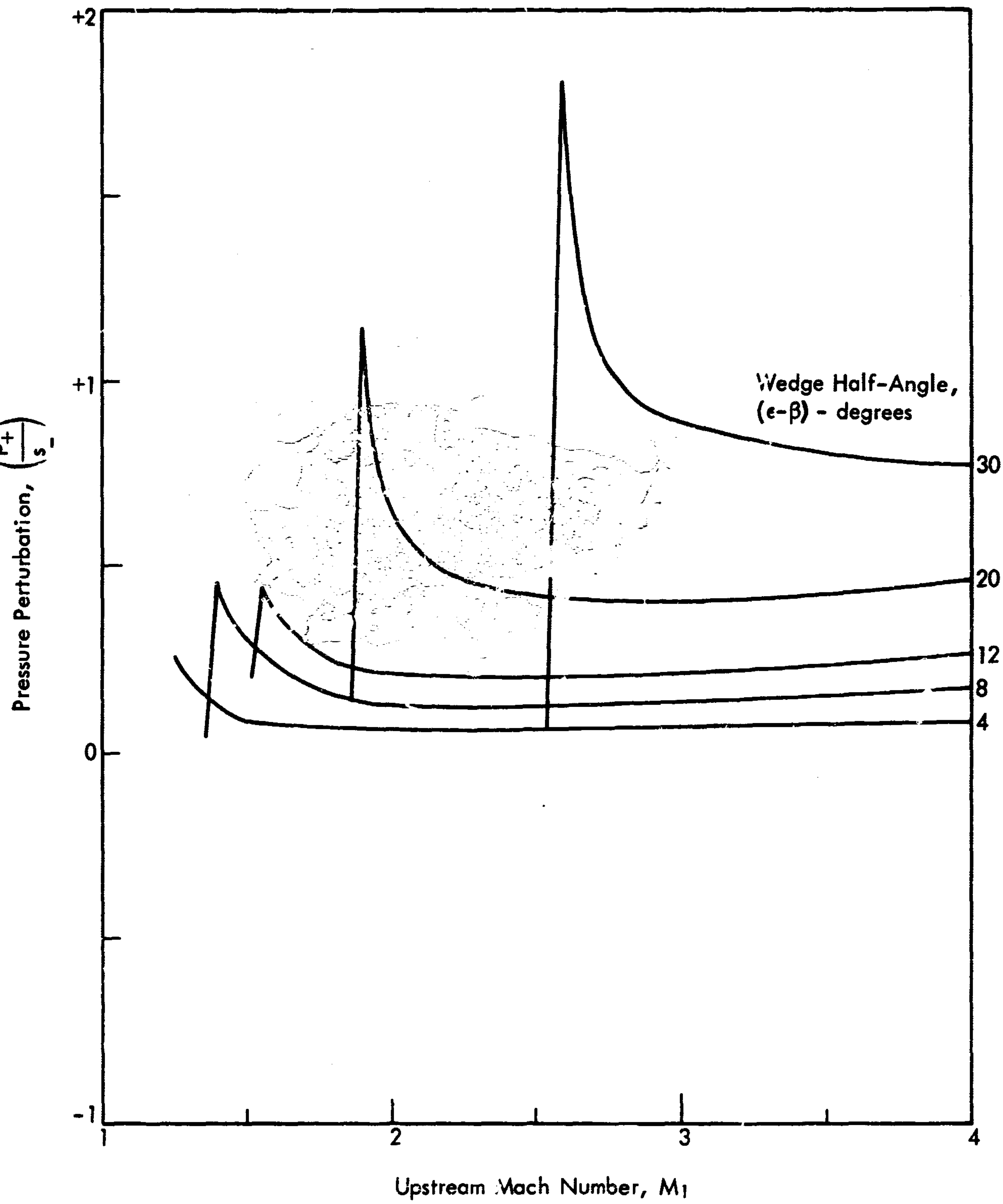

Figure 28. Generated Pressure Disturbance, Oblique Shock Case, $\delta = 89°$

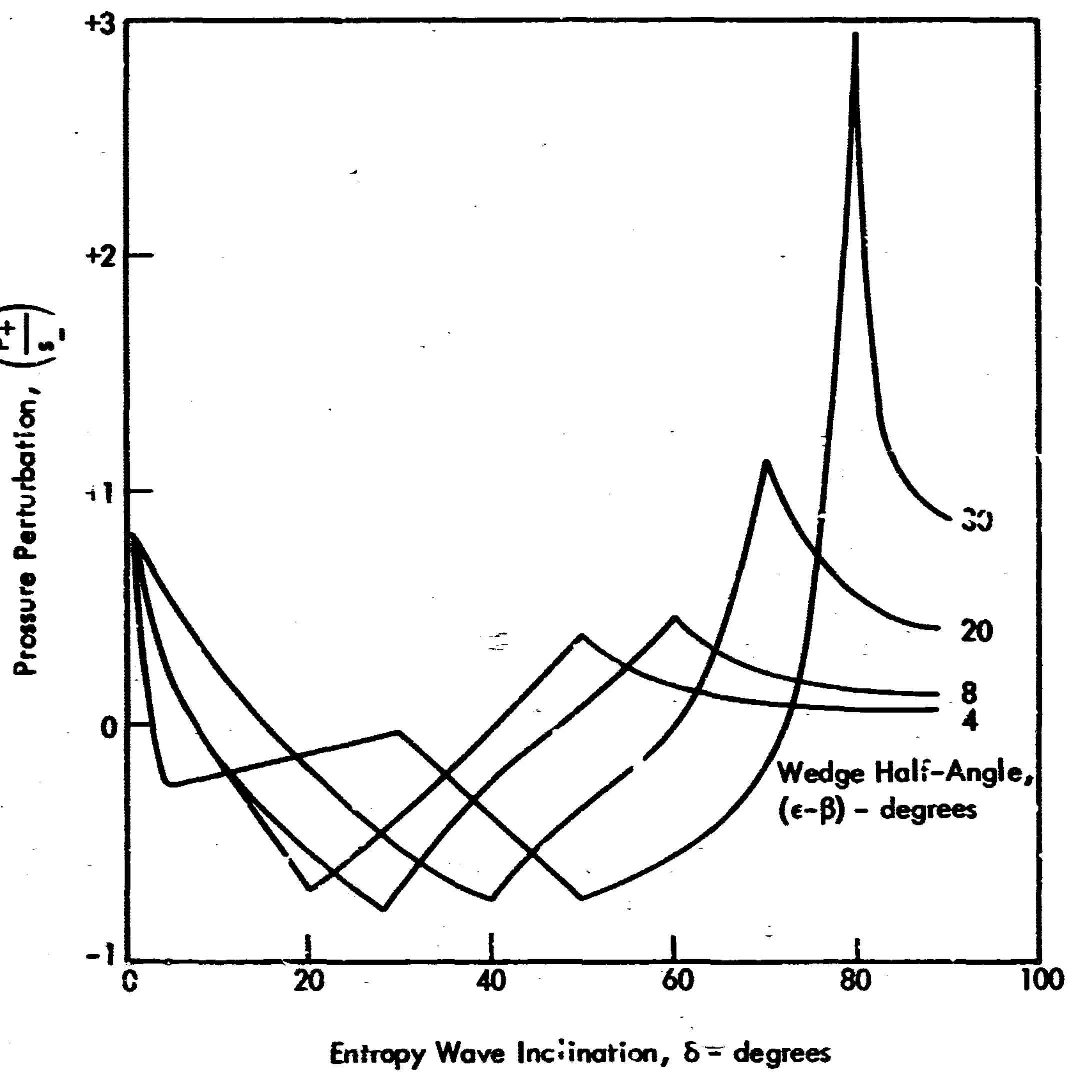

Figure 29. Generated Pressure Disturbance, Oblique Shock Case, $M_1 = 3$

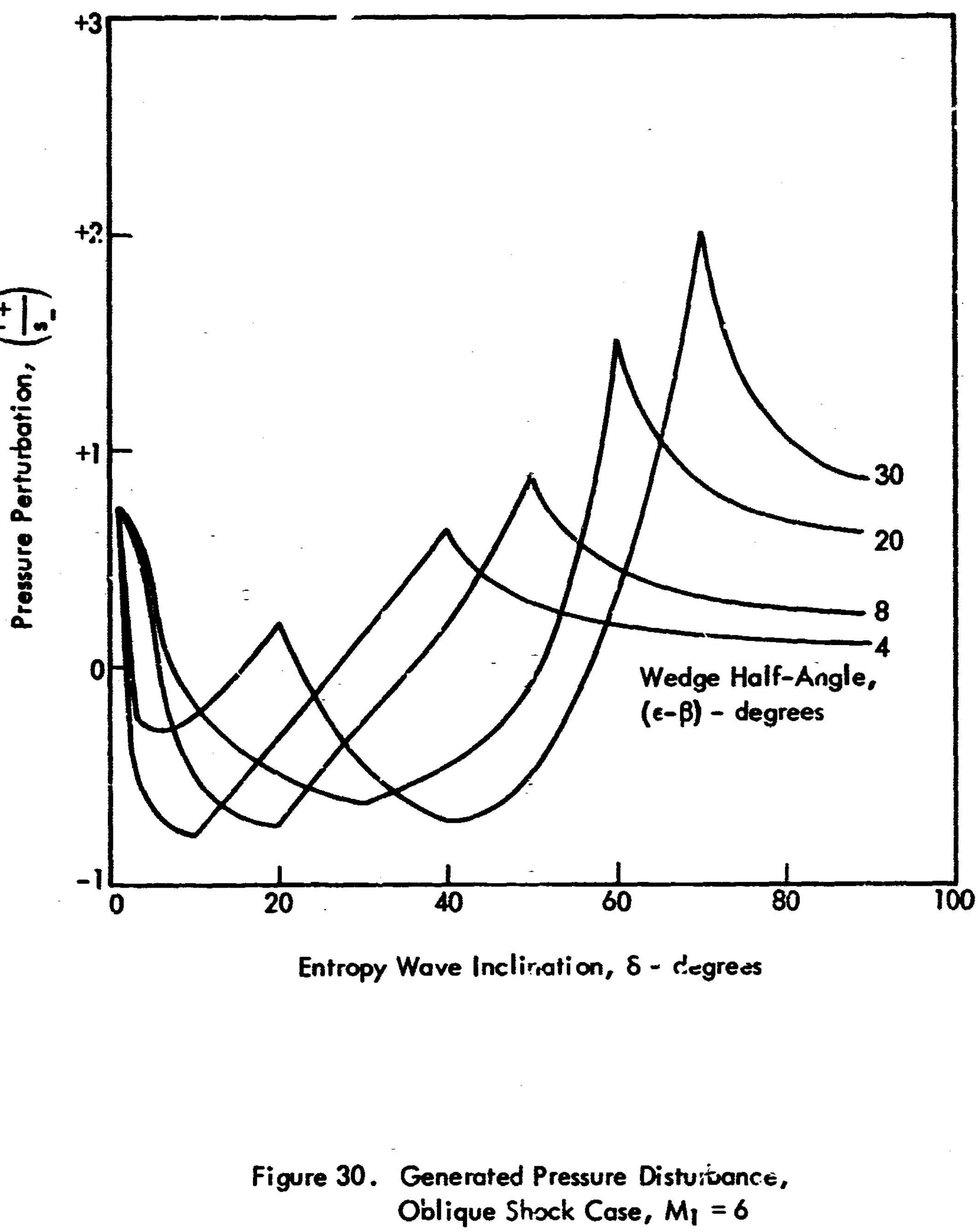

Figure 30. Generated Pressure Disturbance,
Oblique Shock Case, $M_1 = 6$

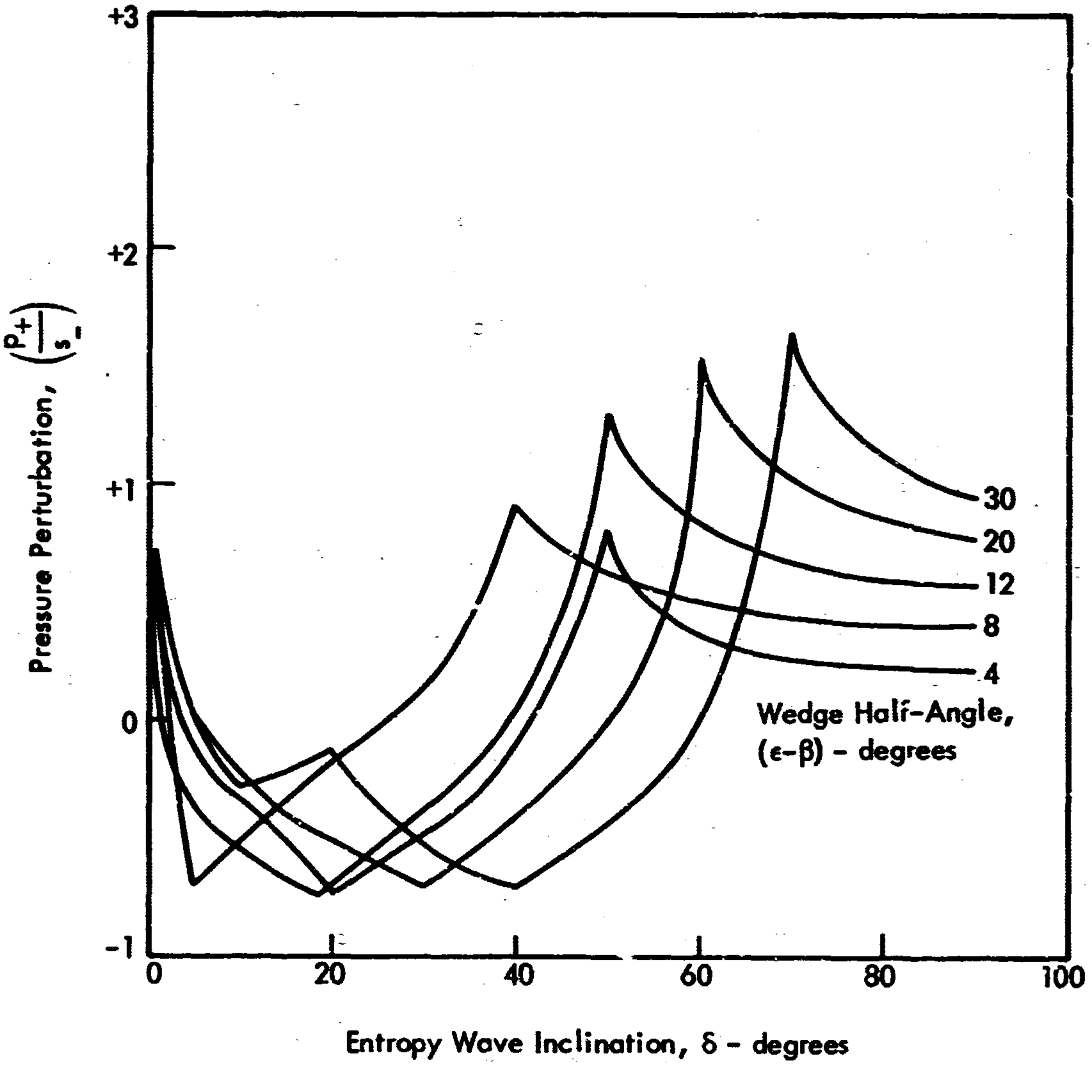

Figure 31. Generated Pressure Disturbance, Oblique Shock Case, $M_1 = 10$

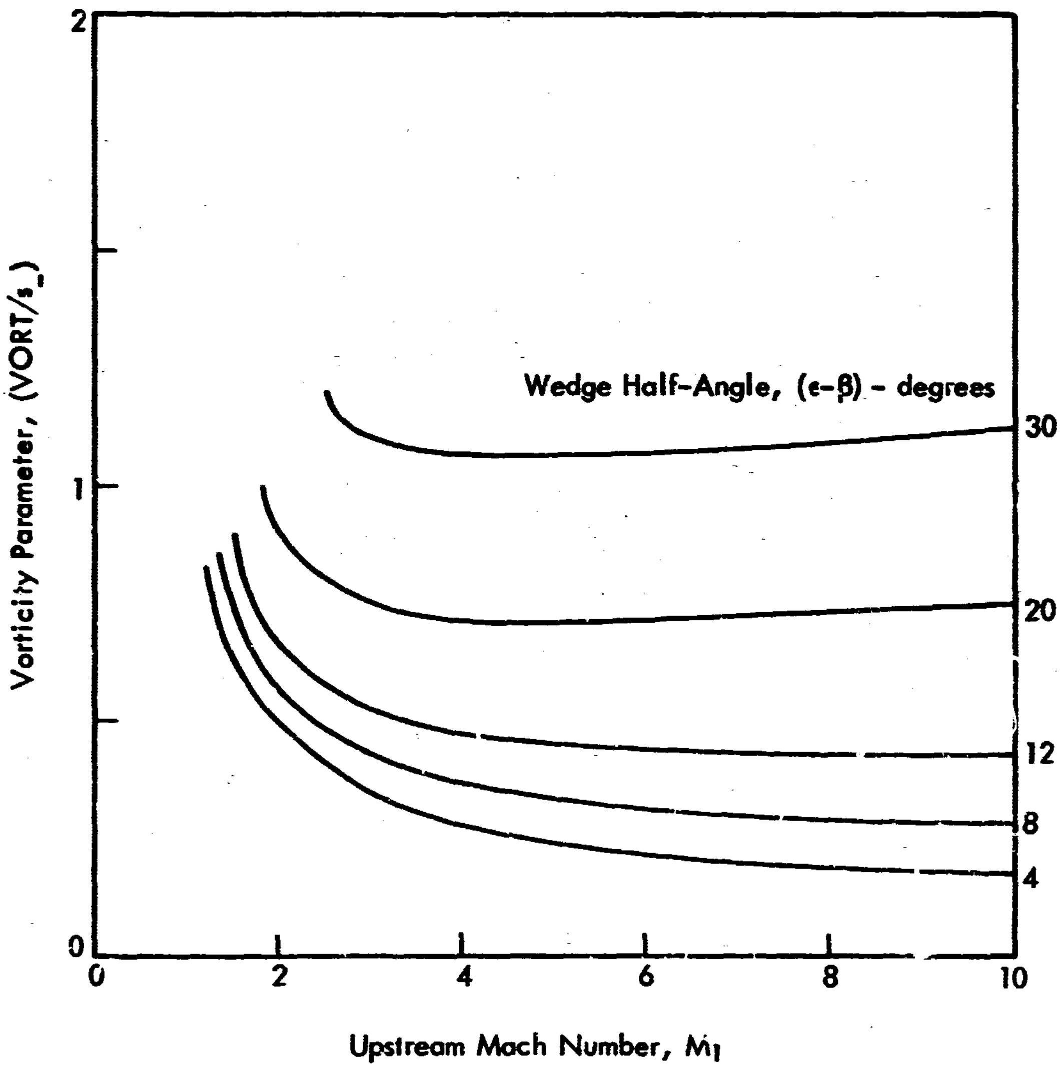

Figure 32. Generated Vorticity,
Oblique Shock Case, $\delta = 1°$

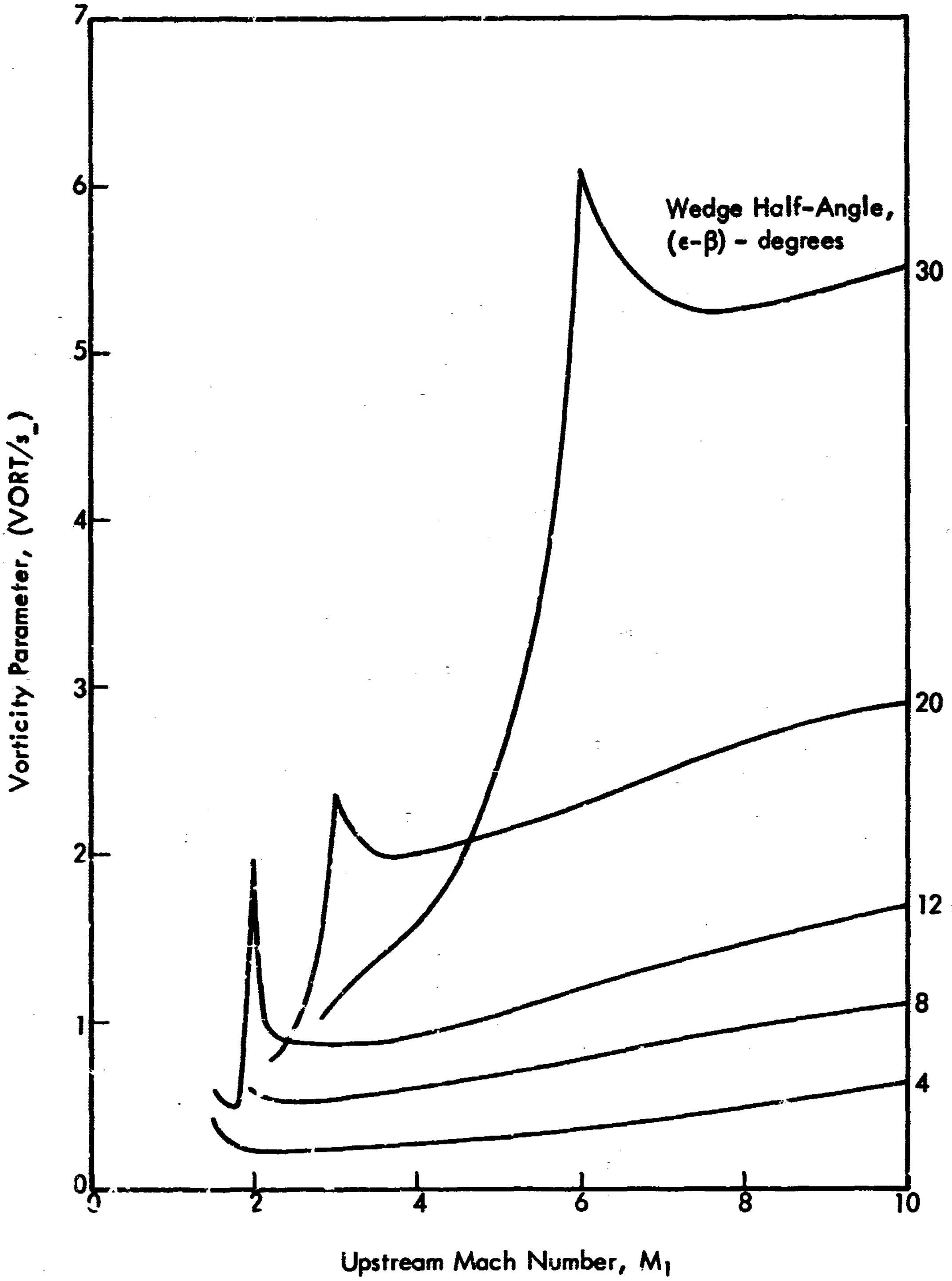

Figure 53. Generated Vorticity,
Oblique Shock Case, $\delta = 70^{o}$

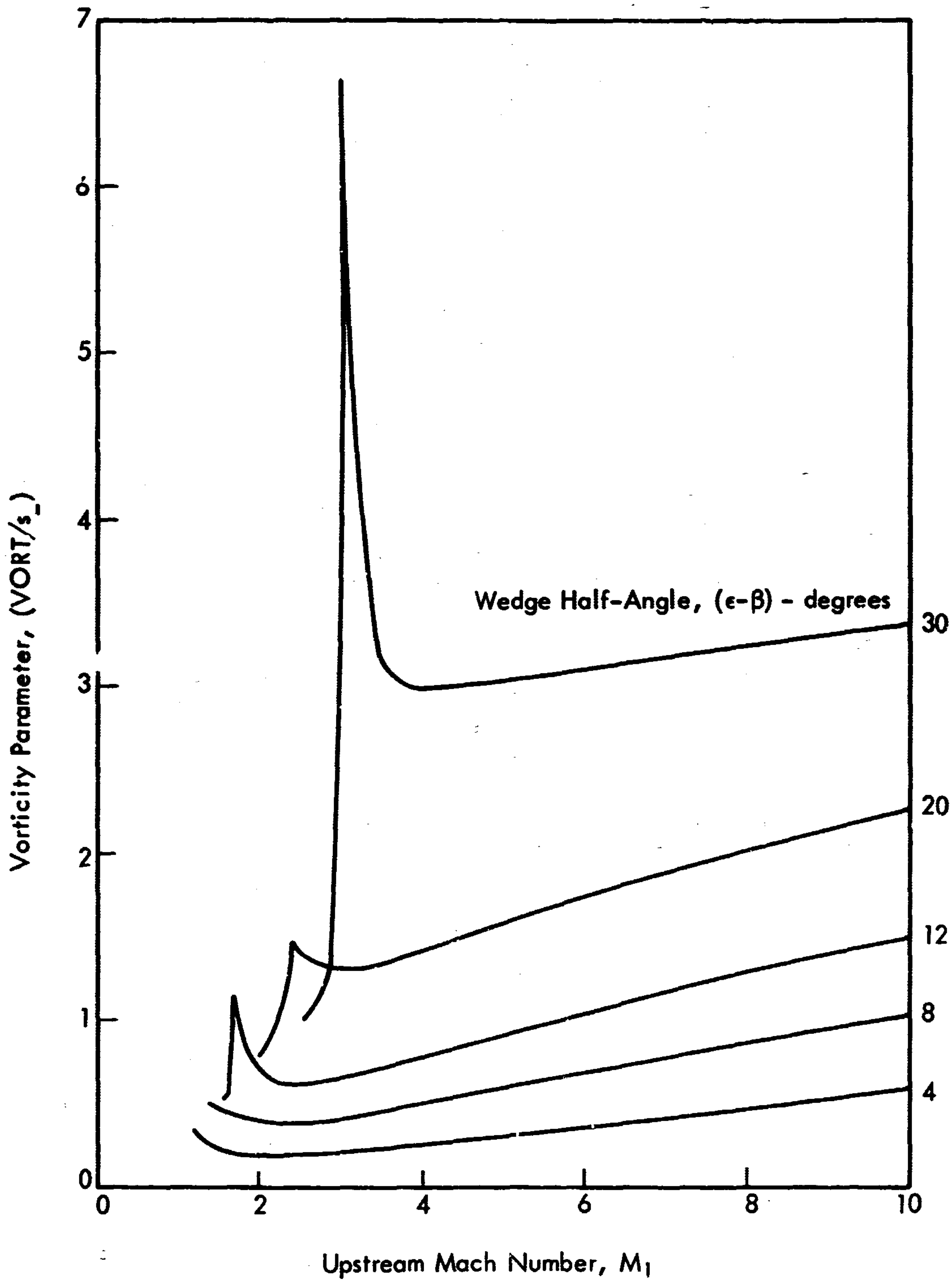

Figure 34. Generated Vorticity, Oblique Shock Case, $\delta = 80°$

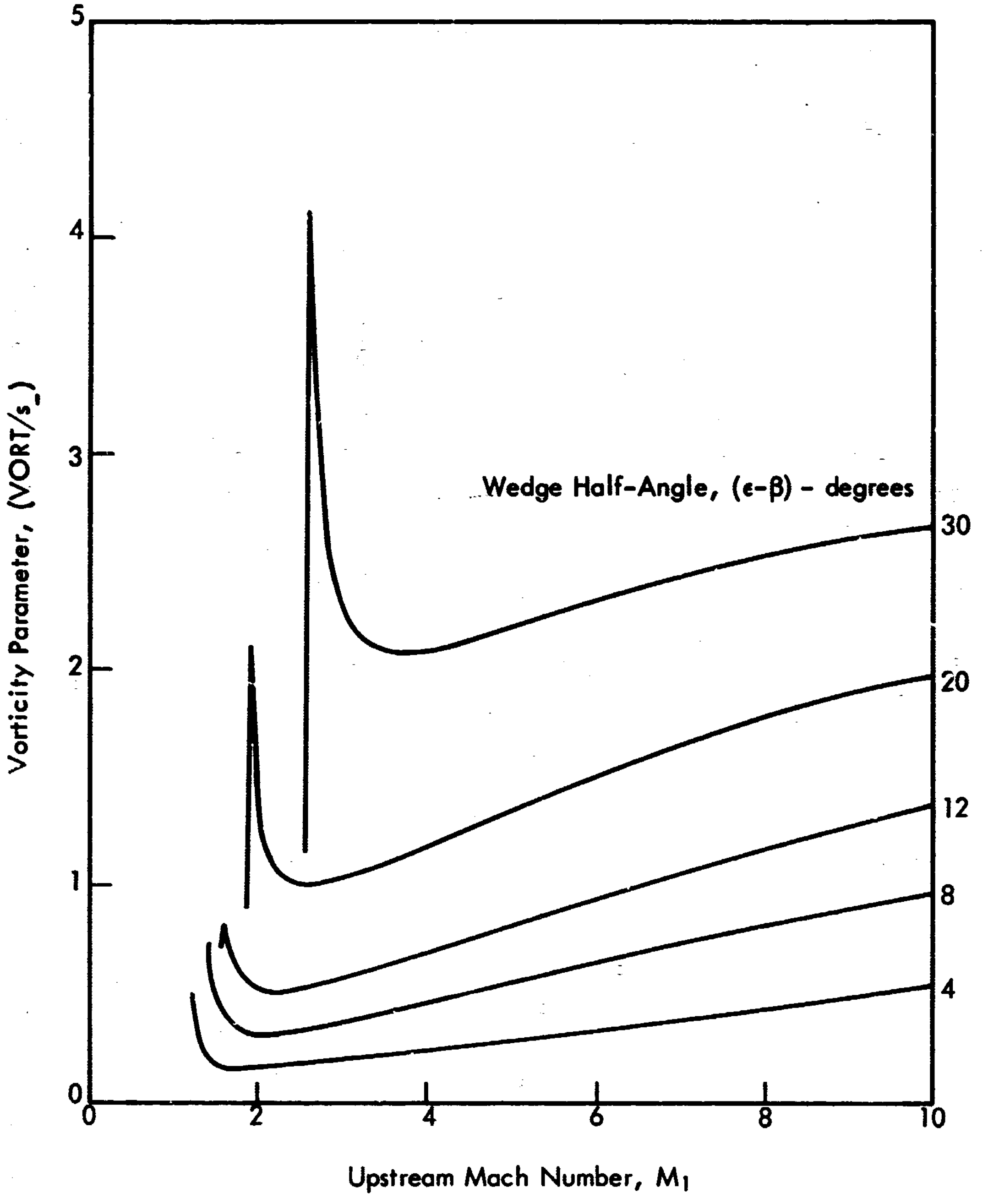

Figure 35. Generated Vorticity
Oblique Shock Case, δ = 89°

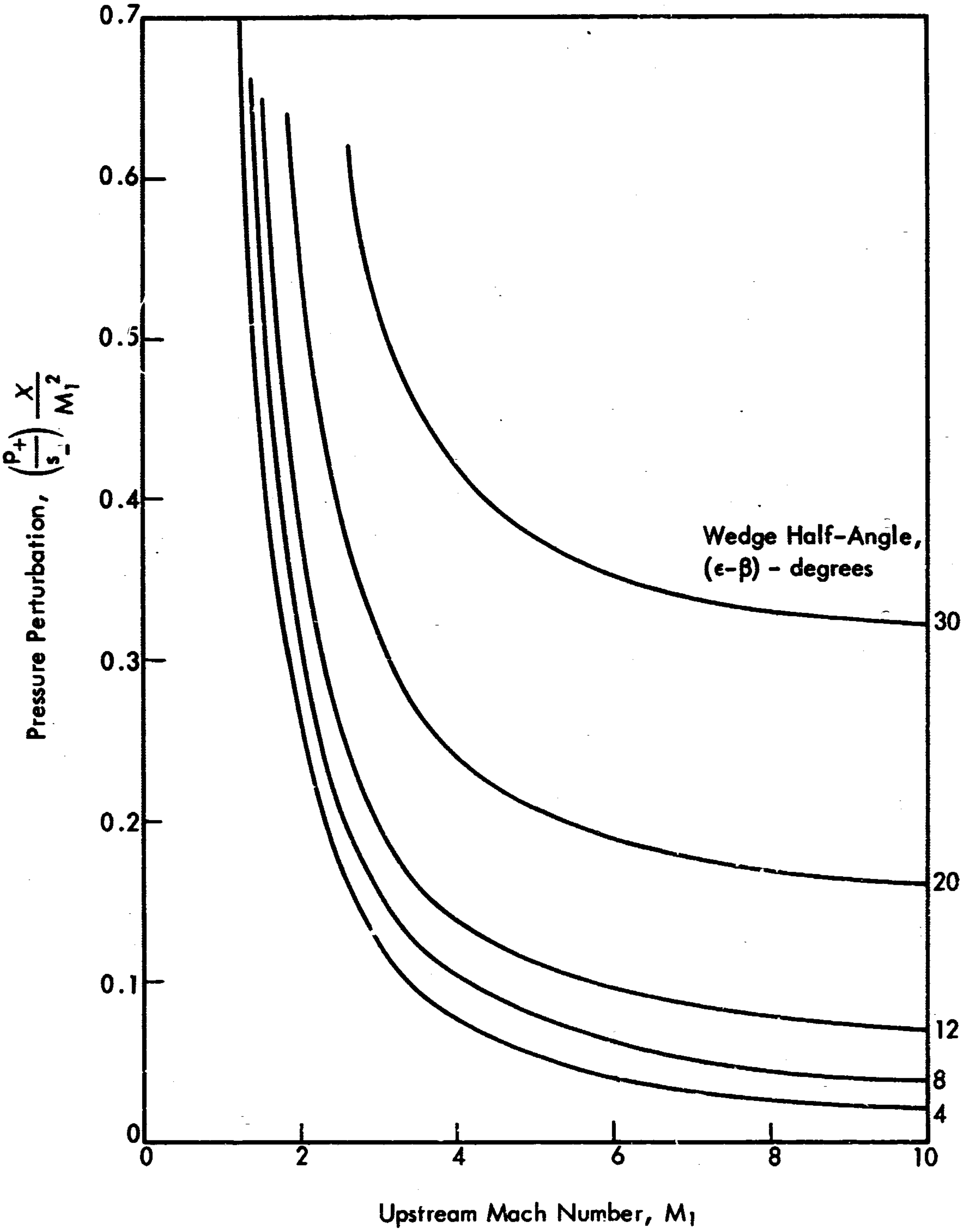

Figure 36. Pressure Disturbance Referenced to Free-Stream Conditions, Oblique Shock Case, $\delta = 1^\circ$

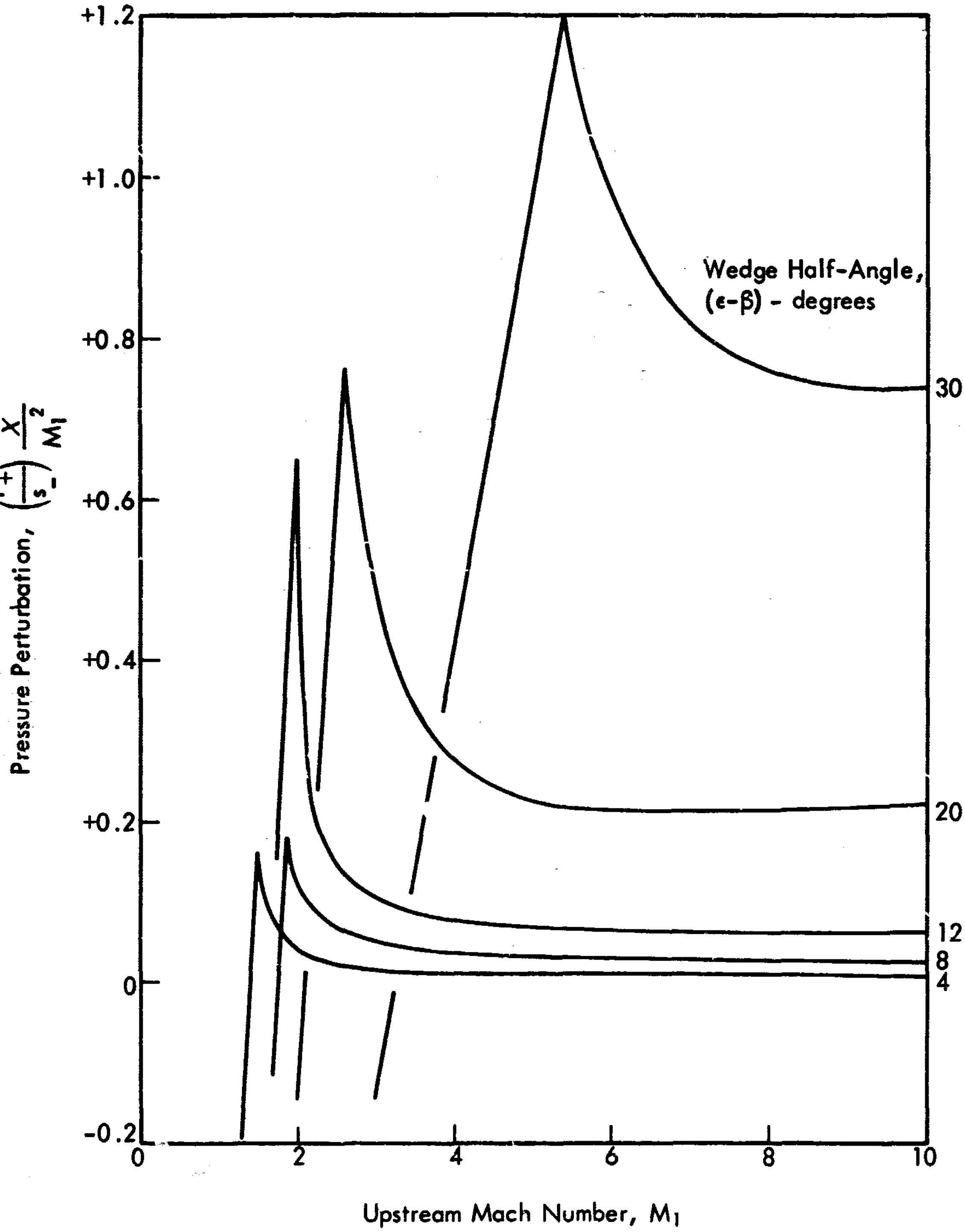

Figure 37. Pressure Disturbance Referenced to Free-Stream Conditions, Oblique Shock Case, $\delta = 70°$

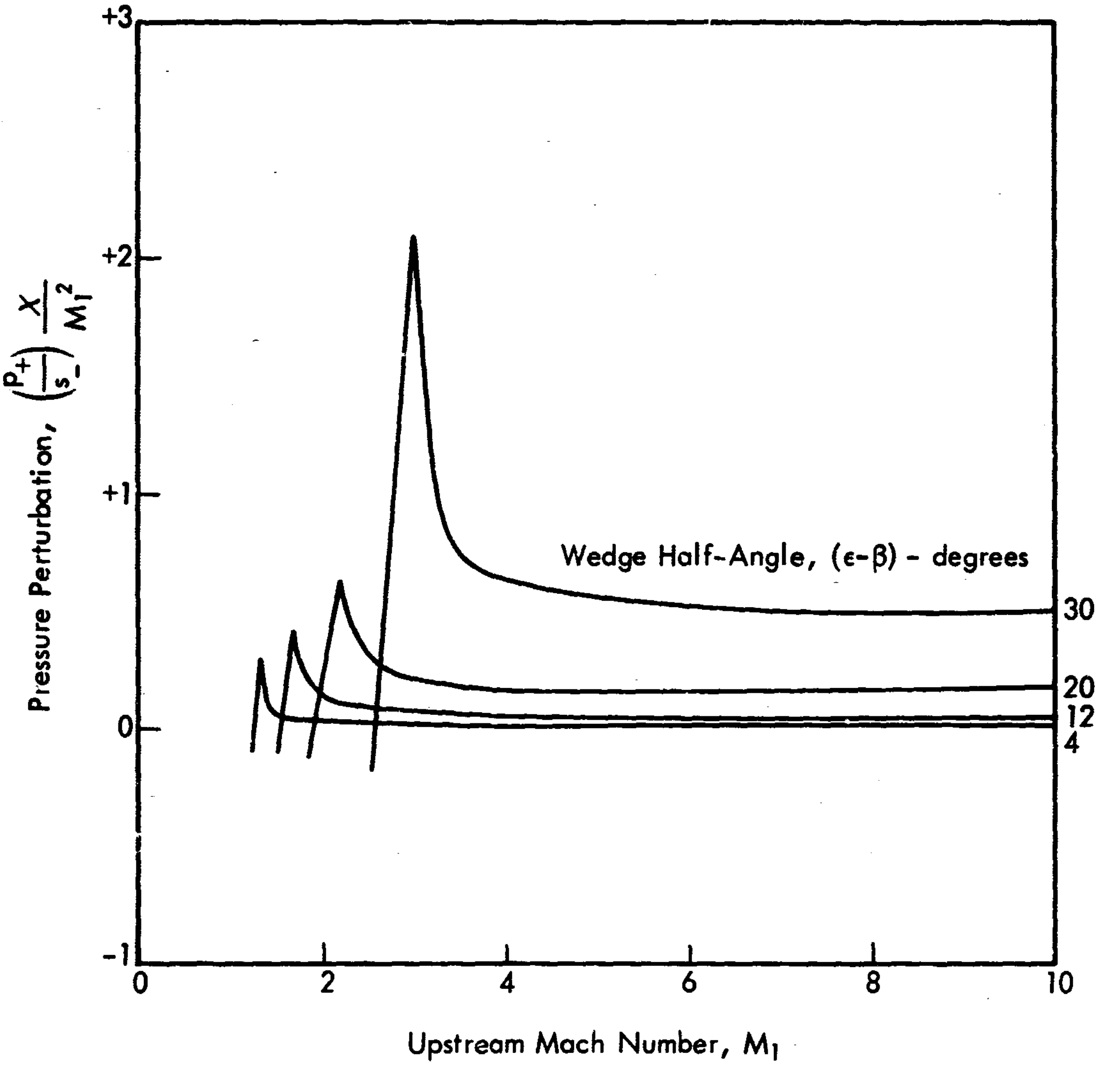

Figure 38. Pressure Disturbance Referenced to Free-Stream Conditions, Oblique Shock Case, $\delta = 80^\circ$

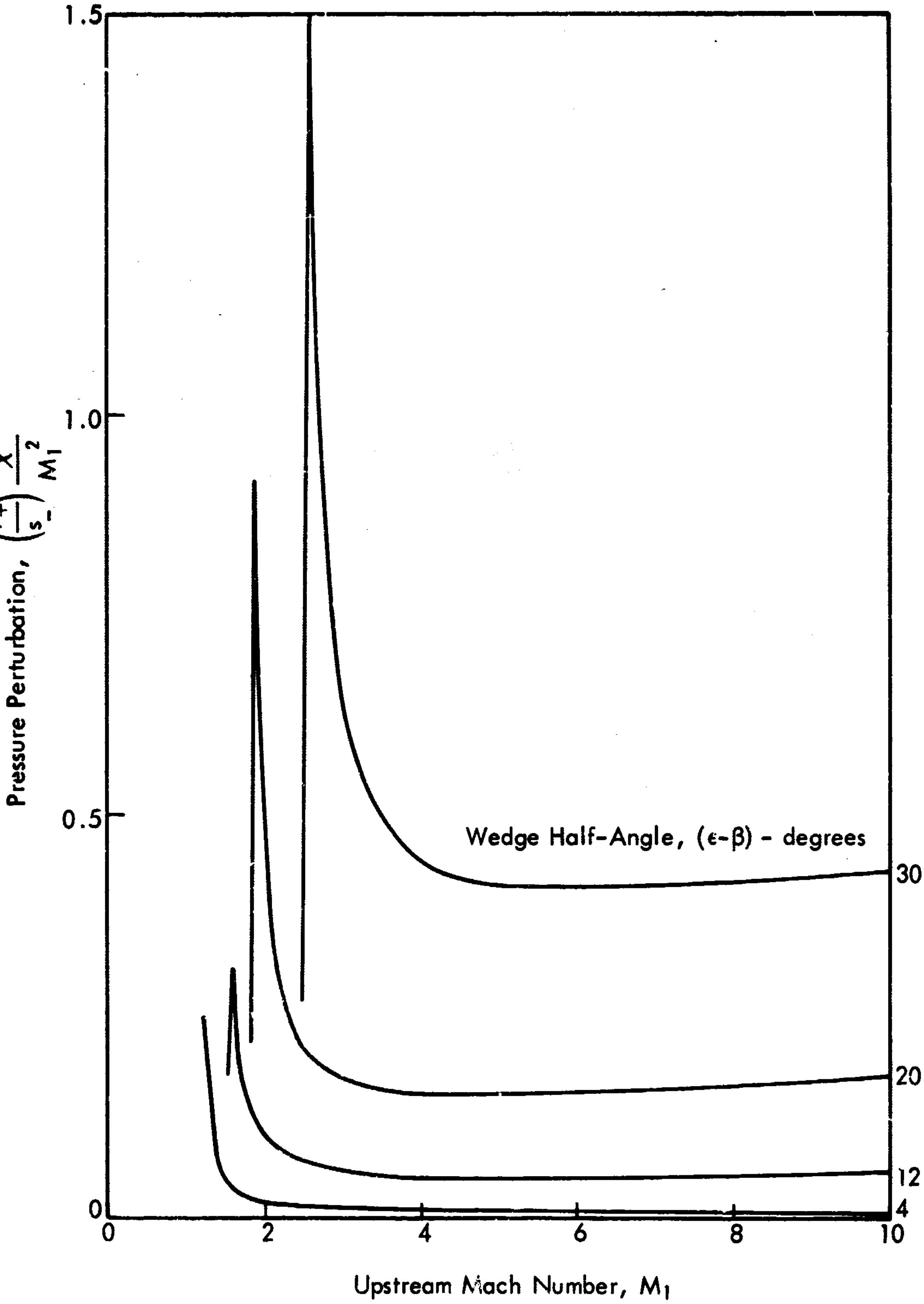

Figure 39. Pressure Disturbance Referenced to Free-Stream Conditions, Oblique Shock Case, $\delta = 89^{\circ}$

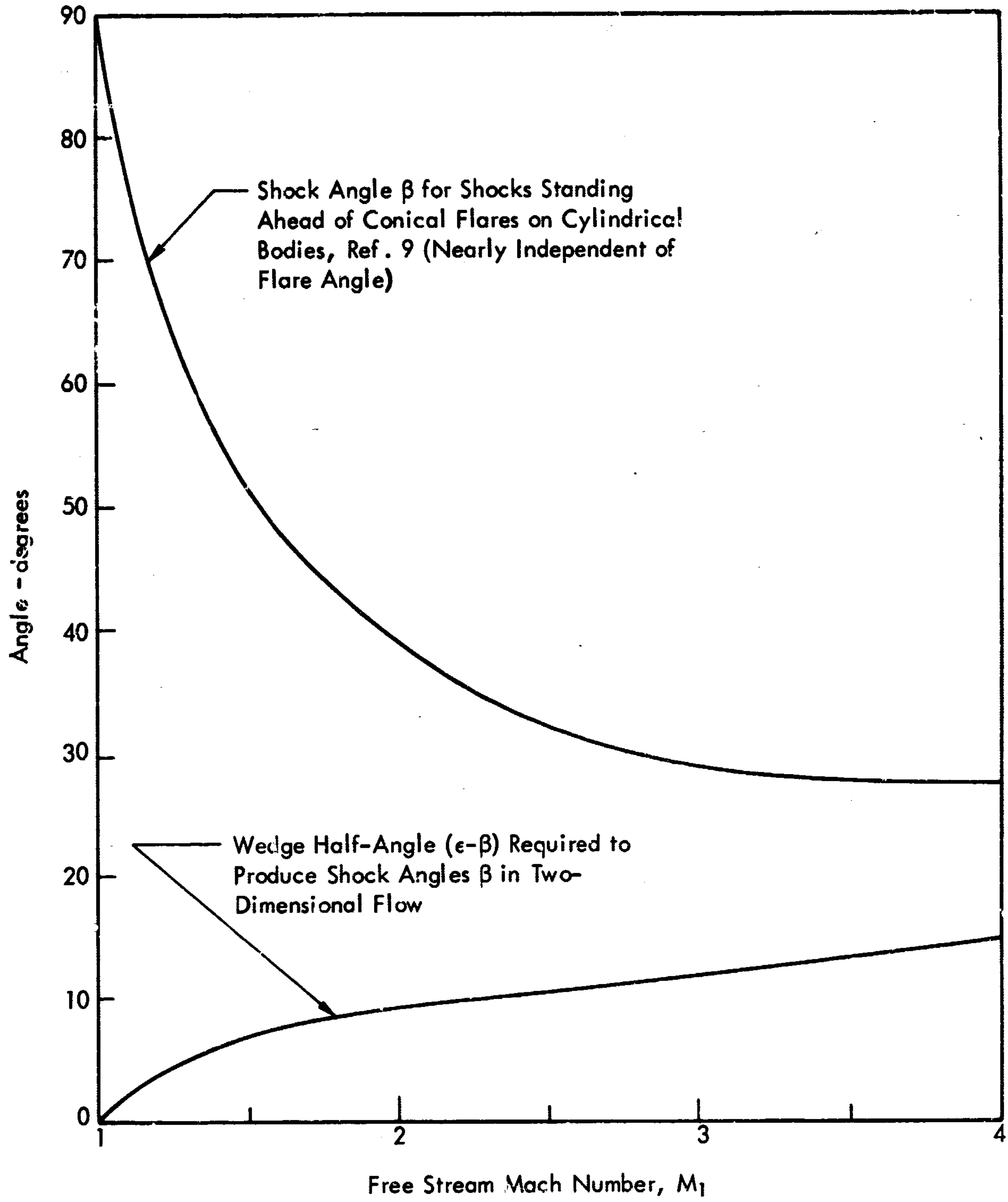

Figure 40. Interpretation for Separation Shocks Before Conical Transitions

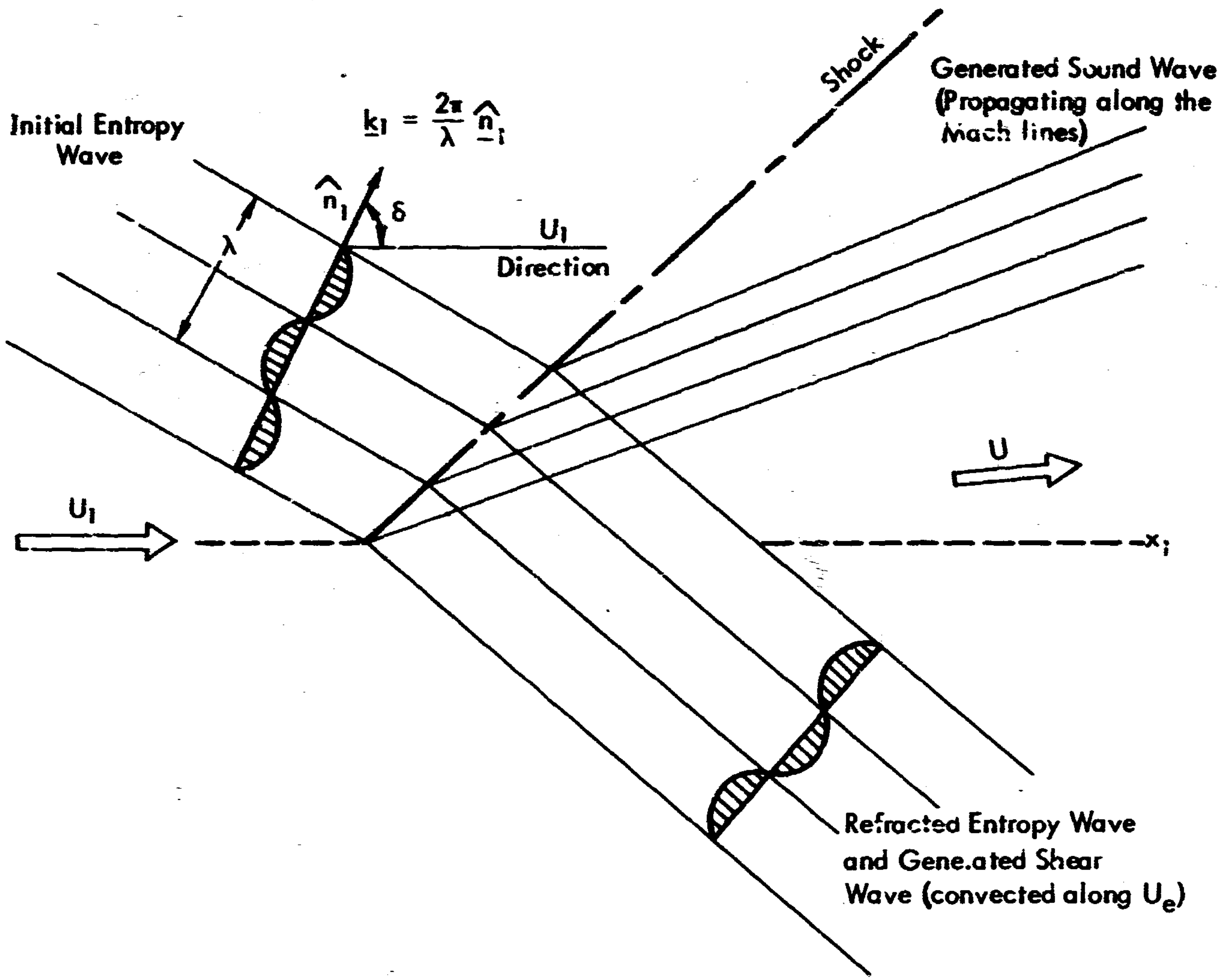

Figure 41. Shock Interaction Diagram For Simple Harmonic Entropy Waves

APPENDIX A

COMPUTER PROGRAM TO CALCULATE VARIOUS QUANTITIES ASSOCIATED WITH SHOCK ENTROPY INTERACTION

By

David M. Lister

APPENDIX A

COMPUTER PROGRAM TO CALCULATE VARIOUS QUANTITIES ASSOCIATED WITH SHOCK ENTROPY INTERACTION

Contents:

Sections:

Definition of Input Format

Quantities input are:

(1) The date of the run, e.g. 10/23/67, columns 1 through 8, format 2A4

(2) s_-, ϵ, β, M_1, γ, δ, A_1, ISW, ISW2 format 7F10.0, 2I5

(3) Repeat (2) for as many inputs as required.

Note that the quantities s_- through A_1 are defined in Section A.2.

If $\gamma \le 0$ then the run is terminated

If ISW > 1 then "δ^*" routine omitted

If ISW2 = 0 then full anotated output is obtained

If ISW2 $\neq$ 0 then the results for this case will appear only in the summary tables.

Definition of Output Alternatives

For each set of input data a full set of annotated results is output if ISW2 = 0 (see Section A.5).

At the end of each run or when the number of sets of input data equals a multiple of fifty, tables of the variable sets of input data with their calculated output quantities are printed (see Section A.5).

Note that all angles are quoted in degrees and radians.

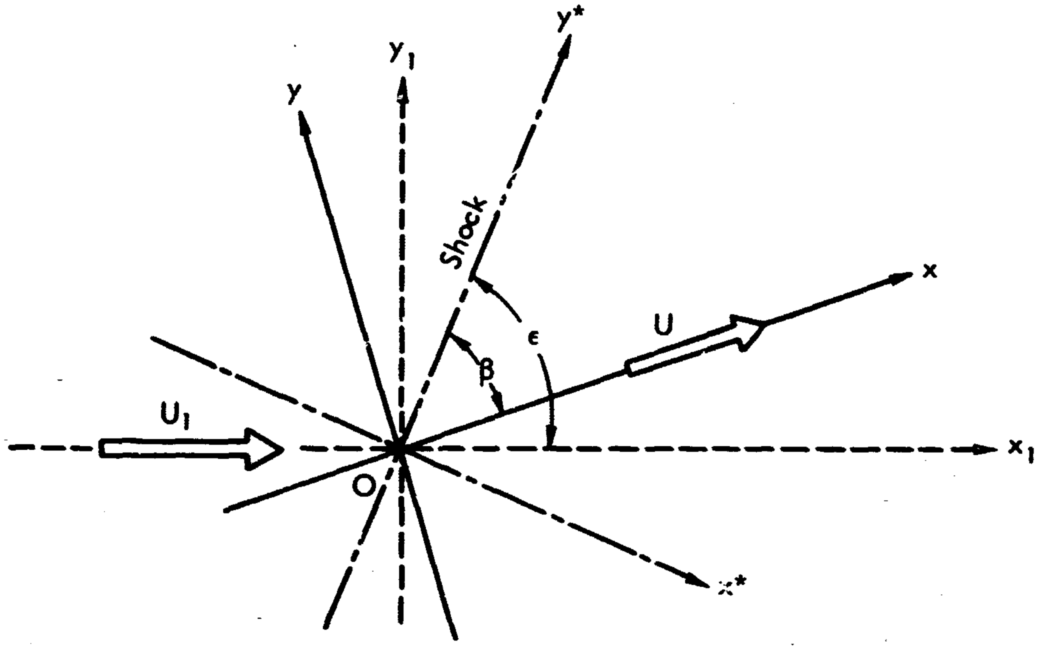

Figure A1. Basic Flow Coordinate Systems

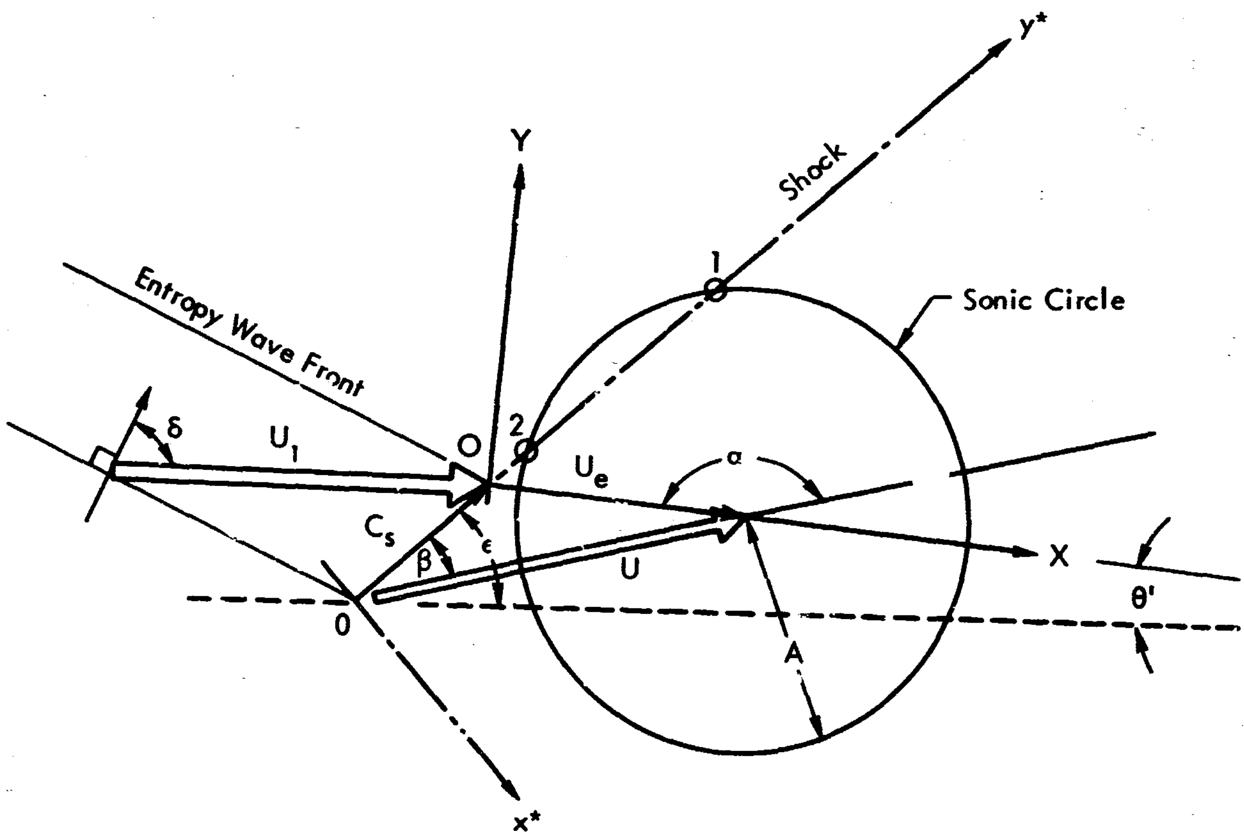

Figure A2. Intrinsic Frame of Reference with Respect to Downstream Flow Field

A.1 SHOCK ENTROPY INTERACTION

The given input quantities to the program are:

$M_1, \epsilon, \beta, \gamma, A_1, s_-$.

The equations used to compute the various required quantities are:

(1) $$X = \frac{p_m}{p_{1m}} = \frac{7 N_1^2 - 1}{6}$$

(2) $$M = \sqrt{\left(\frac{N_1^2 + 5}{7 N_1^2 - 1}\right) \Big/ \sin^2\beta}$$

(3) $$\frac{A}{A_1} = \sqrt{\frac{(7 N_1^2 - 1)\,(N_1^2 + 5)}{36 N_1^2}}$$

(3.12)

$$\Lambda_{11} = \left(\frac{\rho_m}{\rho_{1m}}\right)^2\left(\frac{N}{N_1}\right)^2 - (\gamma - 1)\left(1 - \frac{\rho_m}{\rho_{1m}}\right) N^2 \qquad (19)$$

$$\Lambda_{21} = \frac{N^2}{1 - N^2}\left\{\left(1 - \frac{\rho_m}{\rho_{1m}}\right)\left[1 + (\gamma - 1)\, N^2\right] + \left[1 - \left(\frac{\rho_m}{\rho_{1m}}\right)^2\left(\frac{N}{N_1}\right)^2\right]\right\}$$

$$\Lambda_{31} = \frac{-N}{1 - N^2}\left\{\left[1 - \left(\frac{\rho_m}{\rho_{1m}}\right)^2\left(\frac{N}{N_1}\right)^2\right] + \left(1 - \frac{\rho_m}{\rho_{1m}}\right)\gamma N^2\right\}$$

$$\Lambda_{12} = (\gamma - 1)\left(1 - \frac{\rho_m}{\rho_{1m}}\right)\left(1 - \frac{1}{N_1^2}\,\frac{\rho_m}{\rho_{1m}}\right) N^2$$

$$\Lambda_{22} = \frac{-N^2}{1-N^2}\left\{\left(1-\frac{\rho_m}{\rho_{1m}}\right) + \left(1-\frac{1}{N_1^2}\,\frac{\rho_m}{\rho_{1m}}\right)\left[1+(\gamma-1)\left(1-\frac{\rho_m}{\rho_{1m}}\right)N^2\right]\right\}$$

$$\Lambda_{32} = \frac{N}{1-N^2}\left\{\left[1-\left(\frac{\rho_m}{\rho_{1m}}\right)^2\left(\frac{N}{N_1}\right)^2\right] + \gamma\left(1-\frac{\rho_m}{\rho_{1m}}\right)\left(1-\frac{1}{N_1^2}\,\frac{\rho_m}{\rho_{1m}}\right)N^2\right\}$$

$$\Lambda_{13} = (\gamma-1)\left(1-\frac{\rho_m}{\rho_{1m}}\right)^2\frac{N^2}{N_1}$$

$$\Lambda_{23} = \frac{-N}{1-N^2}\left(1-\frac{\rho_m}{\rho_{1m}}\right)\left\{2+(\gamma-1)\left(1-\frac{\rho_m}{\rho_{1m}}\right)N^2\right\}\frac{N}{N_1}$$

$$\Lambda_{33} = \frac{1}{1-N^2}\,\frac{N}{N_1}\left\{1-\left(\frac{\rho_m}{\rho_{1m}}\,N\right)^2 + \gamma\left(1-\frac{\rho_m}{\rho_{1m}}\right)^2N^2\right\}$$

$$\Lambda_{44} = \left(\frac{\rho_m}{\rho_{1m}}\right)\frac{N}{N_1}$$

$$\pi_{11} = -(\gamma-1)\left(1-\frac{\rho_{1m}}{\rho_m}\right)^2\left(\frac{\rho_m}{\rho_{1m}}\right)N$$

$$\pi_{21} = \frac{-N}{1-N^2}\left(1-\frac{\rho_{1m}}{\rho_m}\right)\left[2+(\gamma-1)\left(1-\frac{\rho_m}{\rho_{1m}}\right)N^2\right]$$

$$\pi_{31} = \frac{1}{1-N^2}\left(1-\frac{\rho_{1m}}{\rho_m}\right)\left[1+N^2+(\gamma-1)\left(1-\frac{\rho_m}{\rho_{1m}}\right)N^2\right]$$

$$\pi_{41} = \left(\frac{\rho_m}{\rho_{1m}}-1\right)N$$

(3.14) $$N = M \sin\beta \qquad (20)$$

(3.18) $$\frac{\rho_m}{\rho_{im}} = \frac{6\chi + 1}{\chi + 6}$$

(3.13) $$N_1 = M_1 \sin \epsilon \qquad (20)$$

(4) $$A = \left(\frac{A}{A_1}\right) A_1$$

(5) $$U = MA$$

(5.1) $$U_1 = M_1 A_1$$

(6.01) $$C_s = \frac{\cos\delta}{\cos(\delta - \epsilon)} U_1 \qquad (24)$$

(6.10) $$\mu_e = \arcsin\left(\frac{1}{M_e}\right)$$

(6.09) $$\begin{bmatrix} u^* \\ v^* \end{bmatrix} = \begin{bmatrix} \sin(\alpha - \beta) & \cos(\alpha - \beta) \\ -\cos(\alpha - \beta) & \sin(\alpha - \beta) \end{bmatrix} \begin{bmatrix} U_+ \\ V_+ \end{bmatrix}$$ (Matrix Notation) (30)

(6.17) $$\begin{bmatrix} s_+ \\ p_+ \\ U_+ \\ V_+ \end{bmatrix} = \begin{bmatrix} \Lambda_{11} \\ \Lambda_{21} \\ \Lambda_{31} \sin(\alpha - \beta) \\ \Lambda_{31} \cos(\alpha - \beta) \end{bmatrix} s_- + \begin{bmatrix} \pi_{11} & (M\cos\beta - C_s/A) \\ \pi_{21} & (M\cos\beta - C_s/A) \\ \pi_{31} & (M\cos\beta - C_s/A)\sin(\alpha-\beta) - \pi_{41}\cos(\alpha-\beta) \\ \pi_{31} & (M\cos\beta - C_s/A)\cos(\alpha-\beta) - \pi_{41}\sin(\alpha-\beta) \end{bmatrix} \times$$

$$\times \quad \sin(\alpha - \beta)\,\Psi_y \qquad (31)$$

(6.17d) $$V_+ = \Lambda_{31}\cos(\alpha - \beta)\, s_- + \left[\pi_{31}\left(M\cos\beta - \frac{C_s}{A}\right)\cos(\alpha - \beta) + \pi_{41}\sin(\alpha - \beta)\right]\sin(\alpha - \beta)\,\Psi_y$$

(6a,b) $$O = C_s \sin(\alpha - \beta) - U \sin\alpha$$
$$O = U_e \sin(\alpha - \beta) - U\sin\beta$$, simultaneous (27)

(7) $M_e = \dfrac{U_e}{A}$

(7.05) $q = -T_2(\delta)\cos\mu_e\, s_-$ (37)

(7.06) $q = -T_1(\delta)\cos\mu_e\, s_-$ (38)

(7.07)
$$\left[\begin{aligned}
\tilde{A} &= \frac{\pi_{31}}{\pi_{21}} \\
B &= -\frac{\pi_{41}}{\pi_{21}} \\
G &= \frac{B}{M\cos\beta - C_s/A} \\
\Omega_1 &= \Lambda_{21}\ \breve{A} - \Lambda_{31} \\
\Omega_2 &= \Lambda_{21}\, B
\end{aligned}\right.$$

(7.03a) $q = -\Lambda_{21}\cos\mu_e\, s_- - \left[\pi_{21}\left(M\cos\beta - \dfrac{C_s}{A}\right)\cos\mu_e\right]\sin(\alpha-\beta)\,\Psi_y$ (35)

(7.05a) $T_2(\delta) = \dfrac{\Omega_2\cos(\alpha-\beta) - \Lambda_{21}\, G\sin(\alpha-\beta)}{\tilde{A}\cos(\alpha-\beta) - G\sin(\alpha-\beta) + \cos\mu_e}$ (39)

(7.06a) $T_1(\delta) = \dfrac{\Omega_1\cos(\alpha-\beta) - \Lambda_{21}\, G\sin(\alpha-\beta)}{\tilde{A}\cos(\alpha-\beta) - G\sin(\alpha-\beta) - \cos\mu_e}$ (40)

(8) $\begin{bmatrix} u_1 \\ v_1 \end{bmatrix} = \begin{bmatrix} \sin\epsilon & \cos\epsilon \\ -\cos\epsilon & \sin\epsilon \end{bmatrix}\begin{bmatrix} u^* \\ v^* \end{bmatrix}$ (Matrix Notation)

(9) $f(y) = U_+ + \dfrac{p_+}{M_e}$

(10) $$D = \frac{1}{2} \frac{M_e}{\sqrt{1 - M_e^2}} \left\{ \widetilde{A} \cos(\alpha - \beta) - G \sin(\alpha - \beta) \right\}$$

(11) $$C = \left\{ \Omega_1 \cos(\alpha - \beta) - \Lambda_{21} G \sin(\alpha - \beta) \right\} s_-$$

(12) $$g(Y^*) = \frac{D\,C}{1 + D^2} \qquad (54)$$

(13) $$p\Big]_{x^*=0} = \frac{1}{2} \frac{M_e}{\sqrt{1 - M_e^2}} \left\{ g(Y^*) \right\} \qquad (55)$$

(14) $$\Psi_Y = \frac{p\Big]_{x^*=0} - \Lambda_{21}\, s_-}{\pi_{21}\,(M \cos\beta - C_s/A)\, \sin(\alpha - \beta)}$$

(15) $$\left(\frac{d\,p_+}{\gamma\, d\,p_m\, M^2}\right) \Big/ \left(\frac{d\,T_-}{T_{m1}}\right) = \left(\frac{p_+}{s_-}\right) \frac{1}{M^2}$$

(16) $$\left(\frac{d\,p_+}{\gamma\, p_{m1}\, M_1^2}\right) \Big/ \left(\frac{d\,T_-}{T_{m1}}\right) = \left(\frac{p_+}{s_-}\right) \frac{X}{M^2}$$

(20) $$\theta' = \pi - \epsilon - (\alpha - \beta)$$

(21) $$\tan(\delta^*) = \left[\frac{U_1}{C_s} - \cos\epsilon\right] \Big/ \sin\epsilon$$

(22) $$\alpha = \arctan\left[\frac{C_s \sin\beta}{C_s \cos B - U}\right]$$

(23) $$\theta'' = \arcsin\left[\frac{U \sin\beta}{A}\right]$$

(24) $$A\,C^2 = U^2 + A^2 - 2U \left\{ U \sin^2\beta - \cos\beta \sqrt{A^2 - U^2 \sin^2\beta} \right\} = C_{s1}^2$$

(25) $BC = 2A\cos\theta'' = 2\sqrt{A^2 - U^2 \sin^2\beta}$

(26) $AB = AC - BC$ i.e., $C_{S2} = C_{S1} - BC$

Note that the equation numbers on the left hand side are those referred to by the flow charts (Section A.3) and those on the right hand side are those used by E. Cuadra in the report.

Derivation of Equations 23 through 26

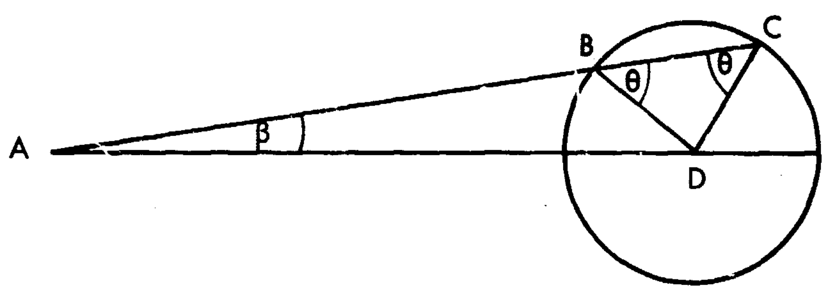

<u>To find</u> AB and AC

i.e., CS2 and CS1

Given $B\hat{A}D = \beta$

$\vec{AD} = U$

$BD = DC = A$

Let $D\hat{B}C = D\hat{C}B = \theta$

Consider ΔDBC then $C\hat{D}B = 180 - 2\theta$

Consider ΔCDA then $C\hat{D}A = 180 - \beta - \theta$

Apply the cosine rule to Δ CDA

$$AC^2 = U^2 + A^2 - 2AU\cos(180 - \beta - \theta)$$

Apply the sine rule to Δ CDA

$$\therefore \frac{A}{\sin\beta} = \frac{U}{\sin\theta}$$

$$\therefore \sin\theta = \frac{U\sin\beta}{A}$$

$$\therefore \cos\theta = \frac{\sqrt{A^2 - U^2\sin^2\beta}}{A}$$

$$AC^2 = U^2 + A^2 - 2U\left[U\sin^2\beta - \cos\beta\sqrt{A^2 - U^2\sin^2\beta}\right]$$

From Δ DBC

$$BC = 2A\cos\theta = 2\sqrt{[A^2 - U^2\sin^2\beta]} \quad \text{and}$$

$$AB = AC - BC$$

Now

$$\theta = \sin^{-1}\left[\frac{U\sin\beta}{A}\right]$$

$$\begin{aligned} \alpha_1^* &= 180 - C\hat{D}A \\ &= 180 - (180 - \beta - \theta) \\ &= \beta + \theta \\ \alpha_2^* &= \beta + 180 - \theta \end{aligned}$$

A.2 TABLE OF SYMBOLS,
THEIR COMPUTER CODE EQUIVALENTS AND DEFINITIONS

Symbol	Computer Code	Description
M_1	EM1	Upstream flow Mach number.
ϵ	ETA EE EV(IC)	Shock wave angle, referenced to the x_i - axis.
β	BETA BB BV(IC)	Angle between the shock wave and the downstream mean flow velocity vector.
γ	GAMMA	Ratio of specific heats.
δ	DELTA DV(ISW, IC) DD DDV(IC)	Inclination of upstream entropy wave with respect to main flow direction.
A_1	A1	Speed of sound in the flow field upstream of the shock.
s_-	SM SMV(IC)	Dimensionless magnitude of the upstream entropy pertubation.
N_1	EN1 EN1V(IC)	Upstream Mach number corresponding to a normal shock of equivalent strength.
χ	CHI CHIV(IC)	Shock strength in terms of the ratio of pressure of the unperturbed flow across the shock.
M	EM	Downstream flow Mach number.
N	EN	Downstream Mach number corresponding to a normal shock of equivalent strength.
ρ_m/ρ_{1m}	RORAT	Density ratio across the shock, downstream to upstream.
A/A_1	ARAT	Ratio of acoustic velocities across the shock, downstream to upstream.

Symbol	Computer Code	Description
U_1	U1	Mean flow velocity downstream of the shock.
A	A	Speed of sound in the flow field upstream of the shock.
U	U	Mean flow velocity downstream of the shock.
Λ_{ij}	OMEGA(I,J)	Transfer coefficients for the interaction (see derivation in text).
π_{ij}	PI(I,J)	Transfer coefficients for the interaction (see derivation in text).
C_s	CS CSV(ISW)	Drift speed of the upstream entropy wave along the shock
α	ALPHA AA AV(ISW,JC)	Inclination of U_e with respect to the downstream mean flow direction U.
U_e	UE	Apparent mean flow velocity downstream of the shock with respect to an observer moving with C_s .
M_e	EME EMEV(IC)	Effective Mach number corresponding to U_e .
μ_e	EMEWE	Effective Mach angle corresponding to M_e .
$\tilde{A}$	ABAR	Ratio of transfer coefficients, π_{31}/π_{21} .
B	B	Ratio of transfer coefficients, $-\pi_{41}/\pi_{21}$
G	G	A nondimensional group in the solution for the Riemann invariants, case $M_e > 1$.
Ω_1	OMEG 1	A convenient grouping of transfer coefficients in the solution for the amplitude function $T_1(\delta)$.
Ω_2	OMEG 2	A convenient grouping of transfer coefficients in the solution for the amplitude function $T_2(\delta)$.

Symbol	Computer Code	Description
C_s	CS 2 CSV(2) CS2V(IC)	Intersection of shock plane and sonic circle lying nearest the origin.
C_s	CS 1 CSV(1) CS1V(IC)	Intersection of shock plane and sonic circle lying farthest from the origin.
$T_2(\delta)$	T 2D	An amplitude function required for the pressure perturbation solution, case $M_e > 1$ (s.a. report text).
$T_1(\delta)$	T 1D	An amplitude function required for the pressure perturbation solution, case $M_e > 1$ (s.a. report text).
q	Q	A dimensionless parameter related to the downstream pressure perturbation, one member of the pair making up the Riemann invariants (s.a. report text).
Ψ_y	PSIY PSIYV(IC)	Local shock deflection owing to the interaction.
s_+	SP SPV(IC)	Dimensionless magnitude of the downstream entropy perturbation.
P_+	PP PPV(IC)	Dimensionless magnitude of the (downstream) generated pressure perturbation.
U_+	UP UPV(IC)	Dimensionless magnitude of the (downstream) velocity perturbation component along downstream mean flow velocity vector.
V_+	VP VPV(IC)	Dimensionless magnitude of the (downstream) velocity perturbation component normal to downstream mean flow velocity vector.
u^*	US	Dimensionless magnitude of the (downstream) velocity perturbation, component along x^* axis (along shock plane).
v^*	VS	Dimensionless magnitude of the (downstream) velocity perturbation, component along y^* axis (normal to shock plane).

Symbol	Computer Code	Description
u_1	UL 1 UL1V(IC)	Dimensionless magnitude of the (downstream) velocity perturbation, component along x_1 axis
v_1	VL 1 VL1(IC)	Dimensionless magnitude of the (downstream) velocity perturbation, component along y_1 axis.
f (Y)	FY FYV(IC)	Vorticity generating function (s.a. report text).
C	C	A convenient grouping in the solution for the equivalent source function $g(Y^*)$; s.a. report text.
$g(Y^*)$	GYS	A function related to the strength of an equivalent source located on the shock plane (s.a. report text), case $M_e < 1$.
$P(x^*=0)$	PCS PCSV(IC)	Dimensionless pressure perturbation immediately behind the shock, for the case $M_e < 1$.
$\left(\frac{P_+}{s_-} \cdot \frac{1}{M^2}\right)$	ANG ANGV(IC)	Dimensionless pressure perturbation referenced to local stream dynamic pressure.
$\left(\frac{P_-}{s_-} \cdot \frac{X}{M^2}\right)$	ANC ANCV(IC)	Dimensionless pressure perturbation referenced to upstream (free stream) dynamic pressure.
θ'	TDD THETAD THDV(IC)	Enclosed angle between U_e and the x_1 - axis.
D	D	A convenient grouping in the solution for the equivalent source function $g(Y^*)$, s.a. report text.
θ	THET	Enclosed angle between the shock plane and the radius vector of the sonic circle ending at the intersection of sonic circle and shock.
VORT	VORT VORTV(IC)	$\sqrt{u_1^2 + v_1^2}$

A.3 FLOW DIAGRAM

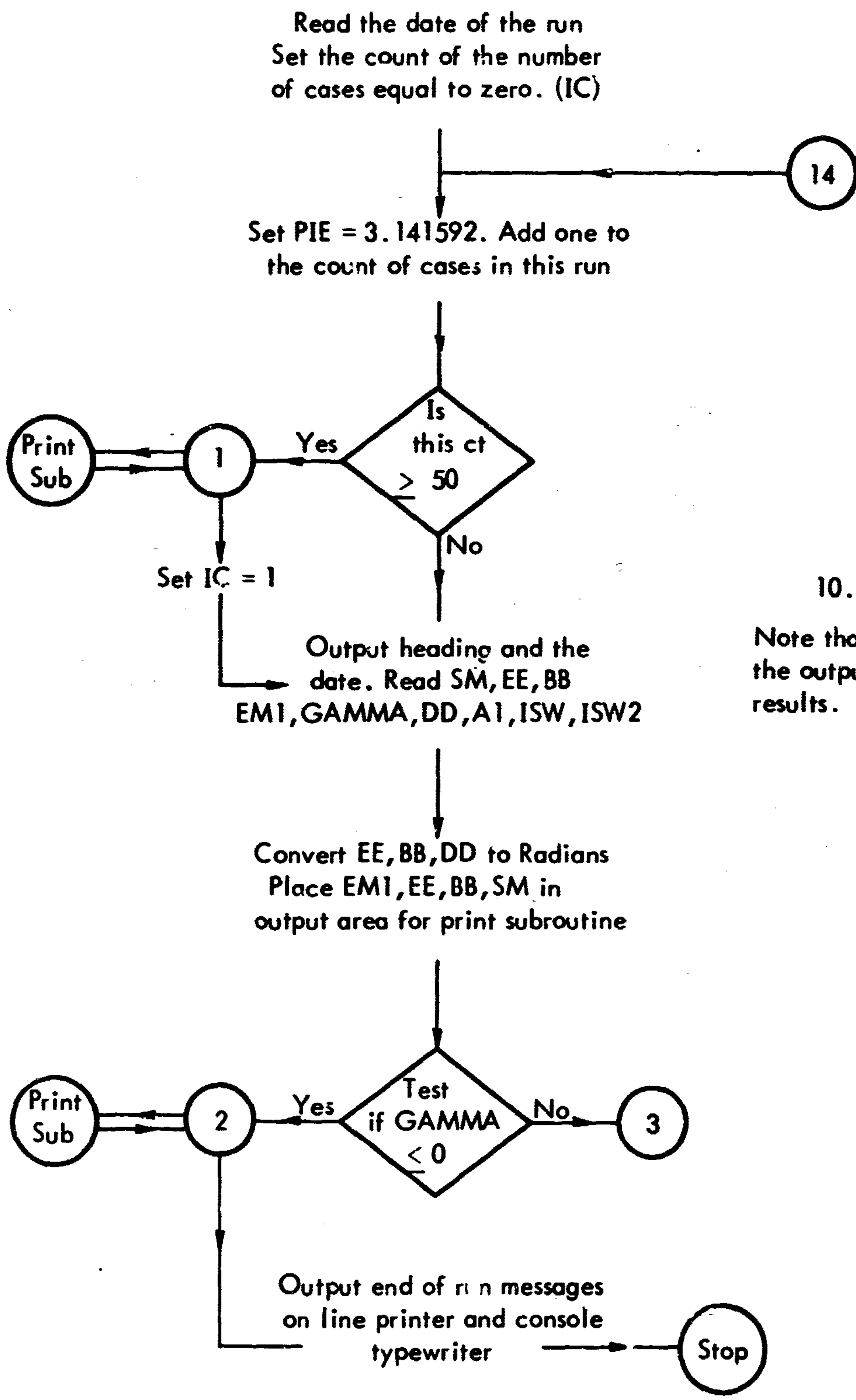

10.19.67

Note that ISW2 determines the output format of the results.

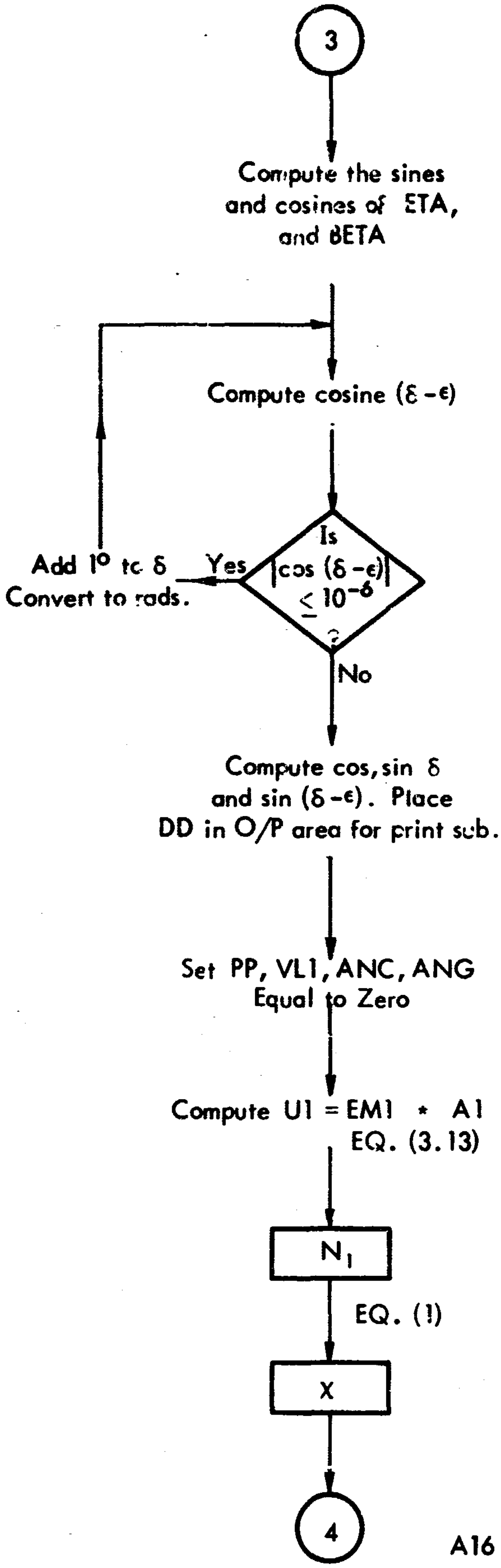

* Note that the value of ISW determines whether CS, CS1 or CS2 is being used to compute values of parameters in the latter part of the program.

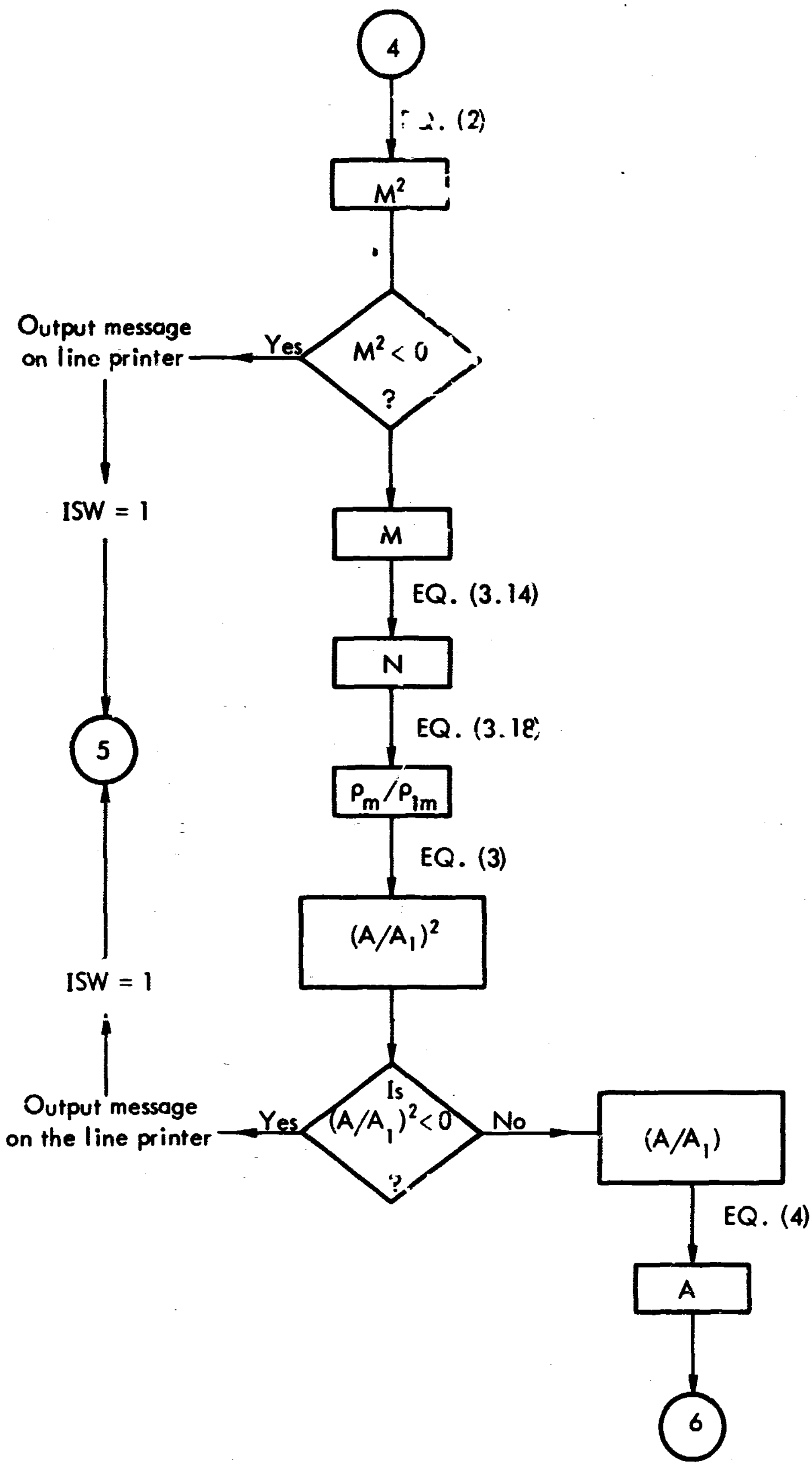
4
EQ. (2)
M^2
Output message
on line printer
Yes
$M^2 < 0$
?
ISW = 1
M
EQ. (3.14)
N
EQ. (3.18)
5
ρ_m/ρ_{1m}
EQ. (3)
$(A/A_1)^2$
ISW = 1
Output message
on the line printer
Yes
Is
$(A/A_1)^2 < 0$
?
No
(A/A_1)
EQ. (4)
A
6

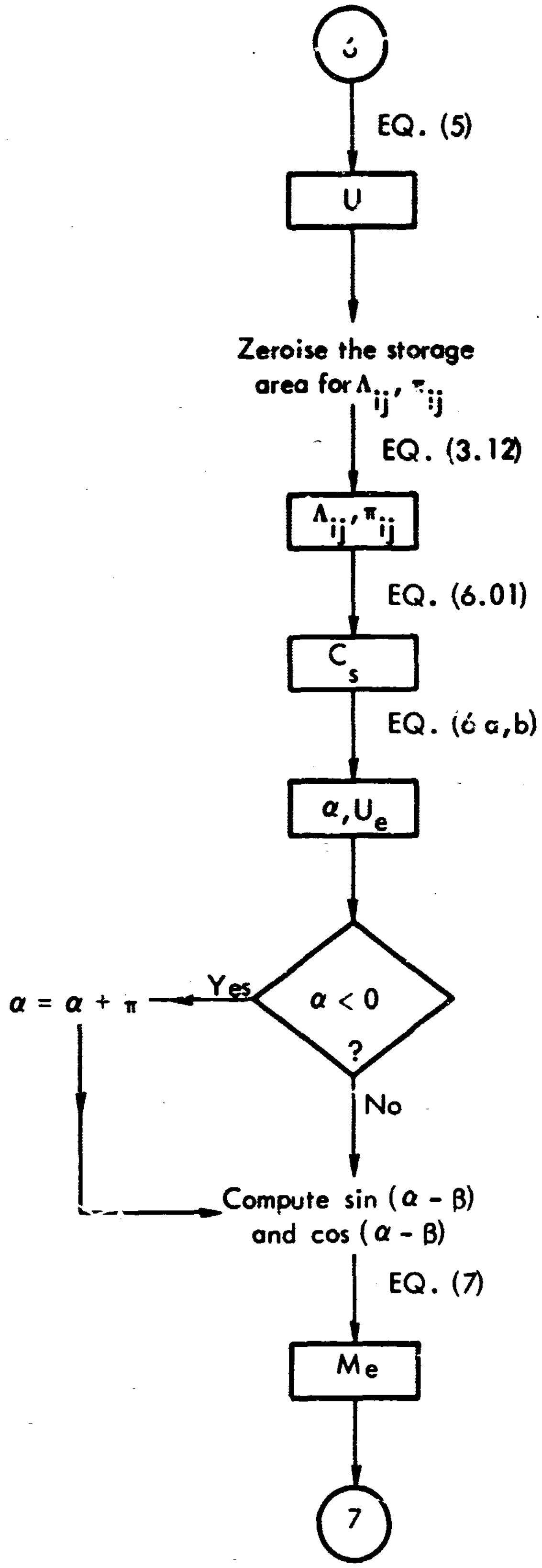
6
EQ. (5)
U
Zeroise the storage area for Λ_{ij}, π_{ij}
EQ. (3.12)
Λ_{ij}, π_{ij}
EQ. (6.01)
C_s
EQ. (6 a,b)
α, U_e
$\alpha < 0$?
Yes
$\alpha = \alpha + \pi$
No
Compute sin $(\alpha - \beta)$ and cos $(\alpha - \beta)$
EQ. (7)
Me
7

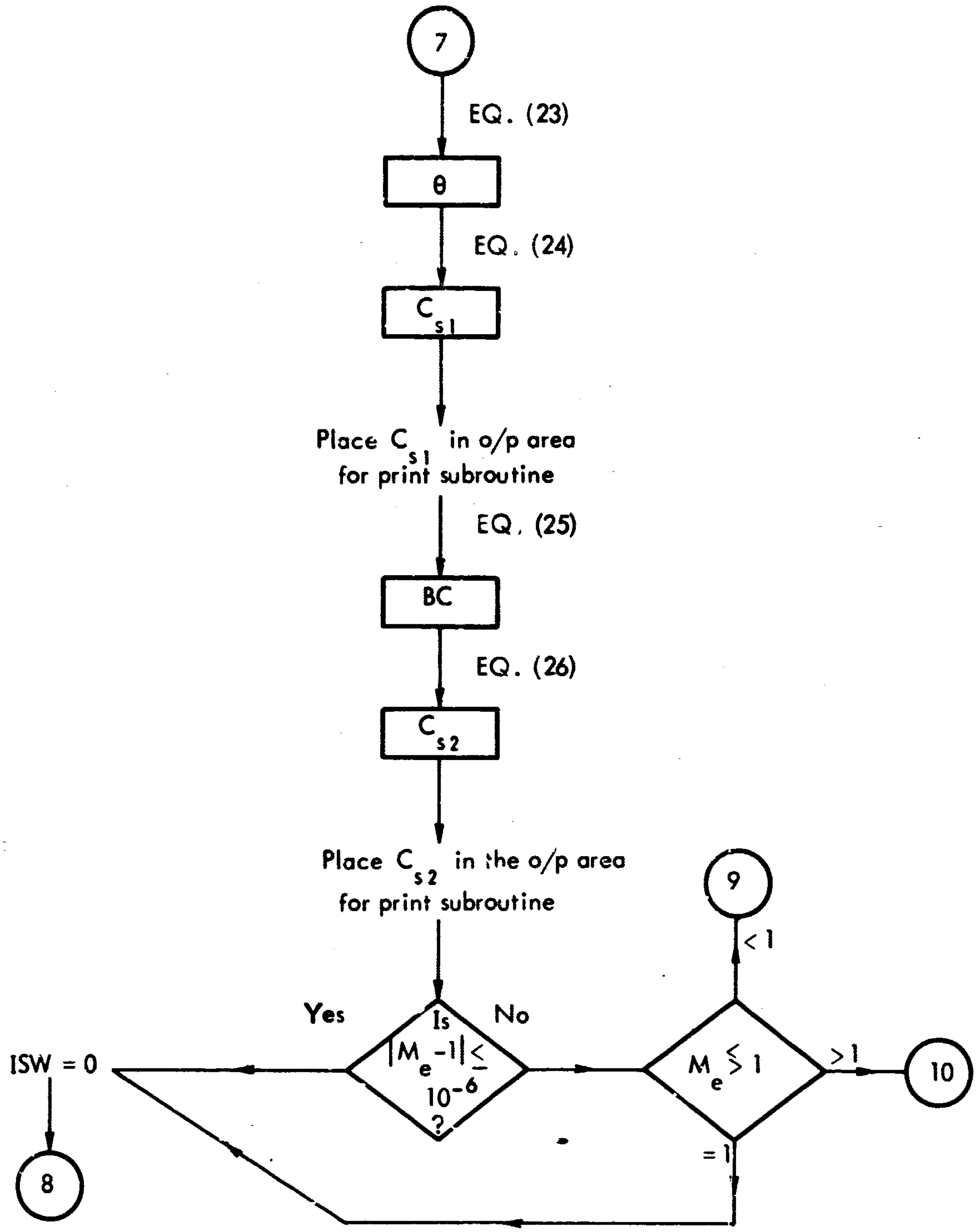

7
EQ. (23)
θ
EQ. (24)
C_{s1}
Place C_{s1} in o/p area for print subroutine
EQ. (25)
BC
EQ. (26)
C_{s2}
Place C_{s2} in the o/p area for print subroutine
Yes
No
Is $|M_e - 1| \leq 10^{-6}$?
ISW = 0
8
9
< 1
$M_e \lessgtr 1$
> 1
10
= 1

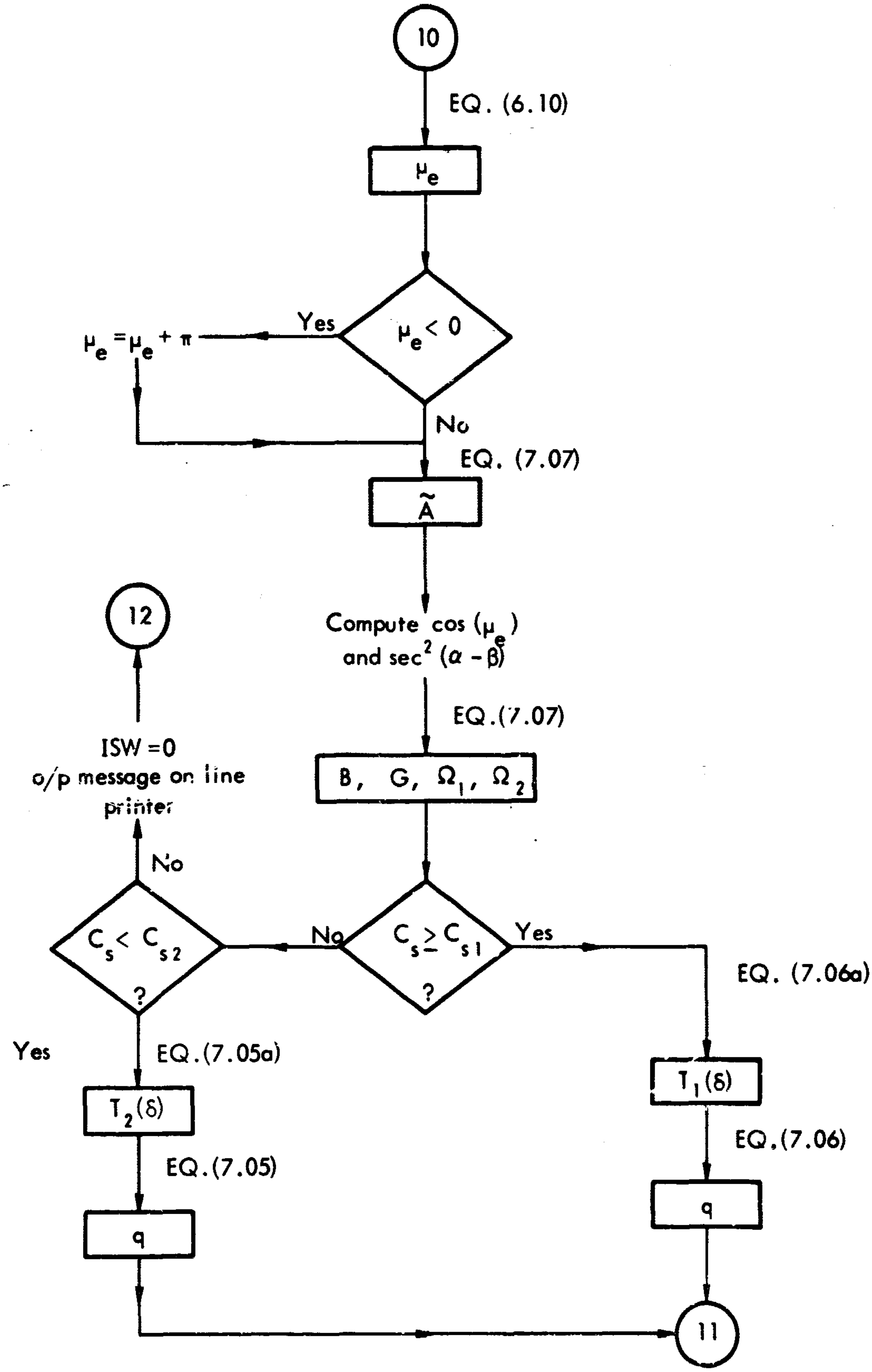

10
EQ. (6.10)
μ_e
$\mu_e < 0$
Yes
$\mu_e = \mu_e + \pi$
No
EQ. (7.07)
$\tilde{A}$
Compute cos (μ_e)
and sec^2 ($\alpha - \beta$)
EQ. (7.07)
B, G, Ω_1, Ω_2
$C_s \geq C_{s1}$
?
Yes
No
EQ. (7.06a)
$T_1(\delta)$
EQ. (7.06)
q
$C_s < C_{s2}$
?
No
ISW = 0
o/p message on line
printer
12
Yes
EQ. (7.05a)
$T_2(\delta)$
EQ. (7.05)
q
11

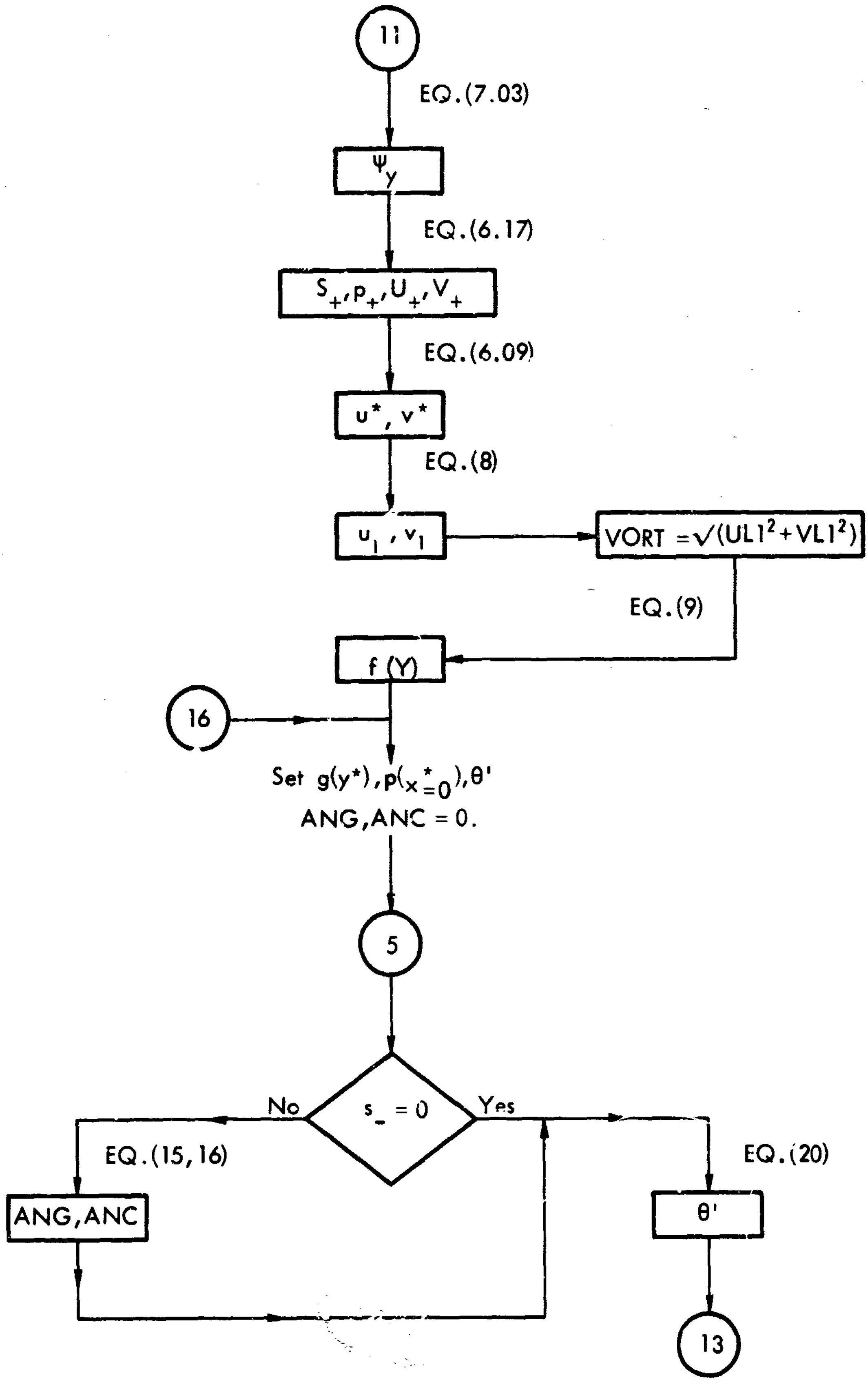
11
EQ.(7.03)
Ψ_y
EQ.(6.17)
S_+, p_+, U_+, V_+
EQ.(6.09)
u^*, v^*
EQ.(8)
u_1, v_1
VORT = $\sqrt{(UL1^2+VL1^2)}$
EQ.(9)
f(Y)
16
Set $g(y^*), p(x^*=0), \theta'$
ANG, ANC = 0.
5
$s_- = 0$
No
Yes
EQ.(15,16)
ANG, ANC
EQ.(20)
θ'
13

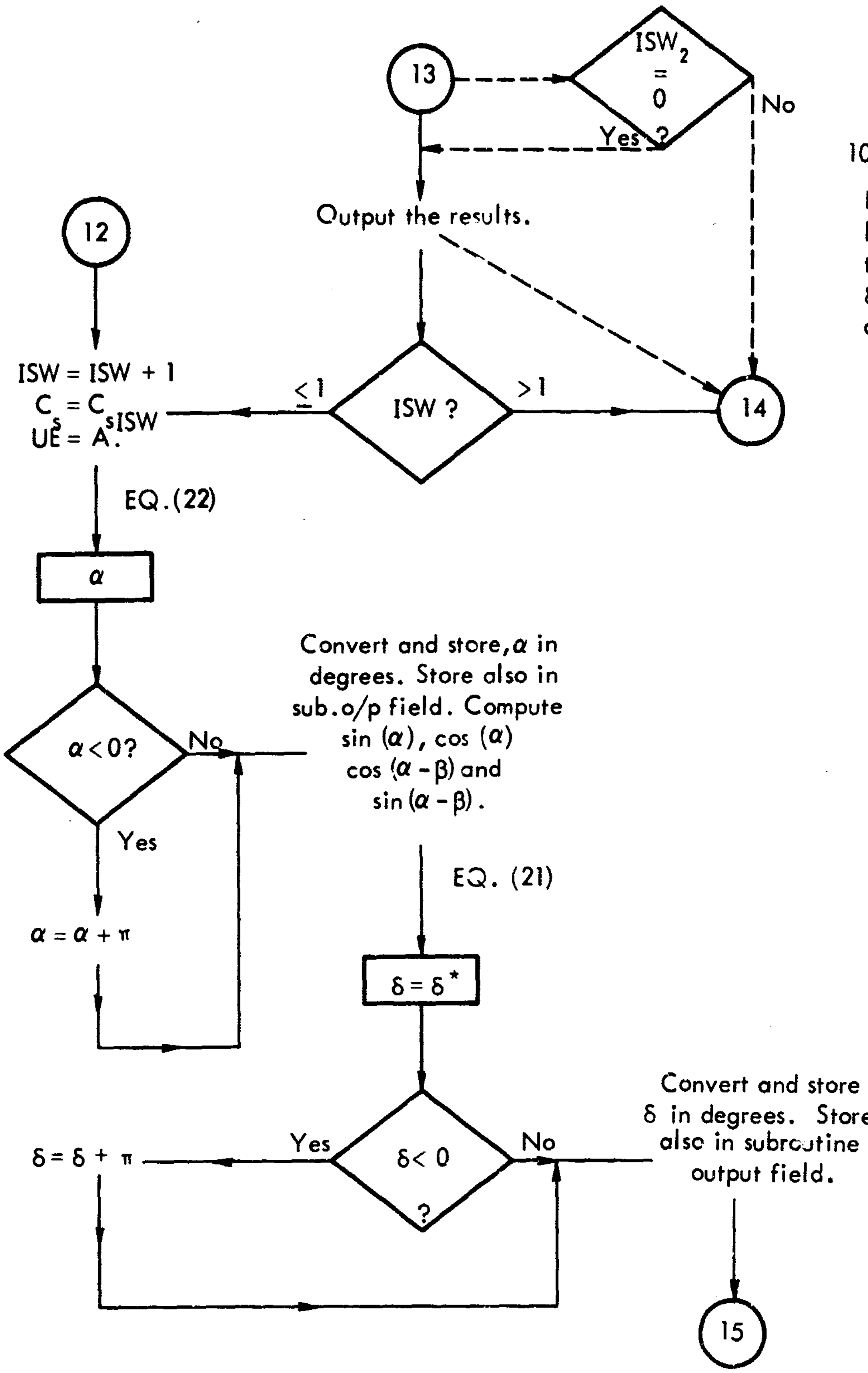

10.9.67

Note that in the latest version of the program the δ* routine is omitted.

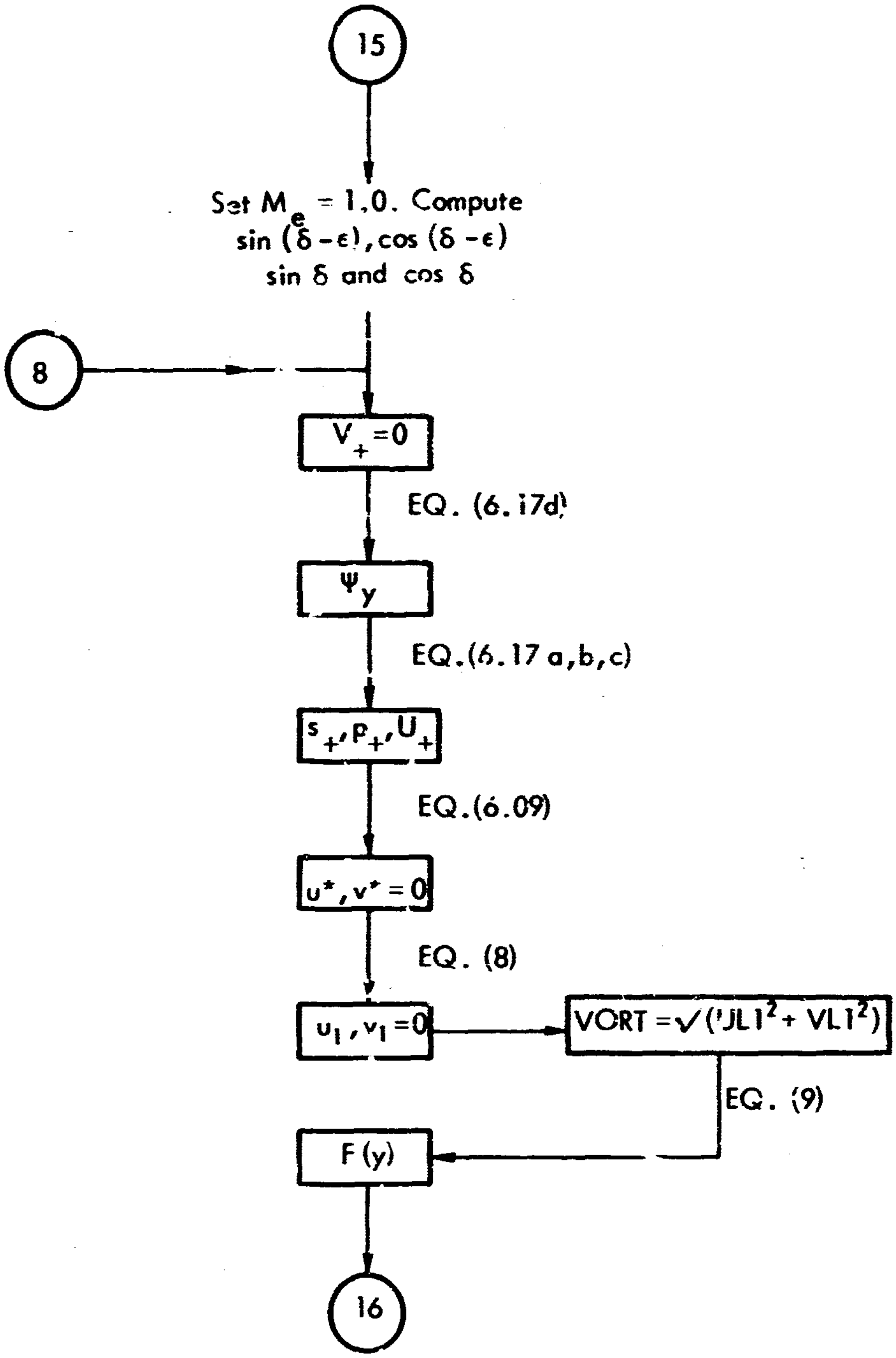
15
Set M e = 1.0. Compute
sin (δ - ε), cos (δ - ε)
sin δ and cos δ
8
V + =0
EQ. (6.17d)
Ψ y
EQ.(6.17 a,b,c)
s +, p +, U +
EQ.(6.09)
u*, v* = 0
EQ. (8)
u 1, v 1 =0
VORT = √(UL1² + VL1²)
EQ. (9)
F (y)
16

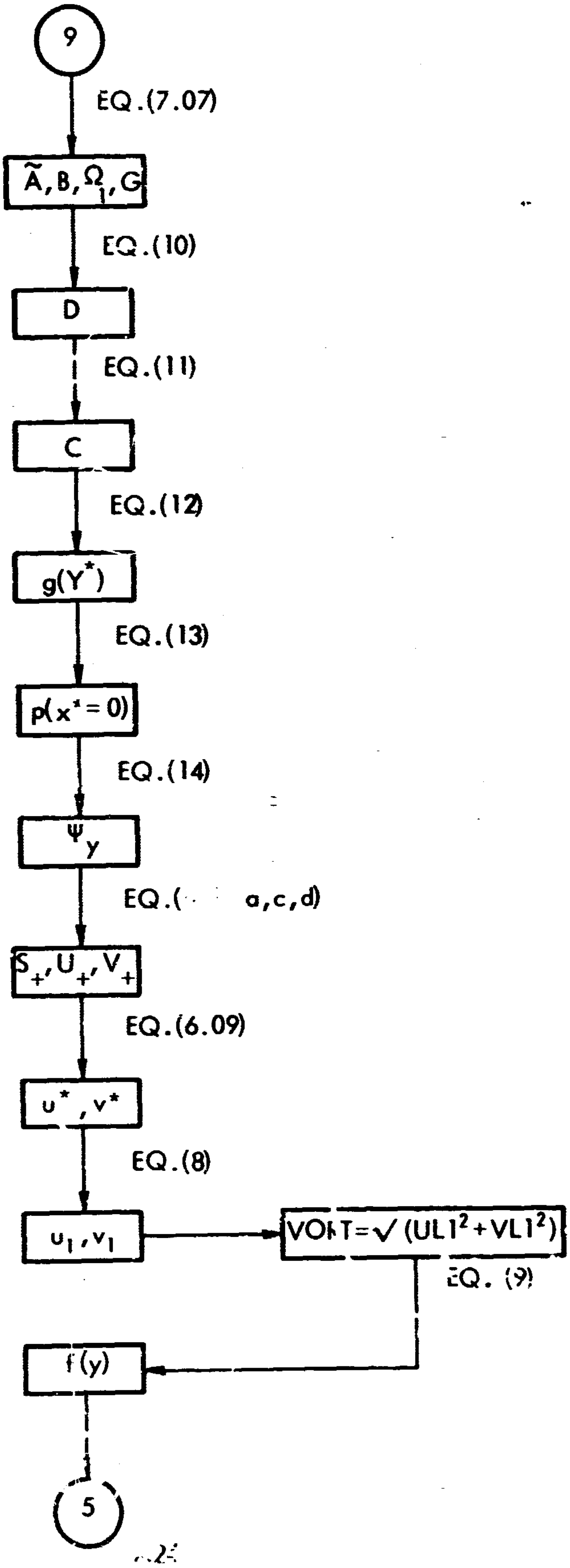
9
EQ.(7.07)
Ã,B,Ω1,G
EQ.(10)
D
EQ.(11)
C
EQ.(12)
g(Y*)
EQ.(13)
p(x*=0)
EQ.(14)
Ψy
EQ.(a,c,d)
S+,U+,V+
EQ.(6.09)
u*,v*
EQ.(8)
u1,v1
VORT=√(UL1²+VL1²)
EQ.(9)
f(y)
5

Flow Charts Continued

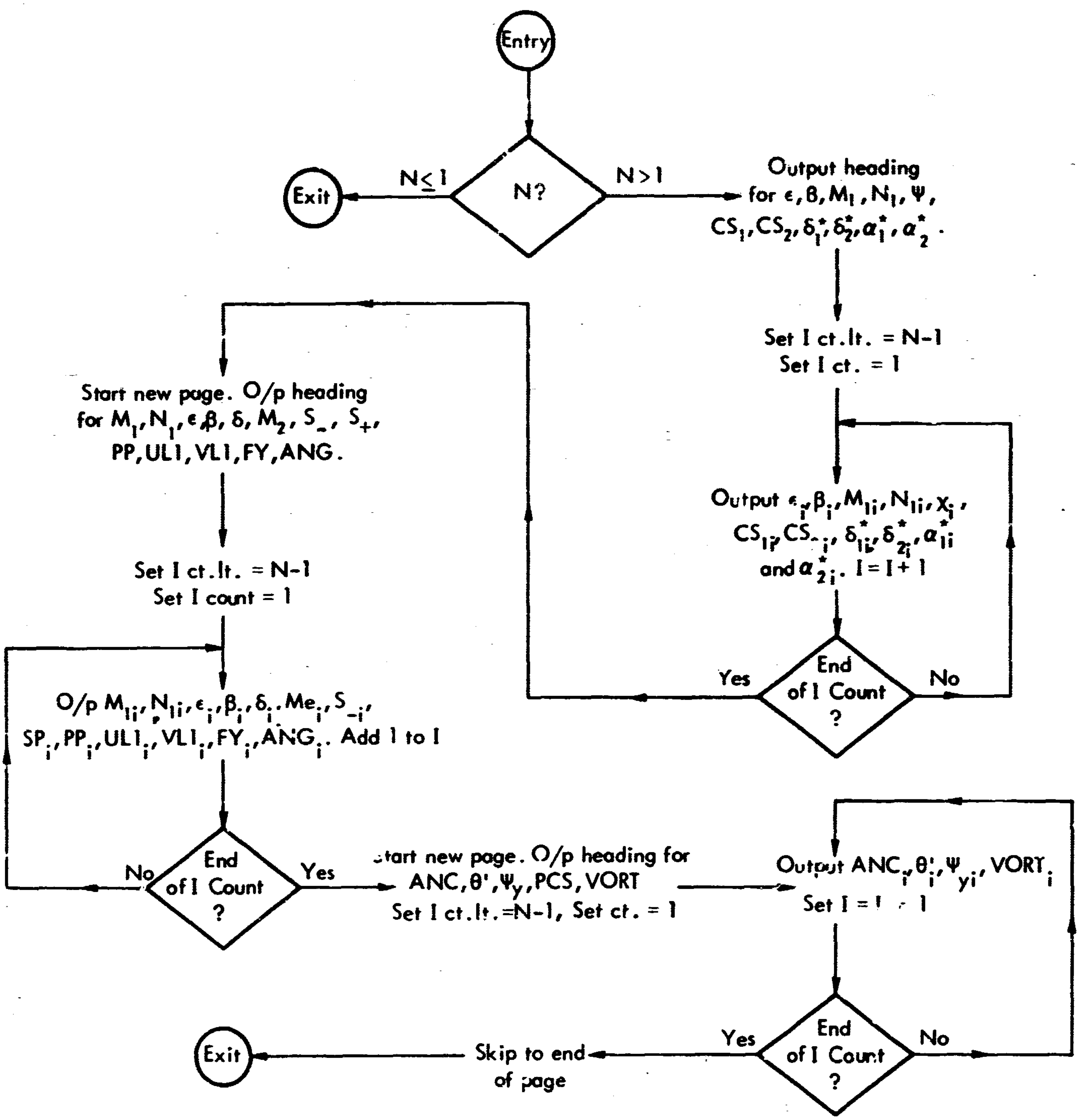

A.4 FORTRAN LISTING OF PROGRAM


```
      PROGRAM HUNT
      COMMON OMEGA(4,4),PI(4,4),CSV(2),CS1V(50),CS2V(50),EV(50),BV(50),E
     1 1V(50),EN1V(50),CHIV(50),DV(2,50),AV(2,50)
      COMMON DDV(50),EMEV(50),SMV(50),SPV(50),PPV(50),VL1V(50),VE1V(50),
     1 V(50),ANGV(50),ANCV(50),THOV(5 ),PSIVV(50),POSV(50),VORTV(50)
      EQUIVALENCE (CSV(1),CS1),(CSV(2),CS2)
      READ (60,201) ID1,ID2
  201 FORMAT (2A4)
      IC=0
  121 PIE=3.141592
      IC=IC+1
      IF (IC-50) 406,406,7
  406 READ (60,200) SM,EE, BM,  EM1,GAMMA,DD,   A1  ,ISW,ISW2
  200 FORMAT (7F10.0,2I5)
      IF (ISW2.EQ.0) 906,907
  906 WRITE(61,300)ID1,ID2
  300 FORMAT (10X,25HSHOCK ENTROPY INTERACTION,25X,2A4)
  907 BETA=BB*PIE/180.0
      ETA=EE*PIE/180.0
      DELTA=DD*PIE/180.0
      EM1V(IC)=EM1
      EV(IC)=EE
      BV(IC)=BM
      SMV(IC)=SM
      IF (GAMMA) 122,122,123
  122 CALL PRINTIT(IC)
      WRITE (61,400)
      WRITE (59,400)
  400 FORMAT (3X,10HEND OF RUN)
      STOP
    7 CALL PRINTIT(IC)
      IC=1
      GO TO 406
  123 SE=SIN(ETA)
      CE=COS(ETA)
      SB=SIN(BETA)
      CB=COS(BETA)
  602 CDME=COS(DELTA-ETA)
      IF (ABS(CDME)-0.000001 ) 600,600,601
  600 DD=DD+1.0
      DELTA=DD*PIE/180.0
      GO TO 602
  601 CD=COS(DELTA)
      SDME=SIN(DELTA-ETA)
      SD=SIN(DELTA)
      DDV(IC)=DD
      PP=0.0
      VL1=0.0
      ANC=0.0
      ANG=0.0
      C1=EM1*A1
      EN1=EM1*SE
      CHI=(EN1*EN1*7.0-1.0)/6.0
      EN1V(IC)=EN1
      CHIV(IC)=CHI
      EM=      ((EN1*EN1+5.0)/(EN1*EN1*7.0-1.0))/SB**2
      IF (EM) 402,403,403
  402 WRITE (61,320)
  320 FORMAT (5X,12HEM IMAGINARY)
      ISW =1
```

```
      GO TO 11
  403 EN=SQRT(EM)
      EN=EN*EB
      RORAI=(EN1*6.0+1.0)/(EN1+6.0)
      ARAI=((7.00*EN1*EN1-1.0)*(EN1*EN1+5.0))/(EN1*EN1*36.0)
      IF (ARAI) 404,405,405
  404 WRITE (61,321)
  321 FORMAT (5X,14HARAI IMAGINARY)
      ISW=1
      GO TO 11
  405 ARAI=SQRT(ARAI)
      A=ARAI*A1
      U=A*A
      DO 1 I=1,4
      DO 1 J=1,4
      OMEGA(I,J)=1.0
1     P(I,J)=0.0
      OMEGA(1,1)=(RORAI*EN/EN1)**2-(GAMMA-1.0)*(1.0-RORAI)*EN*EN
      OMEGA(2,1)=(EN*EN/(1.0-EN*EN))*((1.0-RORAI)*(1.0+(GAMMA-1.0)*EN*E
     1)+(1.0-(RORAI*EN/EN1)**2))
      OMEGA(3,1)=-(EN/(1.0-EN*EN))*((1.0-(RORAI*EN/EN1)**2)+(1.0-RORAI)*
     1GAMMA*EN*EN)
      OMEGA(1,2)=(GAMMA-1.0)*(1.0-RORAI)*(1.0-RORAI/(EN1*EN1))*EN*EN
      OMEGA(2,2)=-(EN*EN/(1.0-EN*EN))*(1.0-RORAI+(1.0-RORAI/(EN1*EN1))*(
     11.0+(GAMMA-1.0)*(1.0-RORAI)*EN*EN))
      OMEGA(3,2)=(EN/(1.0-EN*EN))*(((1.0-(RORAI*EN/EN1)**2)+GAMMA*(1.0-RO
     1RAI)*(1.0-RORAI/(EN1*EN1))*EN*EN)
      OMEGA(1,3)=(GAMMA-1.0)*((1.0-RORAI)*EN)**2/EN1
      OMEGA(2,3)=-(EN/(1.0-EN*EN))*(1.0-RORAI)*(2.0+(GAMMA-1.0)*(1.0-RO
     1RAI)*EN*EN)*EN/EN1
      OMEGA(3,3)=(1.0/(1.0-EN*EN))*(EN/EN1)*(1.0-(RORAI*EN)**2+GAMMA*(1.
     1-RORAI)**2*EN*EN)
      OMEGA(4,4)=RORAI*EN/EN1
      P(1,1)=-(GAMMA-1.0)*((1.0-1.0/RORAI)**2*RORAI*EN
      P(2,1)=-(EN/(1.0-EN*EN))*(1.0-1.0/RORAI)*(2.0+(GAMMA-1.0)*(1.0-RO
     1RAI)*EN*EN)
      P(3,1)=(1.0/(1.0-EN*EN))*(1.0-1.0/RORAI)*(1.0*EN*EN+(GAMMA-1.0)*(
     11.0-RORAI)*EN*EN)
      P(4,1)=EN*(RORAI-1.0)
      CS=1.0/CAMB
      ALPHA=ATAN(SA*CS/(CB*CS-U))
      IF (ALPHA) 20,21,21
   20 ALPHA=PIE+ALPHA
   21 SAMB=SIN(ALPHA-BETA)
      CAMB=COS(ALPHA-BETA)
      U=U*SA/SAMB
      EME=E/A
      EMEV(IC)=EME
      THET=ASIN(U*SB/A)
      CS1=SQRT(U*U+A*A-2.0*A*U*COS(PIE-BETA-THET))
      CS1V(IC)=CS1
      C0=2.0*A*COS(THET)
      CS2=CS1-C0
      CS2V(IC)=CS2
      IF (ABS(EME-1.0)-0.00001)33,33,401
  401 IF (EME-1.0)2,33,4
    4 EMENE=ATAN(1.0/(EME*SQRT(1.0-(1.0/(EME*EME)))))
      IF(E-EXE)22,23,23
   22 EMENE=PIE+EMENE
   23 EMR=P(3,1)/P(2,1)
      CME=COS(EMENE)          TSNAR=1.0/(CAMB*CAMB)
      EE=P(4,1)/P(2,1)
```

```
      Q=V/(E *CB-CS/A)
      OMEG1=OMEGA(2,1)*A+A   MEGA(3,1)
      OMEG2=OMEGA(2,1)*B
      IF(CS-CS1)10,9,9
9     T1 =(OMEG1*CAMB-OMEGA(2,1)*G*SAMB)/(ABAR*CAMB-G*SAMB-CME)
      Q=-T1 *CME*SM
15    PSI =-(G+OMEGA(2,1)* *CME)/(SAMB*(E *CB-CS/A)*PI(2,1)*CME)
      PSIY(IC)=PSI
      SF=O EGA(1,1)*SM+PI(1,1)*(E *CB-CS/A)*SAMB*-SI
      SFV( C)=SF
      FF=  EGA(2,1)*SM+P (2,1)*(E *CB-CS/A)*SAMB*PSI
      FF (IC)=FF
      SF=OMEGA(3,1)*SAMB*SM+(PI(3,1)*(E *CB-CS/A)*SAMB-PI(4,1)*CAMB)*SAM
     1 * S )
      VF=O EGA(3,1)*CAMB*SM-(PI(3,1)*(E *CB-CS/A)*CA B+PI(4,1)*SAMB)*SAM
     1 * SI)
      USI=SF*SAMB+VF*CAMB
      V  =-UF*CAMB+VF*SAMB
      U 1=USI*SE+VSI*CF
      U 1 (IC)=UC1
      VC1=-USI*CF+VSI*SE
      V 1 (IC)=VC1
      FY=  *-F/EME
      F  ( C)=FY
16    S  =0.
      F  =0.
      FC V(IC)=FCS
      -  =0.0
      A  =0.0
      DELTAB=0.0
      GO T  11
10    IF(CS-CS2)12,13,13
13    WRITE(61,301)    EME
301   FORMAT(10X,25HCS1 GR C  GR CS2    A WHAT .,15X,4HME =,E20.10/)
      IS =0
501   IS =IS +1
      CS=CSV(ISK)
      CR=A
      AL HA=ATAN(CS*SB/(CS*C -S))
      IF(ALPHA)40,41,41
40    ALPHA=ALPHA+PIE
41    AA=ALPHA*180.0/PIE
      AA=ALPHA*180.0/PIE
      A (ISK,IC)=AA
      SA=SIN(ALPHA)
      CA=COS(ALPHA)
      CAMB=COS(ALPHA-BE A)
      SAMB=SIN(ALPHA-B  A)
      DELTA =ATAN((C1/CS-CF)/SF)
      IF(DELTA)42,43,43
42    DELTA=DELTA+PIE
43    DD=DELTA*180.0/PIE
      D (ISK,IC)=DD
      E  =1.0
      SDME=SIN(DELTA-ETA)
      CDME=COS(DELTA-ETA)
      SD=SIN(DELTA)
      CD=COS(DELTA)
      GO TO 33
12    T2 =(OMEG2*CAMB-OMEGA(2,1)*G*SAMB)/(ABAR*CAMB-G*SAMB+CME)
      Q=-T2 *CME*S
      GO TO 15
```

```
33    YP=0.0
      PSIY=-OMEGA(3,1)*CAME*SM/(SAMB*(PI(3,1)*(EM*CB-CS/A)*CAMB+PI(4,1)*
     1SAMB))
      PSIYV(IC)=PSIY
      SP=OMEGA(1,1)*SM+PI(1,1)*(EM*CB-CS/A)*SAMB*PSIY
      SPV(IC)=SP
      PP=OMEGA(2,1)*SM+PI(2,1)*(EM*CB-CS/A)*SAMB*PSIY
      PPV(IC)=PP
      UP=OMEGA(3,1)*SAMB*SM+(PI(3,1)*(EM*CB-CS/A)*SAMB-PI(4,1)*CAMB)*SAM
     1B*PSIY
      USI=UP*SAMB
      VSI=0.0
      UL1=USI*SE
      UL1V(IC)=UL1
      VL1=0.0
      VL1V(IC)=VL1
      PY=SP+PP/EME
      PYV(IC)=PY
      GO TO 16
2     ABAR=PI(3,1)/PI(2,1)
      G=-PI(4,1)/PI(2,1)
      OMEG1=OMEGA(2,1)*ABAR-OMEGA(3,1)
      B=-/(EM*CB-CS/A)
      E=EME*0.5*(ABAR*CAMB-G*SAMB)/SQRT(1.0-EME*EME)
      U=B*(OMEG1*CAMB-OMEGA(2,1)*G*SAMB)
      GY=U*G/(1.0+D*D)
      PCS=EMF*GY+0.5/SQRT(1.0-EME*EME)
      PCSV(IC)=PCS
      PSIY=(PCS-OMEGA(2,1)*SM)/(SAMB*PI(2,1)*(EM*CB-CS/A))
      PSIYV(IC)=PSIY
      SP=OMEGA(1,1)*SM+PI(1,1)*(EM*CB-CS/A)*SAMB*PSIY
      SPV(IC)=SP
      PP=OMEGA(2,1)*SM+SAMB*PSIY*(EM*CB-CS/A)*PI(2,1)
      PPV(IC)=PP
      UP=OMEGA(3,1)*SAMB*SM+(PI(3,1)*(EM*CB-CS/A)*SAMB-PI(4,1)*CAMB)*SAM
     1B*PSIY
      VP=OMEGA(3,1)*CAMB*SM+(PI(3,1)*(EM*CB-CS/A)*CAMB+PI(4,1)*SAMB)*SAM
     1B*PSIY
      USI=UP*SAMB+VP*CAMB
      VSI=-UP*CAMB+VP*SAMB
      UL1=USI*SE+VSI*CE
      UL1V(IC)=UL1
      VL1=-USI*CE+VSI*SE
      VL1V(IC)=VL1
      PY=UP+PP/EME
      PYV(IC)=PY
11    IF (SM) 30,31,30
30    ANG=PP/(SB*EB*EM)
      ANGV(IC)=ANG
      ANC=PP*CHI/(SB*EM1*EM1)
      ANCV(IC)=ANC
31    THETAD=BETA-ALPHA-ETA+PIE
      THEV(IC)=THETAD*180.0/PIE
      SQRTV(IC)=SQRT(UL1*UL1+VL1*VL1)
      IF (IS.EQ.0) 906,121
906   WRITE (61,302) EM,EE,ETA,BB,BETA
302   FORMAT (1H ,11HGIVEN DATA.//24X,4HM1 =,E20.10/23X,5HETA =,E20.10,1
     10X,E20.10/22X,6HBETA =,E20.10,10X,E20.10)
      WRITE (61,311) DB,DELTA,SM,A1
311   FORMAT (21X,7HDELTA =,E20.10,10X E20.10/24X,4HSM =,E20.10/24X,4HA1
     1 =,E20.10/)
      WRITE(61,303)EM1,EN,EB,CHI,ROHA,A,U
```

```
 303  FORMAT (13X,8HRESULTS./ 24X,4HN1 =,E20.10/25X,3HK =,E20.10/25X,3HK
     1 =,E20.10/23X,5HCHI =,E20.10/21X,7HRORAT =,E20.10/25X,3HA =,E20.10
     2/25X,3HU =,E20.10)
      WRITE(61,304)
 304  FORMAT(44X,12HOMEGA MATRIX/)
      DO 18 I=1,4
 18   WRITE(61,305) (OMEGA(I,J),J=1,4)
 305  FORMAT(10X,4E20.10)
      WRITE(61,306)
 306  FORMAT (47X,9HPI MATR.X/)
      DO 19 I=1,4
 19   WRITE(61,305)(PI(I,J),J=1,4)
      AA=ALPHA*180.0/PIE
      WRITE (61,310) AA,ALPHA
 310  FORMAT (2X//21X,7HALPHA =,E20.10,10X,E20.10)
      WRITE(61,307) CS,      UE,EMF,CS2,CS1,PSIY
 307  FORMAT          (24X,4HCS =,E20.10/                         24X,4HUE =,E20
     1.10/23X,5HEMF =,E20.10/23X,5HCS2 =,E20.10/23X,5HCS1 =,E20.10/22X,6
     2HPSIY =,E20.10)
      WRITE(61,308)SP,PF,UF,VF,US1,VS1,UL1,VL1
 308  FORMAT (24X,4HSP =,E20.10/24X,4HPF =,E20.10/24X,4HUF =,E20.10/24X,
     14HVF =,E20.10/23X,5HUS1 =,E20.10/23X,5HVS1 =,E20.10/23X,5HUL1 =,E2
     20.10/23X,5HVL1 =,E20.10)
      TDD=THETAD
      THETAD=TDD*180.0/PIE
      WRITE (61,309) FY,GYS,FCS,ANG,ANC,THETAD,TDD
 309  FORMAT (24X,4HFY =,E20.10/23X,5HGYS =,E20.10/23X,5HFCS =,   .10/23
     1X,5HANG =,E20.10/23X,5HANC =E20.10/20X,8HTHETAD =,E20.10,1...,E 0.1
     20)
      WRITE (61,314) VCRIV(10)
 314  FORMAT (22X,6HVCRT =,E20.10)
      WRITE (61,313)
 313  FORMAT (1H1)
      GO TO 121
      END

          3200 FORTRAN DIAGNOSTIC RESULTS - FOR   HOR

NULL STATEMENT NUMBERS
     501
```

```
      SUBROUTINE PRINT1(N)
      COMMON OMEGA(4,4),FI(4,4),CSV(2),CS1V(50),CS2V(50),EV(50),BV(50),E
     1F1V(50),EN1V(50),CHIV(50),DV(2,50),AV(2,50)
      COMMON DDV(50),EMEV(50),SMV(50),SPV(50),PPV(50),UL1V(50),VL1V(50),
     1FYV(50),ANGV(50),ANCV(50),THDV(50),PSIYV(50),FCSV(50),VORTV(50)
      IF(N-1)1,1,2
2     WRITE(61,300)
300   FORMAT (15X,3HETA,6X,4HBETA,8X,2HM1,8X,2HN1,7X,3HCHI,9X,3HCS1,9X,3
     1HCS2)
      M=N-1
      DO 3 I=1,M
    3 WRITE(61,301)EV(I),BV(I),EM1V(I),EN1V(I),CHIV(I),CS1V(I),CS2V(I)
301   FORMAT(10X,5F10.3,2F12.3,2F10.3,2F11.3)
      WRITE(61,302)
302   FORMAT(1H1)
      WRITE (61,303)
 303  FORMAT (15X,3HM1.,6X,3HN1.,6X,4HETA.,5X,5HBETA.,5X,6HDELTA.,5X,3HM
     1E.,5X,3HSM.,7X,3HSP.,6X,3HPP.,5X,4HUL1.,6X,4HVL1.,7X,3HFY.,7X,4HAN
     2G./)
      DO 4 I=1,M
    4 WRITE(61,304) EM1V(I),EN1V(I),EV(I),BV(I),DDV(I),EMEV(I),SMV(I),SP
     1V(I),PPV(I),UL1V(I),VL1V(I),FYV(I),ANGV(I)
 304  FORMAT (10X,2F9.3,3F10.3,F9.3,F10.5,2F9.4,3F10.5,F10.4)
      WRITE (61,302)
      WRITE (61,305)
 305  FORMAT (15X,4HANC.,5X,7HTHETAD.,3X,5HPSIY.,6X,4HFCS.,5X,5HVORT.,5X
     1,2HM1,8X,2HN1,7X,3HETA,6X,4HBETA,5X,5HDELTA/)
      DO 5 I=1,M
    5 WRITE (61,306) ANCV(I),THDV(I),PSIYV(I),FCSV(I),VORTV( I),EM1V(I),
     1EN1V(I),EV(I),BV(I),DDV(I)
 306  FORMAT (10X,F10.4,F11.3,3F10.5,2F9.3,3F10.3)
      WRITE (61,302)
1     RETURN
      END
```

3200 FORTRAN DIAGNOSTIC RESULTS - FOR PRINT1

```
NO ERRORS
LOAD,56
RUN,1
```

```
SHOCK ENTROPY INTERACTION                              10/20/67

GIVEN DATA

         M1 =     1.2500000000E 00
        ETA =     6.2000000000E 01                1.0821039111E 00
       BETA =     5.7999999999E 1                 1.0122907555E 00
      DELTA =     1.0000000  E 00                 1.7453288889E-02
         SM =     1.0000000000E-02
         A1 =     1.1170000000E 03

  RESULTS.
         M1 =     1.1036843590E 00
          N =     4.  8915159555E- 1
          M =     1.  717.32677E 00
        CHI =     1.2544723583E  0
      RORAT =     1.1753699841E 00
          A =     1.1539552436E 03
          U =     1.2367890999E 03
                                 OMEGA MATRIX

   9.9491739606E-01   -2.0330415678E-03    9.2102490710E-03                   0
  -8.0916427305E-0     6.7632629065 -01    1.4665327727E 00                   0
   7.5036019687E-01    2.9234407889E-01   -5.0067250166E-01                   0
                  0                   0                   0    9.6790676172E-01
                                  PI MATRIX

  -9.5150466335E-03                   0                   0                   0
  -1.5146585992E 00                   0                   0                   0
   1.5174461208E 00                   0                   0                   0
   1.5941461541E-01                   0                   0                   0


      ALPHA =     8.3247360347E 01                1.4529405785E 00
         CS =     2.8795566926E 03
         UE =     2.4596606392E 03
        EME =     2.1309659479E  0
        CS2 =     1.7421621546E 02
        CS1 =     1.1365795948E 03
       FSTY =     6.2554904720E-03
         SP =     9.9981058585E-03
         PP =    -3.0155986087E-04
         DP =    -5.9583940845E-04
         VP =    -2.6629374247E-04
        UST =    -4.9499772554E-04
        VST =     4.2534011055E-04
        ULT =    -2.3737182696E- 4
        VLT =     6.0794043600E-04
         FY =    -7.3735263213E-04
        GYS =                    0
        FGS =                    0
        ANG =    -2.6252320221E-02
        ANC =    -2.4211104630E-02
     THETAD =     9.2752619656E 01                1.6188382661E 00
       VORT =     6.5263845884E-04
```

SHOCK ENTROPY INTERACTION 10/20/67

GIVEN DATA.

M1 =	1.7000000000E 00	
ETA =	4.0000000000E 01	6.9813155556E-01
BETA =	3.6000000000E 01	6.2831839999E-01
DELTA =	1.0000000000E 00	1.7453288889E-02
SM =	1.0000000000E-02	
A1 =	1.1170000000E 03	

RESULTS.

M1 =	1.0927367473E 00
V =	9.1747097669E-01
M =	1.5608951402E 00
CHI =	1.2264242982E 00
RORAT =	1.1566641321E 00
A =	1.1501908597E 03
U =	1.7955273233E 03

OMEGA MATRIX

9.9586606172E-01	-1.6527752961E-03	7.5625363300E-03	0
-8.1135458278E-01	6.7545816683E-01	1.4849927943E 00	0
7.4060334972E-01	2.9624134005E-01	-5.1569249666E-01	0
0	0	0	9.7114 [illegible]7205E-01

PI MATRIX

-7.7872517125E-03	0	0	0
-1.5291162979E 00	0	0	0
1.5312218753E 00	0	0	0
1.4373479464E-01	0	0	0

ALPHA =	8.2610299059E 01	1.4453120725E 00
CS =	2.4436553140E 03	
UE =	1.4473720565E 03	
EME =	1.2563755507E 00	
CS2 =	9.5490071179E 2	
CS1 =	1.9099988146E 03	
PSIY =	8.5620395397E-03	
SP =	1.0000645627E-02	
PP =	1.2677655923E-04	
UP =	-1.2520758378E-03	
VP =	7.6957771170E-05	
UST =	-8.4562493612E-04	
VST =	8.9936190490E-04	
UE1 =	1.4539413627E-04	
VE1 =	1.2256849513E-03	
FY =	-1.1313296344E-03	
GYS =	0	
FCS =	0	
ANG =	5.2034514132E-03	
ANC =	5.3799949024E-03	
THETAD =	9.3189700940E 01	1.6264667720E 00
VCRT =	1.2344769615E-03	

SHOCK ENTROPY INTERACTION   10/20/67

GIVEN DATA.

```
      M1 =   2.4000000000E 00
     ETA =   2.7600000000E 01        4.8520148110E-01
    BETA =   2.3799999999E 01        4.1538827555E-01
   DELTA =   1.0000000000E 00        1.7453288869E-02
      SM =   1.0000000000E-02
      A1 =   1.1170000000E 03
```

RESULTS.

```
      M1 =   1.1193277225E 00
       V =   8.9706254739E-01
       N =   2.2229542290E 00
     CHI =   1.2950436421E 00
   KORAL =   1.2022219656E 00
       A =   1.1593192367E 03
       U =   2.5771136000E 03
```

OMEGA MATRIX

9.9341836930E-01	-2.6326442566E-03	1.1759935023E-02	0
-6.0621127950E-01	6.7751548818E-01	1.4405276730E 00	0
7.1731782765E-01	2.8692713142E-01	-4.0326426703E-01	0
0	0	0	9.8349647669E-01

PI MATRIX

-1.2295477974E-02	0	0	0
-1.4951042957E 00	0	0	0
1.4984528065E 00	0	0	0
1.8140576953E-01	0	0	0

```
   ALPHA =   8.1992852236E 01        1.4310449369E 00
      CS =   3.0029511047E 03
      CE =   1.2237573861E 03
     EPS =   1.0555827483E 00
     CS2 =   1.8456470767E 03
     CS1 =   2.8702617504E 03
    FSTY =   1.3572615436E-02
      SS =   1.0012509318E-02
      PP =   1.5323251301E-03
      UP =  -3.1767748685E-03
      VP =   4.9067684483E-04
     UST =  -2.4427910719E-03
     VST =   2.0924017862E-03
     UE1 =   7.1161400285E-04
     VE1 =   3.1567146734E-03
      FY =  -1.7271377207E-03
     G/S =                  0
     PCS =                  0
     ANG =   3.1009111026E-02
     ANC =   3.4451828597E-02
  THE AO =   9.4007147762E 01        1.6407339075E 00
    VUPT =   3.2164224585E-03
```

SH[illegible] [illegible]RY [illegible]ERAC[illegible] 10/29/87

[illegible] [illegible]A.

[illegible]1 =	4.[illegible]E 00	
E[illegible]A =	1.[illegible]E 01	3.0194109[illegible]E [illegible]1
[illegible]TA =	1.3[illegible]E [illegible]1	2.3212874222E [illegible]1
[illegible]TA =	1.[illegible]E 00	1.74532[illegible]E [illegible]2
[illegible] =	1.[illegible]E-02	
[illegible]1 =	1.117[illegible]E 03	

[illegible]S.

[illegible]1 =	1.1[illegible]264E 00
[illegible] =	8.4[illegible]7156715E-01
[illegible] =	3.6[illegible]1443E 00
[illegible] =	1.4[illegible]946E [illegible]0
[illegible]RAT =	1.32[illegible]9392[illegible]E 00
[illegible]A =	1.[illegible]E 03
[illegible] =	4.364[illegible]12433E 03

O[illegible]EGA [illegible]ATRIX

[illegible].[illegible]4[illegible]3110226E-01	-6.[illegible]27559[illegible]810E-03	2.5536539937E-02	0
-7.[illegible]456324416E-01	6.[illegible]2[illegible]232E-01	1.3356610[illegible]12E 00	0
[illegible].[illegible]15[illegible]36032E-01	2.[illegible]4[illegible]2555540E-01	-3.[illegible]0[illegible]26E-01	0
0	0	0	9.4431927251E-01

[illegible] A[illegible]I[illegible]

-2.[illegible]E-02	0	0	0
-1.41[illegible]0[illegible]2[illegible]5E 00	0	0	0
1.4222995770E 00	0	0	0
[illegible].[illegible]440[illegible]534E-01	0	0	0

ALP[illegible]A =	[illegible].1[illegible]1[illegible]3481E 01	1.41750[illegible]332E 00
[illegible] =	4.[illegible]17443E 03	
[illegible] =	1.[illegible]048E 03	
E[illegible] =	9.15[illegible]32[illegible]1[illegible]3E-01	
[illegible]2 =	3.621720635[illegible]E [illegible]3	
[illegible]1 =	4.872[illegible]40[illegible]721E [illegible]3	
[illegible] =	1.61[illegible]5[illegible]8[illegible]76E-02	
[illegible] =	9.9[illegible]3[illegible]7[illegible]1E-03	
[illegible] =	-6.6[illegible]1[illegible]032E-04	
[illegible] =	-2.1[illegible]4[illegible]2557E-03	
[illegible] =	3.5[illegible]7590444[illegible]E-03	
[illegible] =	-7.[illegible]3[illegible]6[illegible]334E-04	
VS[illegible] =	4.1[illegible]29[illegible]5[illegible]965E-03	
[illegible]1 =	3.7[illegible]95763E-03	
V[illegible]1 =	1.615[illegible]1341[illegible]5E-03	
[illegible]Y =	-2.92[illegible]47[illegible]2[illegible]1E-03	
[illegible] =	-5.8279224627E-04	
[illegible] =	-[illegible].[illegible]5[illegible]81[illegible]5041E-04	
A[illegible] =	-4.[illegible]57[illegible]7[illegible]977E-03	
A[illegible] =	-6.[illegible]0[illegible]7[illegible]7[illegible]8E-03	
[illegible] =	9.47[illegible]83[illegible]52[illegible]E 01	1.6541942113E 00
[illegible] =	4.[illegible]44[illegible]4[illegible]043E-03	

SHOCK ENTROPY INTERACTION 10/20/67

ETA	BETA	M1	N1	CHI	CS1	CS2
67.700	63.700	1.210	1.120	1.296	1026.584	1.301
62.000	58.000	1.250	1.104	1.254	1136.580	174.216
46.400	42.400	1.500	1.086	1.210	1602.620	717.198
40.000	36.000	1.700	1.093	1.226	1909.999	994.901
33.400	29.400	2.000	1.101	1.247	2339.680	1388.765
27.800	23.800	2.400	1.119	1.295	2870.262	1845.647
22.400	18.400	3.000	1 143	1.356	3642.425	2532.457
17.300	13.300	4.000	1.189	1.484	4672.604	3621.727
12.300	8.300	6.000	1.278	1.739	7354.595	5891.565

M1.	N1.	ETA.	BETA.	DELTA.	ME.	SM.	SP.	FP.	UL1.	VL1.	FY.	ANG.
1.210	1.120	67.700	63.700	1.000	2.659	.01000	.0100	-0.0004	-0.00034	.00054	-0.00067	-0.0390
1.250	1.104	62.000	58.0-0	1.000	2.131	.01000	.0100	-0.0003	-0.00024	.00061	-0.00074	-0.0263
1.500	1.086	46.400	42.400	1.000	1.411	.01000	.0100	-0.0001	.00001	.00091	-0.00094	-0.0028
1.700	1.093	40.000	36.000	1.000	1.258	.01000	.0100	.0001	.00015	.00123	-0.00113	.0052
2.000	1.101	33.400	29.400	1.000	1.135	.01000	.0100	.0005	.00036	.00182	-0.00136	.0158
2.400	1.119	27.800	23.8-0	1.000	1.056	.01000	.0100	.0015	.00071	.00314	-0.00173	.0310
3.000	1.143	22.400	18.400	1.000	.963	.01000	.0100	.0017	.00194	.00363	-0.00220	.0223
4.000	1.189	17.300	13.300	1.000	.916	.01000	.0100	-0.0007	.00371	.00162	-0.00292	-0.0049
6.000	1.278	12.300	8.300	1.000	.816	.01000	.0098	-0.0043	.00619	-0.00156	-0.00412	-0.0141

A C.	THETAD.	FSTY.	PCS.	VDRT.	M1	N1	ETA	BETA	DELTA
-0.0345	92.569	.00608	0	.00064	1.210	1.120	67.700	63.700	1.000
-0.0242	92.753	.00626	0	.00065	1.250	1.104	62.000	58.000	1.000
-0.0028	92.775	.00752	0	.00091	1.500	1.086	46.400	42.400	1.000
.0054	93.190	.00856	0	.00123	1.700	1.093	40.000	36.000	1.000
.0170	93.240	.01047	0	.00160	2.000	1.101	33.400	29.400	1.000
.0345	94.007	.01357	0	.00322	2.400	1.119	27.800	23.800	1.000
.0262	94.059	.01697	.00173	.00411	3.000	1.143	22.400	18.400	1.000
-0.0062	94.776	.01613	-0.00067	.00404	4.000	1.189	17.300	13.300	1.000
-0.0266	89.963	.01566	-0.00431	.00639	6.000	1.278	12.300	8.300	1.000